8-2018

Engelmann Spruce Survival and Regeneration After an Epidemic Spruce Beetle Outbreak on the Markagunt Plateau in Southern Utah

Jessika M. Pettit
Utah State University

ENGELMANN SPRUCE SURVIVAL AND REGENERATION AFTER AN

EPIDEMIC SPRUCE BEETLE OUTBREAK ON THE MARKAGUNT

PLATEAU IN SOUTHERN UTAH

by

Jessika M. Pettit

A thesis submitted in partial fulfillment
of the requirements for the degree

of

MASTER OF SCIENCE

in

Ecology

Approved:

_____ _____
Julia I. Burton, Ph.D.   Steve L. Voelker, Ph.D.
Co-Major Professor   Co-Major Professor

_____ _____
R. Justin DeRose, Ph.D.   James N. Long, Ph.D.
Committee Member   Committee Member

_____
Mark R. McLellan, Ph.D.
Vice President for Research and
Dean of the School of Graduate Studies

UTAH STATE UNIVERSITY
Logan, Utah

2018

ABSTRACT

Engelmann Spruce Survival and Regeneration after an Epidemic Spruce Beetle Outbreak

on the Markagunt Plateau in Southern Utah

by

Jessika M. Pettit, Master of Science

Utah State University, 2018

Major Professors: Dr. Julia I. Burton and Dr. Steve L. Voelker
Department: Wildland Resources

Climate change may lead to more severe disturbance regimes, and alter successional trajectories following disturbance. Throughout the western United States warmer, drier conditions are leading to an abundance of epidemic bark beetle outbreaks. Drought is often correlated with epidemic beetle outbreaks, but the mechanism behind this correlation—either through promoting beetle populations or by producing more drought stressed trees with less non-structural carbons available for inducible defenses—has not been fully resolved. Engelmann spruce (*Picea engelmannii*) is one such coniferous species that has experienced epidemic spruce beetle (*Dendroctonus rufipennis*) outbreaks across its range with the most recent one on the Markagunt Plateau in the 1990s occurring during a prolonged drought. These epidemic beetle outbreaks alter the microclimate conditions through canopy removal, thus impacting subsequent regeneration. Our research analyzes the mortality of Engelmann spruce during the outbreak as well as the patterns of regeneration in the following decades. We compared carbon isotopes from crossdated annual rings of Engelmann spruce that were determined

to have succumbed to the beetle either very early or very late during the epidemic outbreak to assess the extent to which tree drought stress influences beetle outbreaks. The annual carbon isotope discrimination ($\Delta^{13}C$) in tree-rings was most sensitive to changes in climatic moisture deficit (CMD), and there were significant differences between early- and late-dying trees when accounting for size. Small trees were similar in their sensitivity to climate, whereas large early-dying trees were more drought sensitive than late-dying ones. Additionally, we examined Engelmann spruce seedling regeneration across a climate gradient on the Markagunt Plateau. Using multiple lines of evidence, we identified a shift in factors influencing regeneration where the density of pre-outbreak seedlings appears to have been influenced by historical competition with overstory trees, as opposed to post-outbreak seedlings which are more related to current microclimate conditions. In the context of climate change, having an abundance of advance (pre-outbreak) regeneration provides some resilience to climate-disturbance interactions.

(129 pages)

PUBLIC ABSTRACT

Engelmann Spruce Survival and Regeneration after an Epidemic Spruce Beetle Outbreak

on the Markagunt Plateau in Southern Utah

Jessika M. Pettit

Bark beetle outbreaks are becoming more intense and severe when coupled with the effects of climate change. Engelmann spruce (*Picea engelmannii*) is one such species facing large-scale, epidemic spruce beetle outbreaks. Large-scale disturbances, such as beetle outbreaks, have major consequences for the future success of the ecosystem, thus highlighting the importance of understanding what promotes amplified outbreaks as well as their effects on future seedling establishment. Our research focused on two parts of a large-scale beetle outbreak: the mortality of spruce trees and the subsequent regeneration of seedlings. Our first study examined the timing of spruce mortality during an outbreak in order to identify the extent to which drought promotes host species mortality. Trees that are drought stressed have less resources to defend themselves against beetle attacks, however, the warmer temperatures associated with droughts also promote a more rapid population expansion of spruce beetles. We were specifically interested in determining the contribution that host drought stress plays during an epidemic outbreak. Our second study analyzed the patterns of regenerating seedlings with an aim to identify changes associated with the outbreak. Specifically, we were interested in how an epidemic outbreak changes the drivers of seedling establishment.

ACKNOWLEDGMENTS

CONTENTS

LIST OF TABLES

LIST OF FIGURES

CHAPTER 1

INTRODUCTION

High elevation forests dominated by Engelmann spruce (*Picea engelmannii*) and subalpine fir (*Abies lasiocarpa*) constitute an important ecosystem in North America due in part to the wide variety of wildlife species they support. Engelmann spruce can be found as far north as British Columbia, Canada and as far south as New Mexico and Arizona, USA. These subalpine forests face numerous disturbances each with their own severity, return interval, and potential to interact. The two main disturbances I'll be focusing on are climate change and spruce beetle (*Dendroctonus rufipennis*) outbreaks, and specifically, how they impact Engelmann spruce forests. In order to conserve spruce habitat today and in the future, we need to understand how these disturbances are affecting the survival and regeneration of spruce trees separately as well as how they interact.

Climate and Engelmann spruce

The distribution of Engelmann spruce is confined to a range with a particular climate. Spruce, especially new seedlings, are sensitive to drought, and prefer a cool, wet climate characterized by long, cold winters and short, cool summers (Noble and Alexander 1977, Alexander and Shepperd 1984, Alexander 1987, Gill et al. 2015). Their seedling life-history traits signify this as well. Spruce seeds have a higher germination and recruitment survival rate on mineral soil and decaying wood (Macek et al. 2017), as opposed to areas with thicker litter that tend to dry out faster (Knapp and Smith 1982). Engelmann spruce also have relatively small seeds compared to other trees in its range

(e.g. *Abies lasiocarpa*). These small seeds are able to germinate faster and at lower temperatures to help them avoid late growing season drought stress (Knapp and Smith 1982), but this puts them at risk during extremely dry or shorter seasons. Dendrochronological studies have supported this preference of spruce for cool, wet climates as well. Spruce growth patterns have shown that growth is generally most limited by warm, dry previous year growing season conditions (Peterson and Peterson 1994, Villalba et al. 1994). Further studies have shown an increase in mortality of spruce trees following droughts (Bigler et al. 2007).

With future climate projections indicating warmer, drier climates throughout the range of Engelmann spruce, suitable habitat for spruce trees will be at higher elevations from their historical range (Rehfeldt et al. 2006). Based on current temperature and precipitation trends, models indicate a reduction in potential spruce habitat, including its elimination from areas in the current southern range of spruce (Rehfeldt et al. 2006). The future survival of spruce trees appears to lie in their ability to move upslope in areas where suitable growing space still exists at higher elevations. Numerous studies have already documented this shift throughout its range (Bekker 2005, Jump and Penuelas 2005, Sakulich 2015). Not only is climate affecting the temperature and precipitation throughout the range of Engelmann spruce, but it is also affecting the severity of large disturbances, which can contribute to spruce mortality. Fire regimes are more prominent and of higher intensity in areas where drought occurs (Bigler et al. 2005), as are spruce beetle outbreaks.

Spruce beetle and Engelmann spruce

Unlike fires or other landscape-wide disturbances, spruce beetle outbreaks are host-specific. Spruce beetles have coexisted and evolved with Engelmann spruce (Raffa and Berryman 1987). Spruce beetle populations are attracted to blowdowns and freshly cut logs where they are afforded winter protection from cold temperatures and predators (e.g., woodpeckers) by the snow (Knight 1958, Schmid and Frye 1977, Schmid 1981), and where they can accumulate in large numbers in hosts with weakened defenses. Mature, adult spruce beetles lay eggs in the phloem of spruce trees which generally have a two year life-cycle. When the eggs hatch, the larvae spend two winters inside their host tree feeding on key nutrients in the phloem until they become adults and tunnel outward to attack new hosts (Schmid and Frye 1977). These feeding galleries prevent spruce trees from transporting photosynthetic sugars, effectively killing them. In response to gallery-excavation, spruce trees have evolved mechanisms by which they can defend themselves against an attack: these are generally characterized as constitutive and induced. Constitutive defenses are baseline defenses that include having thicker bark which inhibits the ability of beetles to burrow into them. Induced defenses can include the ability of some trees to upregulate novel resin formation in epithelial cells that line traumatic resin ducts, providing additional resin to expel bark beetles during an on-going attack. However, this defense mechanism only works for trees that have the capacity for induced defenses and enough non-structural carbon resources to expel mass amounts of resin (Paine et al. 1997).

Background-level, endemic spruce beetle populations are a common occurrence in spruce forests. However, when the beetle population grows to epidemic levels, these

outbreaks overwhelm the population of spruce trees and their defenses. Natural spruce beetle predators, such as woodpeckers and other insects, are unable to impose meaningful controls on population growth during epidemic outbreaks (Knight 1958, Schmid and Frye 1977). Not only does the population density of spruce beetles increase in an epidemic outbreak, but also the area of spruce trees attacked. At endemic levels, large diameter at breast height (DBH) spruce trees are the only trees targeted. These slow-growing, older trees have fewer resources to ward off beetles from attacking their phloem even at endemic levels (Hard et al. 1983, Holsten 1984, Hard 1987, Doak 2004). By contrast, spruce trees as small as 10 cm DBH have been attacked and killed during an epidemic outbreak (Bakaj et al. 2016, Mielke 1950).

Climate and spruce beetle interactions

Understanding the interactions between disturbances and climate change is one of the biggest challenges facing scientists and forest managers today. Changing disturbances and/or climate affects the resiliency of an ecosystem when it is used to a historical range of variability and the new disturbance and/or climate is outside of that range (DeRose and Long 2014, Johnstone et al. 2016). Recent climate change, including warmer, drier conditions throughout much of the range of Engelmann spruce (Easterling et al. 2000, Rehfeldt et al. 2006, Seager et al. 2007) have helped turn endemic spruce beetle outbreaks into epidemic ones (DeRose and Long 2007, Hart et al. 2014, Csank et al. 2016). On the Kenai Peninsula in Alaska, Berg et al. (2006) found one of the biggest predictors of spruce beetle outbreaks in white (*Picea glauca*), Sitka (*P. sitchensis*), and Lutz spruce (*P.* x *luztii*) to be the summer temperature in the five to six years prior to an

outbreak. Whereas in Utah and Colorado, Hebertson and Jenkins (Hebertson and Jenkins 2008) found the mean temperature, precipitation, and Palmer-Drought Severity Index (PDSI) of various months before an attack to be the most important indicators. Overall, across the range of Engelmann spruce, antecedent warmth and drought facilitate epidemic spruce beetle outbreaks.

There are several mechanisms, both direct and indirect, leading to the correlations between warmer, drier years and increased spruce beetle outbreaks. Direct effects include the ways in which temperature regulates spruce beetle life-history traits. Even though beetles can withstand temperatures as low as -34°C, spruce beetles are sensitive to extremely cold winter temperatures, therefore, there is a higher overwinter survival rate of spruce beetles in warmer winters with less extreme cold events (Hebertson and Jenkins 2008, Massey and Wygant 1954). Some spruce beetles also have the ability to mature in only one year instead of two (transition from semivoltine to univoltine) due to higher summer temperatures preventing a second year of diapause (e.g., environment induced dormancy; Hansen et al. 2001a, 2001b, Bentz et al. 2010). When spruce beetles mature during their first year of life, they amplify the population by reproducing during that first year, as well as re-emerging and reproducing again during their second year (Hansen and Bentz 2003). Additionally, since dispersal and flight of spruce beetles is temperature dependent (i.e., beetles need a threshold of 16.1°C in order to fly), warmer temperatures allow the beetles to more rapidly colonize new hosts and decimate a population of spruce trees (Schmid and Frye 1977). Warmer temperatures allow spruce beetles to more easily survive winter, reproduce faster and therefore more often, and then allow them to spread to other trees sooner all of which helps to create epidemic outbreaks.

Indirect effects include the ways in which temperature increases host susceptibility and by extension spruce beetle success. In drought years, spruce trees close their stomata in order to prevent excess water loss through their needles. This in turn decreases the carbon assimilated by the plant, which affects the way in which the remaining carbon is allocated (Cregg 1994, Hartmann et al. 2013). So, in agreement with the growth differentiation balance hypothesis (GDBH, Herms and Mattson 1992), in warmer and drier years, resource-deficient spruce trees are unable to employ adequate defenses to dispel spruce beetles which increases tree mortality rates (Bentz et al. 2010, Csank et al. 2016). Additionally, the symbiotic relationships that spruce beetles have with other organisms (e.g., nematodes, mites, and fungi) can be dramatically impacted by a warming climate as well (Cardoza et al. 2008). So not only does the population of spruce beetles drastically increase in warmer years, but also the susceptibility of spruce trees to attack: amplifying the effect of spruce beetles on Engelmann spruce survival.

In light of this climate-mediated disturbance outside of the range of historic variability, our study looks at both the mortality of Engelmann spruce during the epidemic beetle outbreak (Chapter 2) and the subsequent regeneration (Chapter 3). For Chapter 2, we were specifically interested in the progression of beetle mortality throughout a stand. We looked at Engelmann spruce that died before the year of peak mortality and after it to identify factors related to timing of mortality. For Chapter 3, we were interested in how an epidemic outbreak changes factors related to seedling establishment. We compared seedlings that established before the outbreak to those that established during and after it in terms of their density across sites, spatial relationships to snags, and relationship with coarse woody debris.

LITERATURE CITED

Alexander, R. R. 1987. Ecology, silviculture, and management of the Engelmann spruce-subalpine fir type in the central and southern Rocky Mountains.

Alexander, R.R., and W.D. Shepperd. 1984. Silvicultural characteristics of Engelmann spruce. Rocky Mountain Research Station Publications 4:412-417.

Bakaj, F., N. Mietkiewicz, T. T. Veblen, and D. Kulakowski. 2016. The relative importance of tree and stand properties in susceptibility to spruce beetle outbreak in the mid-20th century. Ecosphere 7:1-17.

Bekker, M.F. 2005. Positive feedback between tree establishment and patterns of subalpine forest advancement, Glacier National Park, Montana, USA. Arctic, Antarctic, and Alpine Research 37:97-107.

Bentz, B.J., J. Régnière, C. J. Fettig, E. M. Hansen, J. L. Hayes, J. A. Hicke, R. G. Kelsey, J. F. Negrón, and S. J. Seybold. 2010. Climate change and bark beetles of the western United States and Canada: direct and indirect effects. BioScience 60:602-613.

Berg, E.E., J. D. Henry, C. L. Fastie, A. D. De Volder, and S. M. Matsuoka. 2006. Spruce beetle outbreaks on the Kenai Peninsula, Alaska, and Kluane National Park and Reserve, Yukon Territory: Relationship to summer temperatures and regional differences in disturbance regimes. Forest Ecology and Management 227:219-232.

Bigler, C., D. G. Gavin, C. Gunning, and T. T. Veblen. 2007. Drought induces lagged tree mortality in a subalpine forest in the Rocky Mountains. Oikos 116:1983-1994.

Bigler, C., D. Kulakowski, and T. T. Veblen. 2005. Multiple disturbance interactions and drought influence fire severity in Rocky Mountain subalpine forests. Ecology 86:3018-3029.

Cardoza, Y.J., J. C. Moser, K. D. Klepzig, and K. F. Raffa. 2008. Multipartite symbioses among fungi, mites, nematodes, and the spruce beetle, *Dendroctonus rufipennis*. Environmental Entomology 37:956-963.

Cregg, B. M. 1994. Carbon allocation, gas exchange, and needle morphology of *Pinus ponderosa* genotypes known to differ in growth and survival under imposed drought. Tree Physiology 14:883-898.

Csank, A. Z., A. E. Miller, R. L. Sherriff, E. E. Berg, J. M. Welker. 2016. Tree-ring isotopes reveal drought sensitivity in trees killed by spruce beetle outbreaks in south-central Alaska. Ecological Applications 26:2001-2020.

DeRose, R. J., and J. N. Long. 2014. Resistance and resilience: a conceptual framework for silviculture. Forest Science 60:1205-1212.

DeRose, R. J., and J. N. Long. 2007. Disturbance, structure, and composition: spruce beetle and Engelmann spruce forests on the Markagunt Plateau, Utah. Forest Ecology and Management 244:16-23.

Doak, P. 2004. The impact of tree and stand characteristics on spruce beetle (Coleoptera: Scolytidae) induced mortality of white spruce in the Copper River Basin, Alaska. Canadian Journal of Forest Research 34:810-816.

Easterling, D. R., G. A. Meehl, C. Parmesan, S. A. Changnon, T. R. Karl, and L. O. Mearns. 2000. Climate extremes: observations, modeling, and impacts. Science 289:2068-2074.

Gill, R. A., C. S. Campbell, and S. M. Karlinsey. 2015. Soil moisture controls Engelmann spruce (*Picea engelmannii*) seedling carbon balance and survivorship at timberline in Utah, USA. Canadian Journal of Forest Research 45:1845-1852.

Hansen, E. M., and B. J. Bentz. 2003. Comparison of reproductive capacity among univoltine, semivoltine, and re-emerged parent spruce beetles (Coleoptera: Scolytidae). The Canadian Entomologist 135:697-712.

Hansen, E. M., B. J. Bentz, and D. L. Turner. 2001a. Temperature-based model for predicting univoltine brood proportions in spruce beetle (Coleoptera : Scolytidae). Canadian Entomologist 133:827-841.

Hansen, E. M., B. J. Bentz, and D. L. Turner. 2001b. Physiological basis for flexible voltinism in the spruce beetle (Coleoptera: Scolytidae). The Canadian Entomologist 133:805-817.

Hard, J. S. 1987. Vulnerability of white spruce with slowly expanding lower boles on dry, cold sites to early seasonal attack by spruce beetles in south central Alaska. Canadian Journal of Forest Research 17:428-435.

Hard, J. S., R. A. Werner, and E. H. Holsten. 1983. Susceptibility of white spruce to attack by spruce beetles during the early years of an outbreak in Alaska. Canadian Journal of Forest Research 13:678-684.

Hart, S. J., T. T. Veblen, K. S. Eisenhart, D. Jarvis, and D. Kulakowski. 2014. Drought induces spruce beetle (*Dendroctonus rufipennis*) outbreaks across northwestern Colorado. Ecology 95:930-939.

Hartmann, H., W. Ziegler, O. Kolle, and S. Trumbore. 2013. Thirst beats hunger - declining hydration during drought prevents carbon starvation in Norway spruce saplings. New Phytologist 200:340-349.

Hebertson, E. G., and M. J. Jenkins. 2008. Climate factors associated with historic spruce beetle (Coleoptera: Curculionidae) outbreaks in Utah and Colorado. Environmental Entomology 37:281-292.

Herms, D. A., and W. J. Mattson. 1992. The dilemma of plants: to grow or defend. The quarterly review of Biology 67:283-335.

Holsten, E. H. 1984. Factors of susceptibility in spruce beetle attack on white spruce in Alaska. Journal of the Entomological Society of British Columbia 81:39-45.

Johnstone, J. F., et al. 2016. Changing disturbance regimes, ecological memory, and forest resilience. Frontiers in Ecology and the Environment 14:369-378.

Jump, A. S., and J. Penuelas. 2005. Running to stand still: adaptation and the response of plants to rapid climate change. Ecology Letters 8:1010-1020.

Knapp, A. K., and W. K. Smith. 1982. Factors influencing understory seedling establishment of Engelmann Spruce (*Picea engelmannii*) and Subalpine Fir (*Abies lasiocarpa*) in Southeast Wyoming. Canadian Journal of Botany 60:2753-2761.

Knight, F. B. 1958. The effects of woodpeckers on populations of the Engelmann spruce beetle. Journal of Economic Entomology 51:603-607.

Macek, M., J. Wild, M. Kopeckỳ, J. Červenka, M. Svoboda, J. Zenáhlíková, J. Brŭna, R. Mosandl, and A. Fischer. 2017. Life and death of *Picea abies* after bark-beetle outbreak: ecological processes driving seedling recruitment. Ecological Applications 27:156-167.

Massey, C. L., and N. D. Wygant. 1954. Biology and control of the Engelmann spruce beetle in Colorado. US Department of Agriculture; Washington.

Mielke, J. L. 1950. Rate of deterioration of beetle killed Engelmann Spruce. Journal of Forestry.

Noble, D. L., and R. R. Alexander. 1977. Environmental factors affecting natural regeneration of Engelmann spruce in the centeral Rocky Mountains. Forest Science 23:420-429.

Paine, T. D., K. F. Raffa, and T. C. Harrington. 1997. Interactions among scolytid bark beetles, their associated fungi, and live host conifers. Annual review of Entomology 42:179-206.

Peterson, D. W., and D. L. Peterson. 1994. Effects of climate on radial growth of subalpine conifers in the North Cascade Mountains. Canadian Journal of Forest Research 24:1921-1932.

Raffa, K. F., and A. A. Berryman. 1987. Interacting selective pressures in conifer-bark beetle systems: a basis for reciprocal adaptations? American Naturalist 129:234-262.

Rehfeldt, G. E., N. L. Crookston, M. V. Warwell, and J. S. Evans. 2006. Empirical analyses of plant-climate relationships for the western United States. International Journal of Plant Sciences 167:1123-1150.

Sakulich, J. 2015. Reconstruction and spatial analysis of alpine treeline in the Elk
    Mountains, Colorado, USA. Physical Geography 36:471-488.

Schmid, J. M. 1981. Spruce beetles in blowdown. USDA Forest Service, Rocky
    Mountain Forest and Range Experiment Station Research Note RM-411.

Schmid, J. M., and R. H. Frye. 1977. Spruce beetles in the Rockies. USDA Forest Service
    General Technician Report, Rocky Mountain Forest and Range Experiment
    Station No. RM-49.

Seager, R., et al. 2007. Model Projections of an Imminent Transition to a More Arid
    Climate in Southwestern North America. Science 316:1178-1181.

Villalba, R., T. T. Veblen, and J. Ogden. 1994. Climatic influences on the growth of
    subalpine trees in the Colorado Front Range. Ecology 75:1450-1462.

CHAPTER 2

CARBON ISOTOPE ANALYSIS REVEALS STAND-SPECIFIC IMPORTANCE OF

DROUGHT SENSITIVITY IN TIMING OF DEATH OF ENGELMANN SPRUCE

DURING AN EPIDEMIC BEETLE OUTBREAK

Abstract

Throughout the western United States, warmer and drier conditions have increasing led to epidemic bark beetle outbreaks. The amplifying effects that warmer temperatures have on beetle populations are well understood. Less well understood is the contribution that host susceptibility adds in creating epidemic beetle outbreaks. Drought is often correlated with epidemic beetle outbreaks, but the mechanism behind this correlation—either through promoting beetle populations or by producing more drought stressed trees with less non-structural carbon available for inducible defenses—has not been fully resolved. Engelmann spruce (*Picea engelmannii*) is one such coniferous species that has experienced epidemic spruce beetle (*Dendroctonus rufipennis*) outbreaks across its range with the most recent one in the 1990s occurring during a prolonged drought. We compared carbon isotope discrimination ($\Delta^{13}C$) from crossdated annual rings of Engelmann spruce that were determined to have succumbed to the beetle either very early or very late during the epidemic outbreak to assess the extent to which tree drought stress influences beetle outbreaks. The sensitivity of tree ring $\Delta^{13}C$ to climatic moisture deficit (CMD) was significantly different between early- and late-dying trees when accounting for size. Small trees were similar in their sensitivity to climate irrespective of time of death, whereas large early-dying trees were more sensitive than

late-dying ones. Timing of spruce death within a stand was most significantly related to tree size, but there was a trade-off in the importance of size versus tree susceptibility that was mediated by stand structure. Timing of death was related to tree vigor in stands composed of large trees, whereby more drought stressed or shade grown were more susceptible to early beetle attacks. In contrast, stands containing few large trees presented a limited local supply of preferred host habitat, and thereby these large trees died early in the outbreak, followed by more abundant and less preferred smaller trees later in the outbreak.

Introduction

Ecosystem resilience can be affected when climate change-mediated disturbances are outside the historical range of variability (DeRose and Long 2014; Johnstone et al. 2016). Bark beetles are one such disturbance agent of forests that is greatly influenced by climate (Berg et al. 2006; Bentz et al. 2010; Hart et al. 2014a, 2017). Recent climate change, including warmer, drier conditions throughout much of the range of Engelmann spruce (*Picea engelmannii*; Easterling et al. 2000; Rehfeldt et al. 2006; Seager et al. 2007) have escalated endemic spruce beetle (*Dendroctonus rufipennis*) outbreaks into epidemic ones (DeRose and Long 2007; Hart et al. 2014a), and knowing which trees within individual stands the spruce beetle is likely to attack is important for assessing resilience and management in the face of these disturbances.

Spruce beetle outbreaks interact with climate causing both indirect and direct effects. Indirect effects include the increased susceptibility of host trees following droughts where individuals have less non-structural carbon available for inducible

defenses (Paine et al. 1997). Direct effects include warmer temperatures promoting an amplified lifecycle, resulting in spruce beetles reproducing sooner and more often (Hansen and Bentz 2003), as well as larger broods due to a decrease in overwinter mortality (Massey and Wygant 1954). At endemic population levels, spruce beetles tend to select only slow-growing large trees, but as the spruce beetle population grows to epidemic levels, all trees are attacked, including smaller trees (Massey and Wygant 1954; Holsten 1984; Hard 1985; Doak 2004). These climate-mediated effects allow the spruce beetle population to grow to epidemic levels in a setting where hosts are more susceptible, thus changing the ecology of the outbreak.

During the transition from endemic to epidemic spruce beetle population levels, the direct effects of temperature on spruce beetle life-history traits are well-documented as being a driving force (Hansen et al. 2001; Hansen and Bentz 2003; Raffa et al. 2008). However, less is known about the relative contribution that the indirect effects of tree susceptibility add during the progression of a spruce beetle outbreak. Tree-ring reconstructions of drought metrics (e.g., Cook et al. 2010) have been correlated with increased spruce beetle activity in Utah (DeRose et al. 2012a) and Colorado (Hart et al. 2014a, 2017) providing some evidence that drought-stressed hosts contributed to the development of these outbreaks. However, drought stress recorded by montane forests are often associated with a co-occurrence of lower precipitation and warmer temperatures that affect winter snowpack, the length of the growing season and evaporative demand during the growing season (Hu et al. 2010; Pederson et al. 2011; Williams et al. 2013; Diffenbaugh et al. 2015; Belmecheri et al. 2016). Therefore, previous studies of past bark beetle activity cannot differentiate between the direct effect of warmer temperatures on

beetle population growth versus the impacts of how warmer temperatures can cause drought and associated reductions in host susceptibility.

Studies that have started to tease apart the relative contribution of drought stress to the progression of spruce beetle outbreaks have performed paired analyses between live and dead trees of similar size, and looked at metrics of tree vigor and carbon isotope discrimination ($\Delta^{13}C$) climate sensitivity for differences in tree survival. $\Delta^{13}C$ measured from tree-rings can often be used as a metric of drought stress, because in areas with abundant sunlight, tree-ring $\Delta^{13}C$ will primarily indicate how open or closed an individual tree's stomata are for any given year. In the absence of significant drought stress, when stomata are open, there are two processes that affect the ratio of ^{12}C to ^{13}C (McCarroll and Loader 2004). Diffusional fractionation occurs across the boundary of the stomata where ^{12}C diffuses into a leaf at a faster rate than ^{13}C. Thereafter, during the Calvin cycle of photosynthesis ribulose-1, 5-bisphosphate carboxylase/oxygenase (RuBisCO) preferentially fixes ^{12}C rather than ^{13}C during the first step of carbon fixation. Therefore, in the absence of significant drought stress, the carbon fixed in annual rings by photosynthesis has more ^{12}C compared to ^{13}C. However, when a tree is drought stressed, stomatal closure constrains water loss to the atmosphere but also limits plant uptake of carbon dioxide. Therefore drought stress results in less discrimination against ^{13}C relative to ^{12}C (lower $\Delta^{13}C$; Farquhar et al. 1989).

If host drought stress was important for driving the progression of a spruce beetle outbreak, there should be a difference in drought sensitivity between early- and late-dying trees during the course of an outbreak with early-dying trees being hypothetically more drought stressed. This difference in drought sensitivity would then help facilitate

the growth of spruce beetle populations from endemic to epidemic levels. Trees that died early in the outbreak, during endemic level spruce beetle populations, would have been more sensitive to drought and thereby would have had fewer resources to defend themselves. In contrast, trees that succumbed later in the outbreak would simply be overwhelmed by epidemic spruce beetle populations, and their induced defenses would not have mattered. However, if the direct effect of temperature was mainly responsible for the development of outbreaks regardless of host susceptibility, the drought sensitivity would be the same for both early- and late-dying trees.

Herein, we propose a combination of drought stress and tree size as being important during the succession of spruce beetle outbreaks in addition to the direct effects of temperature on spruce beetle populations. To test this hypothesis, we first determined whether trees that died earlier versus later in an outbreak were more sensitive to climate using annual $\Delta^{13}C$ data. Second, we tested whether metrics of tree drought stress, tree size, and tree growth were important for predicting when trees died during an epidemic outbreak. We hypothesize that there would be a difference in sensitivity to drought among trees that died but that it would be mediated by tree size. For example, late-dying trees may have been attacked by spruce beetles early in the outbreak and were able to defend themselves until later because they had more resources (as indicated by a lower sensitivity to drought). For example, induced production of traumatic resin ducts in spruce during this outbreak occurred in trees for as many as four continuous years (DeRose et al. 2017). In contrast, some trees that succumbed later in the outbreak may not have been attacked until after spruce beetle populations were at epidemic population levels and then died rapidly (associated with greater sensitivity to drought; DeRose and

Long 2012b). This distinction is likely mediated by tree size. We would expect large trees that died late in the outbreak to have been less sensitive to drought, whereas small trees that died late in the outbreak to have been more sensitive to drought based on the observed progression of spruce beetle outbreaks with respect to tree size and vigor (Holsten 1984).

To build upon previous findings, we designed a study to determine the relative importance of tree size, drought-sensitivity, and stand structure on the timing of spruce beetle-caused mortality during an extensive, severe spruce beetle outbreak. Spruce beetle mortality was so severe, killing 95% of overstory Engelmann spruce across the study area (DeRose and Long 2007), to preclude the pairing of overstory live and dead spruce. Therefore, we assessed groups of trees that were killed earlier versus later during the outbreak as defined on a stand by stand basis. This design allowed us to examine the temporal component of mortality and the contribution of host susceptibility during the progression of beetle outbreaks with respect to stand structure, tree size, and $\Delta^{13}C$ levels.

Methods

Study site

We used archival increment cores that were originally collected during the summers of 2005-2007 (see DeRose and Long 2012a, 2012b) on the Markagunt Plateau in southern Utah (Table 2-1, Fig. 2-1). The Markagunt Plateau is on the western edge of the Colorado Plateau and is largely managed by the USDA Forest Service. The Markagunt Plateau experienced an epidemic spruce beetle outbreak in the 1990s, which was characterized by mortality rates of over ninety five percent of overstory spruce trees

(DeRose and Long 2007; DeRose et al. 2017). The dominant forest type on the plateau
was Engelmann spruce-subalpine fir, however, after the spruce beetle outbreak there was
a high abundance of subalpine fir (DeRose and Long 2010). For this study, we focused
on what had been Engelmann spruce-dominated stands that varied in elevation from 3202
to 2879 m and in basal area spruce composition from 91.3 to 55.5% (Table 2-1).

Increment core preparation for stable isotope analyses

Of the sites previously sampled, only six sites were chosen for further analyses
based on the abundance and quality of the increment cores. The date of last year of
growth was verified for every core using visual crossdating and COFECHA software
(Holmes 1983; Yamaguchi 1991; Grissino-Mayer 2001). Histograms of last year of
growth were made to identify trees that died early in the outbreak during endemic
population levels or later in the outbreak during epidemic population levels per site (Fig.
A-1). Early- and late-dying trees were those that died during years occupying the
respective tails of the mortality-year distribution within each stand, after excluding any
outliers that may have died previous to any significant spruce beetle activity. Ranges of
dates were picked for each site that met two criteria: 1) trees died before (early) or after
(late) the peak of death dates and 2) enough cores were available for stable isotope
analyses (minimum of 5 cores per group). Cores earmarked for stable isotope analyses
were re-measured to include earlywood- and latewood-specific growth back to 1930
using a Velmex measuring system. Annual basal area increment (BAI) was calculated for
each tree by first calculating the diameter inside the bark from the diameter outside the
bark (Myers and Alexander 1972), and then using ring-width values to calculate areal

growth on an annual basis assuming annual rings could be generalized as concentric circles. Trees identified for stable isotope analyses were determined on a site by site basis to obtain the greatest separation of early- and late-dying trees that included at least five dead trees within each group to ensure a large enough sample (Table 2-1; Fig. A-1).

We composited the latewood of tree-rings across a site and within timing categories (i.e., each site had two sets of samples for each year that were distinguished by trees that died early versus late). Compositing rings by year for stable isotope analyses is a common procedure that assures sufficient cellulose for stable isotope analyses when rings of trees are very small (e.g., Tardif et al. 2008; Voelker et al. 2014; Csank et al. 2016). Even though we could not sample tree-ring isotopes on an individual tree basis, using 4-5 trees typically yields an expressed population signal greater than 0.85 (Leavitt 2010). Latewood was excised from each ring to better isolate moisture stress during the summer months (Parker and Henoch 1971; Faulstich et al. 2013). Latewood pieces were ground into wood powder using a Wiley mill before extracting to holocellulose (Leavitt and Danzer 1993; Laumer et al. 2009). Holocellulose was immersed in distilled water within a 2 mL microcentrifuge tube, homogenized using a 500-W ultrasonic probe, freeze-dried to remove the water, and weighed into tin capsules on a microbalance. These samples were analyzed on a Thermo Delta V Advantage isotope ratio mass spectrometer at the Newell Stable Isotope Laboratory located at Utah State University (http://www.usu.edu/geo/newell/Newell_Website/Stable_Isotope_Lab.html). Precision across replicate ^{13}C analyses of cellulose was $1\sigma = 0.12$ ‰. Stable isotope analyses extended back to the tree-ring formed in 1960 for all sites to include a common period of climatic variability in the decades leading up to the spruce beetle outbreak.

Δ^{13}C data were detrended using a 50-year spline (50% frequency cut-off;

combined using the biweight mean). Standard, residual, and ARSTAN Δ^{13}C index

chronologies were calculated for each site/timing combination (i.e., 12 total chronologies,

regardless of detrending) using ARSTAN software (Cook and Holmes 1986; Cook and

Krusik 2014). Indices characterized by a mean of one were then multiplied by the Δ^{13}C

average per site/timing combination to retain the site and group-specific differences in

Δ^{13}C. One Δ^{13}C outlier was removed after data inspection (the 1960 values for the early-

dying trees at site HPT). Ring width data (earlywood, latewood, and total ring width)

were also detrended using a 50-year spline. Detrending was done using the "dplR"

package in R (Bunn 2008; R Core Team 2016) and ARSTAN software (Cook and

Holmes 1986).

Drought sensitivity assessment

We first compared correlations between Δ^{13}C and monthly climate variables from

Climate WNA (after Wang et al. 2016) to identify which metric and months best captured

drought stress at our sites. Variables of interest included climatic moisture deficit (CMD)

defined as precipitation minus reference evapotranspiration for June, July, and August

(after the Hargreaves method, Yates and Strzepek 1994), temperature, and the palmer-

drought severity index (PDSI, Guttman and Quayle 1996). To determine if the climate

sensitivity of Δ^{13}C varied between the trees that died early versus late in the outbreak, we

conducted mixed-effects modeling with repeated-measures that accounted for the nested

design of early- and late-dying trees per site. The repeated measurement was detrended

Δ^{13}C. Because Δ^{13}C should not differ among early- and late-mortality in wet years but

should differ under increasingly dry conditions, we ran the model multiple times, each with progressively drier years included (100%, upper 66%, upper 50%, and upper 33% of years as ranked by CMD). We tested $\Delta^{13}C$ responses with two competing models at each level of CMD. The first model contained the interaction between CMD and timing of death (early or late), whereas the second model included the three-way interaction of CMD, timing of death, and mean diameter at breast height (DBH) for the isotope-cores belonging to early- or late-dying trees. If the interaction between CMD and timing of death was significant in the first model, that would support the importance of drought-sensitivity during the progression of beetle outbreaks. The second model was based on our hypothesis that drought-sensitivity would be mediated by tree size, wherein a significant three-way interaction would support our theory. The model residuals were normally distributed. All analyses were conducted using the "nlme" and "visreg" packages in R (R Core Team 2016; Breheny and Burchett 2017; Pinheiro et al. 2017).

Predicting date of death

Even though $\Delta^{13}C$ data were measured as an average of all early- or late-dying trees from a site, predicting date of death was conducted at the tree-level. More specifically, tests of date of death used annually resolved $\Delta^{13}C$ data averaged across all the trees by site, and by time of death, whereas tree size (DBH) and growth rate (BAI) data were used on the individual tree-level. $\Delta^{13}C$ values for each site and timing category were applied to all trees within it (e.g., all early-dying trees at the ASH site were given the same $\Delta^{13}C$ value for a given year). A generalized linear model was used to predict date of death per tree, which was standardized, among plots due to the variability among

plots (Table 2-1), around the year of highest mortality per site (positive values indicate years later in the outbreak, and negative, years early in the outbreak). The model was fitted with all hypothesized main effects (BAI, DBH, Δ^{13}C, and their interactions) and interpreted in terms that were significant ($P < 0.05$). To highlight the differences in early- versus late-dying trees, and based on the drought-sensitivity analysis (Table 2-2) and the assumption that Δ^{13}C was more sensitive to climate during drier years, another model was run on a subset of the data for years where CMD was in the top 66% of all years analyzed. Random effects were used to account for the nested nature of years repeated for trees within sites. All analyses were done using the "nlme" and "visreg" packages in R (R Core Team 2016; Breheny and Burchett 2017; Pinheiro et al. 2017).

Results

Δ^{13}C was more strongly correlated with monthly climate variables when compared to ring width, latewood width, and earlywood width. In particular, it was most highly correlated to climatic moisture deficit (CMD) for the months of June, July, and August (Table A-1).

Models assessing the sensitivity of Δ^{13}C to drought (i.e., CMD) after accounting for the timing of death (early or late mortality) and tree size (DBH) revealed that the most significant models included Δ^{13}C data from only the top two-thirds of years as ranked by CMD values (Table 2-2). The model of Δ^{13}C sensitivity without DBH (main effects: CMD, timing of death and the interaction between the two), did not show a significant difference in drought-sensitivity between early- and late-dying trees (Table 2-2; Fig. 2-2). However, the model including DBH, and the three-way interaction between CMD, timing

of death, and DBH did include a significant difference between early- and late-dying trees (Table 2-2; Fig. 2-3). Early-dying trees, regardless of DBH, had similar sensitivities to drought. However, larger early-dying trees had consistently lower Δ^{13}C values compared to small early-dying trees at similar CMD (Figs. 2-3a, 2-4), consistent with larger trees being characterized by larger and taller tree crowns that are subject to greater hydrostatic xylem tensions and received greater irradiance. Depending on DBH, late-dying trees varied not only in the magnitude, but also the sign of the relationship between Δ^{13}C and CMD (Figs. 2-3b, 2-4). Large, late-dying trees showed a positive response of Δ^{13}C to CMD whereas small trees had a negative response (Figs. 2-3b, 2-4). Interestingly, small late-dying trees had lower Δ^{13}C values compared to small early-dying trees at similar CMD (Fig. 2-4). If we were to rank the Δ^{13}C at low CMD, early-dying large trees have the lowest Δ^{13}C, then late-dying small trees, followed by late-dying large trees, and early-dying small trees (Fig. 2-4). Whereas at high CMD, late-dying small trees have the lowest Δ^{13}C, followed by early-dying large trees, early-dying small trees, and late-dying large trees (Fig. 2-4).

The t-tests comparing DBH and Δ^{13}C values between early- and late-dying trees indicated some significant differences among groups depending on the site (Table 2-3). Sites that had a significant difference in DBH did not have significant differences in Δ^{13}C (e.g. ASH, NLS; Table 2-3). However, sites that did not have a significant difference in DBH did have a significant difference in Δ^{13}C (e.g. HPT, SNO; Table 2-3). One site, had marginally significant differences in both categories (e.g. MID; Table 2-3). HCK had significant differences in DBH, and Δ^{13}C, but in the opposite direction as other sites. However, when the 10 years leading up to death were compared, the difference in D13C

was no longer significant (Table 2-3). Additionally, at sites where there was not a significant difference in DBH from early- to late-dying trees, there is a marked difference in their correlation with CMD; early-dying trees were more strongly correlated with CMD than late-dying trees (e.g. HPT, SNO; Table 2-3). When analyzing all the sites combined, significantly larger trees died early in the outbreak, and they had significantly lower $\Delta^{13}C$ values than trees that died later in the outbreak (Table 2-3).

When identifying the factors that predict the timing of death (either early or late), from a model with $\Delta^{13}C$, DBH, and BAI, as well as all the possible two-way interactions, and the three-way interaction, the only significant fixed effect ($P < 0.05$) was DBH (Fig. 2-4). As DBH increased, timing of death also occurred sooner at a threshold of 57 cm (Fig. 2-4). When the DBH of a tree was less than 57 cm it tended to succumb to the spruce beetle later in the outbreak, whereas if DBH was greater than 57 cm, it was more likely to succumb earlier in the outbreak (Fig. 2-4).

Discussion

Temperature and host susceptibility are known to impact spruce beetle populations but little is known of whether and how drought stress may influence the success of beetle attacks that fosters a transition between endemic and outbreak phases of population dynamics. To shed light on these questions, our study specified early- and late-dying trees within an outbreak and assessed their sizes and drought-sensitivity leading up to the outbreak to identify how drought stress interacts with tree size to influence the success of beetle attacks. More specifically, we found that the sensitivity of $\Delta^{13}C$ to CMD (i.e., drought) did not differ based on timing of death until tree size (i.e.,

DBH) was also included. Large trees that died early in the outbreak, during the transition from endemic to outbreak beetle populations, were significantly more sensitive to drought than those that died once beetle populations had reached epidemic levels. The effects of drought on host vigor were important for facilitating the growth of spruce beetle populations to epidemic levels in stands with an abundance of large DBH trees.

The climate sensitivity of trees that died during the outbreak is not only related to stomatal conductance but also to irradiance. When comparing the discrimination of large and small early-dying trees, the lower discrimination of large trees across years is consistent with size related differences in $\Delta^{13}C$ (Figs. 2-3a, 2-4). Large trees often close their stomata earlier than small trees because they have a higher hydrostatic gradient at the top of the tree (Schafer et al. 2000; Koch et al. 2004). Additionally, large trees that are dominant in the canopy receive greater solar radiation than smaller trees that are more often shaded throughout the day. This difference in sunlight exposure allows for higher assimilation rates in larger trees (Farquhar and Sharkey 1982). Taken together, these two factors would result in a lower $\Delta^{13}C$ signal from tree rings in these larger early-dying trees.

When comparing the sensitivity of small trees that died early in the outbreak to those that died later (Figs. 2-3, 2-4a), we see the effect of irradiance explaining differences in their sensitivity of $\Delta^{13}C$ to CMD. Lower $\Delta^{13}C$ in small late-dying trees compared to small early-dying trees at low CMD, when drought stress should not be a factor, suggests that there was a difference in sun exposure between the two groups. Small early-dying trees were likely growing in more shaded environments compared to small late-dying trees and therefore would have had lower canopy-integrated

photosynthetic rates (Farquhar and Sharkey 1982; Whitehead 1998). These early-dying trees would then have less stored carbons for induced defenses when attacked by beetle. This mechanism would explain why some small trees were attacked early in the outbreak, given spruce beetles generally prefer large trees (e.g., Schmid and Frye 1976; Holsten 1984; Hard 1985). In contrast, small late-dying trees were likely growing under conditions with much greater access to sunlight and would therefore have had greater canopy-integrated photosynthetic rates compared to small early-dying trees. Hence, small late-dying trees likely had greater non-structural carbon available and were thereby able to defend themselves longer against beetle attacks. Finally, this difference in growing conditions would account for the greater $\Delta^{13}C$ sensitivity to CMD in small late- compared to early-dying trees, and thus their respective differences in timing of death.

When comparing sensitivity of $\Delta^{13}C$ to drought for large trees, the large late-dying trees had a positive relationship between $\Delta^{13}C$ and CMD whereas early-dying trees showed the opposite, a negative response between $\Delta^{13}C$ and CMD (Figs. 2-3, 2-4b). Both groups were likely in similar canopy positions with little difference in their sun exposure. Large early-dying trees were characterized by the expected negative response to CMD, suggesting that they had lower stomatal conductance in response to greater CMD and drought stress, in agreement with other recent research on spruce (Csank et al. 2016). On the other hand, the positive response between $\Delta^{13}C$ and CMD for large late-dying trees was initially puzzling.

Interestingly, large late-dying trees had a positive relationship between $\Delta^{13}C$ and CMD (Figs. 2-3b, 2-4b). As conditions got warmer and drier, these trees kept their stomata open longer suggesting that they were not water limited. Large, late-dying trees

tended to occur on high elevation sites with greater open areas characterized by higher snowpack, slower snow ablation, and thus shorter growing seasons with lower soil and local air temperatures (Hart and Lomas 1979; Hubbart et al. 2015). Together, these microclimate conditions would cause greater stomatal limitations to photosynthesis during cool, low CMD years (DeLucia and Smith 1987; Day et al. 1989). On the contrary, during warmer, high CMD years these stresses would be alleviated resulting in increased photosynthesis. Therefore, as CMD increased, snowpack decreased and soil and air temperatures increased, leading to increased stomatal conductance in these large late-dying trees.

When accounting for DBH, trees that died early in the outbreak during endemic spruce beetle populations versus later in the outbreak during epidemic populations, varied in their $\Delta^{13}C$ sensitivity to CMD, thus highlighting the importance of host drought stress in facilitating the progression of spruce beetle outbreaks. Large trees that were attacked and killed early in the outbreak were those that more rapidly closed their stomata to prevent water loss as CMD increased, indicative of greater moisture stress (Farquhar et al. 1989; Csank et al. 2016). However, large trees that did not die until later, were characterized by leaf gas-exchange responses (i.e., $\Delta^{13}C$) that responded favorably to increased CMD and were likely to have been better able to defend themselves against the beetle during drought years when other trees were more susceptible. Small DBH trees that died early in the outbreak were less sensitive to climate, but $\Delta^{13}C$ indicate these trees had been growing in more shaded conditions. Therefore they likely had less stored non-structural carbon for defense and were thereby susceptible to bark beetles when populations had not yet reached epidemic levels. Small late-dying trees, in comparison,

were growing in locations with greater sunlight. Therefore they had comparatively greater $\Delta^{13}C$ sensitivity to CMD and more stored non-structural carbon available for defenses.

The few large trees that did survive the outbreak (not sampled in this study because of they were so infrequent), would most likely have had $\Delta^{13}C$ sensitivity to CMD that was similar to large late-dying trees. When surviving trees on the Markagunt Plateau were measured for a different study (DeRose et al. 2017), no difference was found between live versus beetle-killed trees in age, ring-width, or BAI, but only in the abundance of traumatic resin ducts. Hence, a lower sensitivity of leaf gas-exchange to drought in Engelmann spruce was associated with successful defense against endemic beetle attacks and defenses against epidemic bark beetle populations for years before death. Tree survival during an epidemic bark beetle attack may nearly require greater resin delivery capacity (Ferrenberg et al. 2014; DeRose et al. 2017). Less than five percent of overstory Engelmann spruce survived the outbreak on the Markagunt Plateau, but late-dying trees, by our designation, represented approximately 12% of the population. Since late-dying trees survived for an average of seven years more than early-dying trees and about three years more than trees that died during the peak of the outbreak, late-dying trees would have produced seed crops and seedlings during a period of newly abundant resources across a substantial part of the forested landscape.

The timing of death of Engelmann spruce was most significantly related to DBH when testing aspects of tree vigor, growth, and size (Fig. 2-5), highlighting the importance of available spruce beetle habitat, but also some of the limitations of our study design (as addressed below). However, a different trend emerges when among site

variability is examined. More specifically, a trade-off in importance of DBH versus $\Delta^{13}C$ emerges; either DBH or $\Delta^{13}C$ was significantly different between early- and late-dying trees from site to site but rarely both (Table 2-3). When taken together with the stand characteristics of each site, this pattern suggests that the importance of DBH versus $\Delta^{13}C$ depends on the diameter distributions and associated stand structural components of each site (Fig. A-2), since other stand attributes such as species richness/diversity did not co-vary with this trend (Fig. A-3). Sites that did not have a significant difference in DBH for early- versus late-dying trees, had a unimodal diameter distribution with an abundance of large diameter trees (e.g. HPT, SNO; Table 2-3; Fig. A-2). By contrast, sites that had a significant difference in DBH from early- to late-dying trees either had a bimodal diameter distribution (e.g. ASH; Table 2-3; Fig. A-2) or unimodal with fewer large trees (e.g. HCK, NLS, MID; Table 2-3; Fig. A-2).

Hence, we propose that stand structure can mediate the progression of an epidemic outbreak within a stand via interactions among how structure impacts available beetle habitat, snowpack accumulation and associated drought stress. Other studies on spruce beetle mortality including aspects of stand structure, have only looked at how it affects the percentage mortality on an areal basis, whether an individual will survive or die, or the spread across the landscape (e.g., Doak 2004; Hart et al. 2014b; Bakaj et al. 2016; Temperli et al. 2014). These studies have found individual tree characteristics to be the best predictors of tree mortality (i.e., DBH) with less importance on stand structure (i.e., lower stem densities and larger trees; Bakaj et al. 2016). Our proposed conceptual model does not indicate how stand structure affects the landscape-level spread of a spruce

beetle outbreak or which trees will survive or die, but instead, once spruce beetles are in a stand, how the timing of individual tree mortality will proceed.

From a landscape-level perspective, spruce beetles will either encounter an even-aged or an uneven-aged stand. Once a spruce beetle population grows within a stand, the subsequent timing of death of Engelmann spruce will be based on the drought-sensitivity of leaf-gas exchange and tree size, but the importance of each will depend on the stand characteristics (Fig. 2-6). More specifically, in mature stands where there is an abundance of large trees, the difference in timing of death will be determined in part by the sensitivity of $\Delta^{13}C$ to drought or in this case CMD (e.g. SNO; Table 2-3; Fig. 2-3; Fig. A-2). However, in an uneven-aged stand, where there is a mix of large and small Engelmann spruce (e.g. ASH; Fig. A-2), tree size will be of greater importance for determining tree susceptibility, beetle preference, and timing of death. At the beginning of an outbreak the few large trees in such stands will be attacked first with a larger number of spruce beetles than in the even-aged stand example, and essentially all these large trees will die regardless of their sensitivity to drought. Under such conditions, the small trees will generally be attacked later in the outbreak after the large ones have been exploited (e.g., Massey and Wygant 1954; Holsten 1984; Dymerski et al. 2001). However, the timing of death of small trees will be mediated by sun exposure where those in the shade will die first followed by those growing in the sun.

Although our design is unique in that we are able to look at timing of death and the factors that influence it during an epidemic outbreak, it has some limitations worth acknowledging. We could not obtain tree level $\Delta^{13}C$ data since latewood bands were consistently narrow and needed around 5-10 trees per sample in order to run an isotope

analysis. Due to this restriction, our model for predicting timing of death did not have tree-level $\Delta^{13}C$ data but did contain tree level DBH data. Because DBH varied from tree to tree along with timing of death, it was a more significant predictor in our mixed model approach compared to $\Delta^{13}C$ where all trees regardless of individual timing of death had the same $\Delta^{13}C$ values per site/overall timing. Regardless, our study elucidates important information on how the spread of an outbreak occurs across early- and late-dying trees, but further analyses with all data measured on the tree-level could provide additional details and help confirm or deny the conceptual model of the progression of tree mortality within stands during a spruce beetle outbreak.

The importance of stand structure in probability of an individual dying during an outbreak is consistent with other findings (e.g., Temperli et al. 2014; Bakaj et al. 2016), but has yet to be fully resolved for the timing of that mortality. Our data suggest a model that accounts for the indirect effects of drought on host susceptibility in addition to the direct effects of temperature on spruce beetle outbreaks depending on the stand structure, where drought sensitivity in stands with an abundance of large trees helps drive spruce beetle populations to epidemic levels. The difference in individual timing of mortality on a site-by-site basis highlights the unique stand-specific progression of spruce beetle outbreaks that is not consistent across a heterogeneous forest landscape. In stands with abundant large trees, the limiting factor affecting timing of death is tree susceptibility, whereas in sites with fewer large trees, available spruce beetle habitat becomes more limiting and DBH becomes the best predictor of timing of death.

References

Bakaj F, Mietkiewicz N, Veblen TT, Kulakowski D (2016) The relative importance of tree and stand properties in susceptibility to spruce beetle outbreak in the mid-20th century. Ecosphere 7:1-17

Belmecheri S, Babst F, Wahl ER, Stahle DW, Trouet V (2016) Multi-century evaluation of Sierra Nevada snowpack. Nat Clim Change 6:2

Bentz BJ, Régnière J, Fettig CJ, Hansen EM, Hayes JL, Hicke JA, Kelsey RG, Negrón JF, Seybold SJ (2010) Climate change and bark beetles of the western United States and Canada: direct and indirect effects. BioScience 60:602-613

Berg EE, Henry JD, Fastie CL, De Volder AD, Matsuoka SM (2006) Spruce beetle outbreaks on the Kenai Peninsula, Alaska, and Kluane National Park and Reserve, Yukon Territory: relationship to summer temperatures and regional differences in disturbance regimes. For Ecol Manage 227:219-232

Breheny P, Burchett W (2017) Visualization of regression models using visreg. The R Journal 9:56-71

Bunn AG (2008) A dendrochronology program library in R (dplR). Dendrochronologia 26:115-124

Cook ER, Holmes RL (1986) User's manual for program ARSTAN. Laboratory of Tree-Ring Research, University of Arizona, Tucson, USA

Cook ER, Seager R, Geim RR Jr, Vose RS, Herwiejer C, Woodhouse C (2010) Megadroughts in North America: placing IPCC projections of hydroclimatic change in a long-term paleoclimate context. J Quat Sci 25:48-61

Cook ER, Krusic PJ (2014) ARSTAN version 44h3: A tree-ring standardization program
based on detrending and autoregressive time series modeling, with interactive
graphics. Tree-Ring Laboratory, Lamont-Doherty Earth Observatory of
Columbia University, Palisades

Csank AZ, Miller AE, Sherriff RL, Berg EE, Welker JM (2016) Tree-ring isotopes reveal
drought sensitivity in trees killed by spruce beetle outbreaks in South-Central
Alaska. Ecol Appl 26:2001-2020

Day TA, DeLucia EH, Smith WK (1989) Influence of cold soil and snowcover on
photosynthesis and leaf conductance in two Rocky Mountain conifers. Oecologia
80:546-552

DeLucia EH, Smith WK (1987) Air and soil temperature limitations on photosynthesis in
Engelmann spruce during summer. Can J For Res 17:527-533

DeRose RJ, Long JN (2007) Disturbance, structure, and composition: spruce beetle and
Engelmann spruce forests on the Markagunt Plateau, Utah. For Ecol Manage
244:16-23

DeRose RJ, Long JN (2010) Regeneration response and seedling bank dynamics on a
Dendroctonus rufipennis-killed *Picea engelmannii* landscape. J Veg Sci 21:377-
387

DeRose RJ, Long JN (2012a) Drought-driven disturbance history characterizes a
southern Rocky Mountain subalpine forest. Can J For Res 42:1649-1660

DeRose RJ, Long JN (2012b) Factors influencing the spatial and temporal dynamics of
Engelmann spruce mortality during a spruce beetle outbreak on the Markagunt
Plateau, Utah. For Sci 58:1-14

DeRose RJ, Long JN (2014) Resistance and resilience: A conceptual framework for silviculture. For Sci 60:1205-1212

DeRose RJ, Bekker MB, Long JN (2017) Traumatic resin ducts as indicators of bark beetle outbreaks. Can J For Res 47:1168-1174

Diffenbaugh NS, Swain DL, Touma D (2015) Anthropogenic warming has increased drought risk in California. PNAS 112:3931-3936

Doak P (2004) The impact of tree and stand characteristics on spruce beetle (Coleoptera: Scolytidae) induced mortality of white spruce in the Copper River Basin, Alaska. Can J For Res 34:810-816

Dymerski AD, Anhold JA, Munson AS (2001) Spruce beetle (*Dendroctonus rufipennis*) outbreak in Engelmann spruce (*Picea engelmannii*) in central Utah, 1986-1998. Western N Am Nat 61:19-24

Easterling DR, Meehl GA, Parmesan C, Changnon SA, Karl TA, Mearns LO (2000) Climate extremes: observations, modeling, and impacts. Science 289:2068-2074

Farquhar GD, Ehleringer JR, Hubick KT (1989) Carbon isotope discrimination and photosynthesis. Annu Rev Plant Biol 40:503-537

Farquhar GD, Sharkey TD (1982) Stomatal conductance and photosynthesis. Annu Rev Plant Physiol 33:317-345

Faulstich HL, Woodhouse CA, Griffin D (2013) Reconstructed cool- and warm-season precipitation over the tribal lands of northeastern Arizona. Clim Chang 118:457-468

Ferrenberg S, Kane JM, Mitton JB (2014) Resin duct characteristics associated with tree resistance to bark beetles across lodgepole and limber pines. Oecologia 174:1283-1292

Grissino-Mayer HD (2001) Evaluating crossdating accuracy: a manual and tutorial for the computer program COFECHA. Tree-Ring Res 57:205-221

Guttman NB, Quayle RG (1996) A historical perspective of US climate divisions. Bull Am Meteorol Soc 77:293-303

Hansen EM, Bentz BJ, Turner DL (2001) Temperature-based model for predicting univoltine brood proportions in spruce beetle (Coleoptera: Scolytidae). Can Entomol 133:827-841

Hansen EM, Bentz BJ (2003) Comparison of reproductive capacity among univoltine, semivoltine, and re-emerged parent spruce beetles (Coleoptera: Scolytidae). Can Entomol 135:697-712

Hard JS (1985) Spruce beetles attack slowly growing spruce. For Sci 31:839-850

Hart GE, Lomas DA (1979) Effects of clearcutting on soil water depletion in an Engelmann Spruce stand. Water Resour Res 15:1598-1602

Hart SJ, Veblen TT, Eisenhart KS, Jarvis D, Kulakowski D (2014a) Drought induces spruce beetle (*Dendroctonus rufipennis*) outbreaks across northwestern Colorado. Ecology 95:930-939

Hart SJ, Veblen TT, Kulakowski D (2014b) Do tree and stand-level attributes determine susceptibility of spruce-fir forests to spruce beetle outbreaks in the early 21st century? For Ecol and Manage 318:44-53

Hart SJ, Veblen TT, Schneider D, Molotch NP (2017) Summer and winter drought drive the initiation and spread of spruce beetle outbreak. Ecology 98:2698-2707

Holmes RL (1983) Computer-assisted quality control in tree-ring dating and measurement. Tree-Ring Bull 43:69-78

Holsten EH (1984) Factors of susceptibility in spruce beetle attack on white spruce in Alaska. J Entomol Soc BC 81:39-45

Hu J, Moore DJP, Burns SP, Monson RK (2010) Longer growing seasons lead to less carbon sequestration by a subalpine forest. Glob Chang Biol 16:771-783

Hubbart JA, Link TE, Gravelle JA (2015) Forest canopy reduction and snowpack dynamics in a northern Idaho watershed of the Continental-Maritime Region, United States. For Sci 61:882-894

Johnstone JF, Allen CD, Franklin JF, Frelich LE, Harvey BJ, Higuera PE, Mack MC, Meentemeyer RK, Metz MR, Perry GLW, Schoennagel T, Turner MG (2016) Changing disturbance regimes, ecological memory, and forest resilience. Fron Ecol Environ 14:369-378

Koch GW, Sillett SC, Jennings GM, Davis SD (2004) The limits to tree height. Nature 428:851

Laumer W, Andreu L, Helle G, Schleser GH, Wieloch T, Wissel H (2009) A novel approach for the homogenization of cellulose to use micro-amounts for stable isotope analyses. Rapid Commun Mass Spectrom 23:1934-1940

Leavitt SW (2010) Tree-ring C–H–O isotope variability and sampling. Sci Tot Environ 408:5244-5253

Leavitt SW, Danzer SR (1993) Method for batch processing small wood samples to holocellulose for stable-carbon isotope analysis. Anal Chem 65:87-89

Massey CL, Wygant ND (1954) Biology and control of the Engelmann spruce beetle in Colorado. US Department of Agriculture; Washington

McCarroll D, Loader NJ (2004) Stable isotopes in tree rings. Quat Sci Rev 23:771-801

Myers CA, Alexander RR (1972) Bark thickness and past diameters of Engelmann spruce in Colorado and Wyoming. USDA Forest Service Research Note, Rocky Mountain Forest and Range Experiment Station 217

Paine TD, Raffa KF, Harrington TC (1997) Interactions among scolytid bark beetles, their associated fungi, and live host conifers. Annu Rev Entomol 42:179-206

Parker ML, Henoch WES (1971) The use of Engelmann spruce latewood density for dendrochronological purposes. Can J For Res 1:90-98

Pederson GT, Gray ST, Woodhouse CA, Betancourt JL, Fagre DB, Littell JS, Watson E, Luckman BH, Graumlich LJ (2011) The unusual nature of recent snowpack declines in the North American Cordillera. Science 333:332-335

Pinheiro J, Bates D, DebRoy S, Sarkar D, R Core Team (2017) nlme: linear and nonlinear mixed effects models. R package version 3.1-131

R Core Team (2016) R: a language and environment for statistical computing. R Foundation for Statistical Computing, Vienna, Austria

Raffa KF, Aukema BH, Bentz BJ, Carroll AL, Hicke JA, Turner MG, Romme WH (2008) Cross-scale drivers of natural disturbances prone to anthropogenic amplification: the dynamics of bark beetle eruptions. BioScience 58:501-517

Rehfeldt GE, Crookston NL, Warwell MV, Evans JS (2006) Empirical analyses of plant-climate relationships for the western United States. Int J Plant Sci 167:1123-1150

Schafer KVR, Oren R, Tenhunen JD (2000) The effect of tree height on crown level stomatal conductance. Plant Cell Environ 23:365-75

Schmid JM, Frye RH (1976) Stand ratings for spruce beetles. USDA FS RN-RM-309

Seager R, Ting M, Held I, Kushnir Y, Lu J, Vecchi G, Huang HP, Harnik N, Leetma A, Lau NC, Li C, Velez J, Naik N (2007) Model projections of an imminent transition to a more arid climate in southwestern North America. Science 316:1178-1181

Tardif JC, Conciatori F, Leavitt SW (2008) Tree rings, δ13C and climate in *Picea glauca* growing near Churchill, Subarctic Manitoba, Canada. Chem Geol 252:88-101

Temperli C, Hart SJ, Veblen TT, Kulakowski D, Hicks JJ, Andrus R (2014) Are density reduction treatments effective at managing for resistance or resilience to spruce beetle disturbance in the southern Rocky Mountains? For Ecol Manage 334:53-63

Voelker SL, Meinzer FC, Lachenbruch B, Brooks JR, Guyette RP (2014) Drivers of radial growth and carbon isotope discrimination of bur oak (*Quercus macrocarpa* Michx.) across continental gradients in precipitation, vapour pressure deficit and irradiance. Plant Cell Environ 37:766-779

Wang T, Hamann A, Spittlehouse D, Carroll C (2016) Locally downscaled and spatially customizable climate data for historical and future periods for North America. PloS ONE 116

Whitehead D (1998) Regulation of stomatal conductance and transpiration in forest canopies. Tree Physiol 18:633-644

Williams AP, Allen CD, Macalady AK, Griffin D, Woodhouse CA, Meko DM, Swetnam
TW, Rauscher SA, Seager R, Grissino-Mayer HD, Dean JS, Cook ER,
Gangodagamage C, Cai M, McDowell NG (2013) Temperature as a potent driver
of regional forest drought stress and tree mortality. Nat Clim Chang 3:292-297

Yamaguchi DK (1991) A simple method for cross-dating increment cores from living
trees. Can J For Res 21:414-416

Yates D, Strzepek KM (1994) Potential evapotranspiration methods and their impact on
the assessment of river basin runoff under climate change

Tables and Figures

Table 2-1 Site summary information for the six sites used in isotope analysis broken up by early and late-dying trees. Range and number of years used in isotope analysis per site/timing combination as well as the number of trees and their range in death dates. Average DBH of all Engelmann spruce (ES) in the stand with the standard deviation, percent BA Engelmann spruce, and site elevation.

Site	Timing of death	Isotope dates	# of trees	Range of death dates	Stand ES Mean DBH	Elev (m)	% BA ES
ASH	early	1994-1960	13	1995-1991	51.4 ±	3197	85.9
	late	1998-1960	6	1998	20.43		
HCK	early	1995-1960	13	1995-1990	36.7 ±	3085	72.4
	late	1997-1960	8	1998-1997	10.84		
HPT	early	1996-1961[a]	11	1996-1992	50.0 ±	3073	74.8
	late	2000-1960	5	2004-2000	14.10		
MID	early	1999-1960	10	1999-1991	42.0 ±	2977	65.2
	late	2001-1960	6	2002-2001	16.56		
NLS	early	1997-1960	8	1998-1991	43.0 ±	2914	55.5
	late	2001-1960	9	2006-2001	15.42		
SNO	early	1994-1960	11	1995-1990	54.0 ±	3175	91.3
	late	2000-1960	6	2005-2000	17.45		

[a]: outlier in year 1960 removed

Table 2-2 Sensitivity of $\Delta^{13}C$ to climatic moisture deficit (CMD) assessed using two model structures across all years and three subsets of years with that were characterized by progressively drier conditions. The first model included CMD, timing of death (early/late), diameter at breast height (DBH), the two way interactions of each variable, and the three-way interaction of all variables. The second model did not include DBH, but did include CMD, timing of death, and their two-way interactions. Reported p-values for the three-way interactions in the model with DBH, and the two-way interactions between CMD and timing of death for both models with varying sample size. Results specified in rows give p-values for the above analyses when considering all only years in which CMD was in the top two-thirds (top 66%), above average (top 50%), and in the top one-third (top 33%) of driest years.

	Model with DBH		Model without DBH	# of observations
	CMD*Timing* DBH	CMD*Timing	CMD*Timing	
All CMD years	$p=0.39$	$p=0.10$	$p=0.76$	463
Top 66% CMD years	$p=0.045$	$p=0.026$	$p=0.70$	310
Top 50% CMD years	$p=0.073$	$p=0.24$	$p=0.96$	233
Top 33% CMD years	$p=0.65$	$p=0.69$	$p=0.85$	154

Table 2-3 Comparisons of tree size (i.e., diameter at breast height, DBH), carbon isotope discrimination ($\Delta^{13}C$), and correlation between inter-annual variation in $\Delta^{13}C$ and climatic moisture deficit (CMD) among sites, for trees that died early versus late in the outbreak. $\Delta^{13}C$ was averaged across the entire sampled period as well as across just the 10 years leading up to death of the early-dying trees at each site ($\Delta^{13}C_{10}$). Asterisks denote results from T-tests (see footnotes) with their placement on the larger DBH and smaller $\Delta^{13}C$ value for every site. CMD was averaged June, July and August for $\Delta^{13}C$ versus CMD correlations.

Site	Timing	DBH	$\Delta^{13}C$	$\Delta^{13}C_{10}$	$\Delta^{13}C$ vs. CMD correlation
ASH	early	63.7 ***	15.85	15.57	-0.599
	late	24.3	15.70	15.65	-0.533
HCK	early	40.3*	15.84	15.50	-0.669
	late	29.1	15.22***	15.18	-0.446
HPT[a]	early	47.7	15.09^{+}	14.95	-0.535
	late	34.6	15.27	15.14	-0.049
MID	early	43.3^{+}	15.65^{+}	15.37^{+}	-0.568
	late	29	15.89	15.77	-0.595
NLS	early	58.9**	15.28	15.45	-0.255
	late	41.3	15.42	15.39	-0.431
SNO	early	67.7	15.07***	14.99**	-0.555
	late	60.4	16.22	16.19	-0.117
ALL	early	53.43***	15.47*	15.31*	-0.73
	late	36.5	15.63	15.55	-0.66

Results from t-test on DBH and $\Delta^{13}C$: $^{+}p<0.1$, *$p<0.05$, **$p<0.01$, ***$p<0.001$
[a]: outlier in year 1960 removed
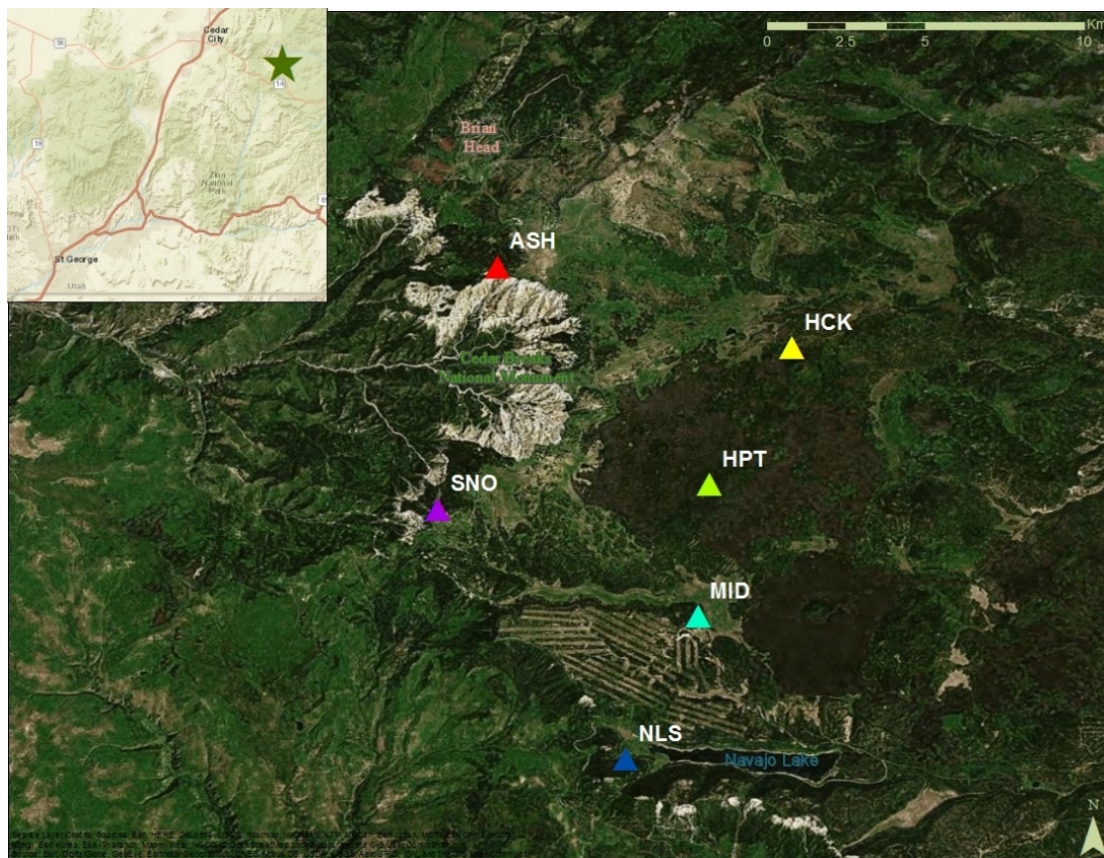
Fig. 2-1 Map of the six sites where tree cores were taken on the Markagunt Plateau in southern Utah in 2006 (DeRose and Long 2007) that were used in the isotope analysis.
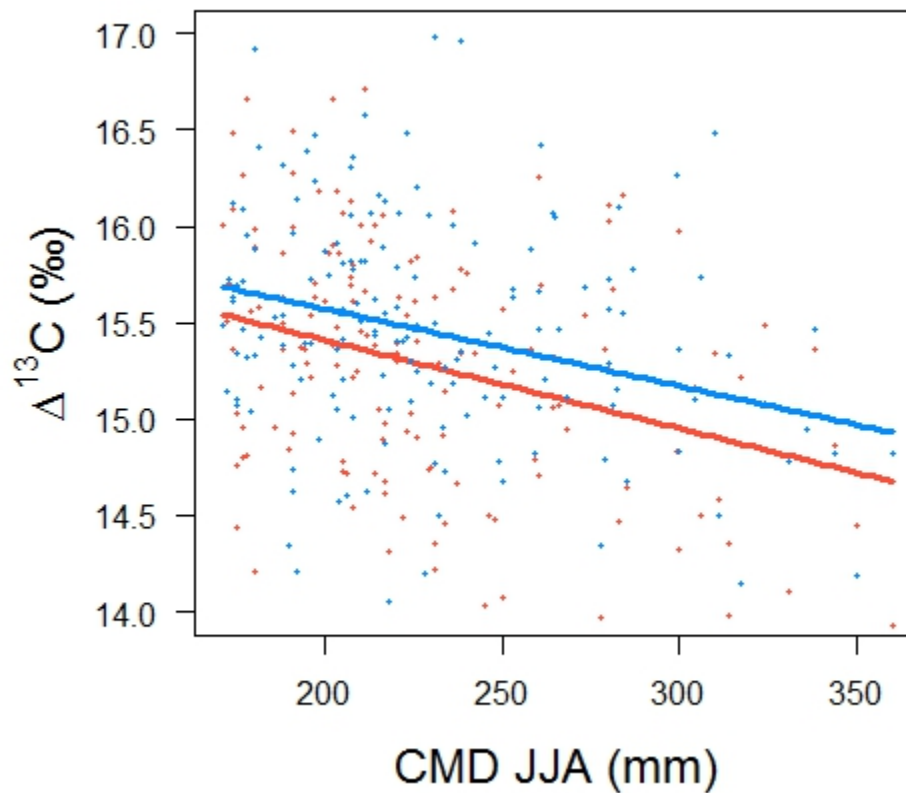
Fig. 2-2 Correlation between $\Delta^{13}C$ values and June, July, August CMD (CMD JJA) for years where CMD is in the top two-thirds (66 %) colored by early/late timing of mortality from repeated measures mixed model without DBH (P = 0.7; Table 2-2). Red dots and line indicate early-dying trees; blue dots and line indicate late-dying trees.
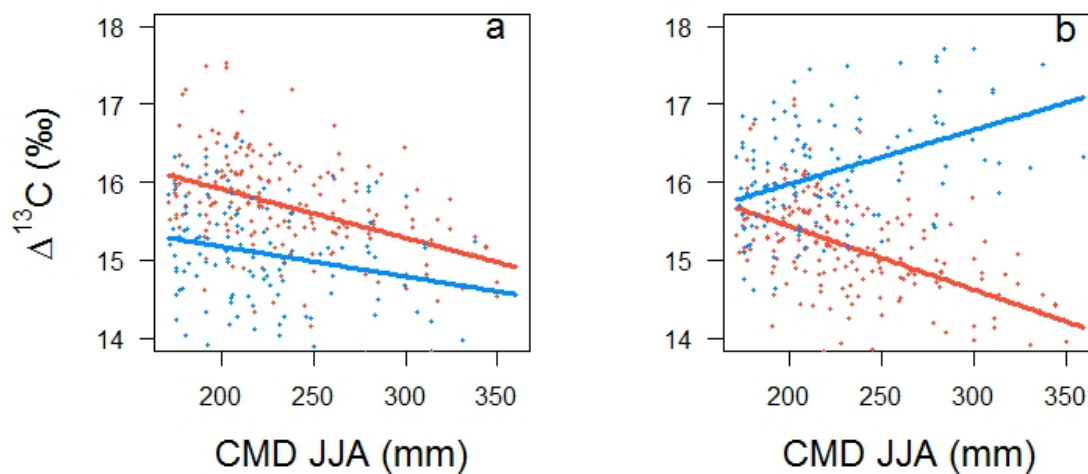
Fig. 2-3 Results of hypothesis testing model of climate sensitivity of $\Delta^{13}C$ for years where CMD is in the top two-thirds (66 %) divided by early-dying (a) and late-dying (b) trees and DBH ($P = 0.045$). Red lines/points indicate small DBH trees (25 cm) and blue indicate large DBH trees (67 cm).
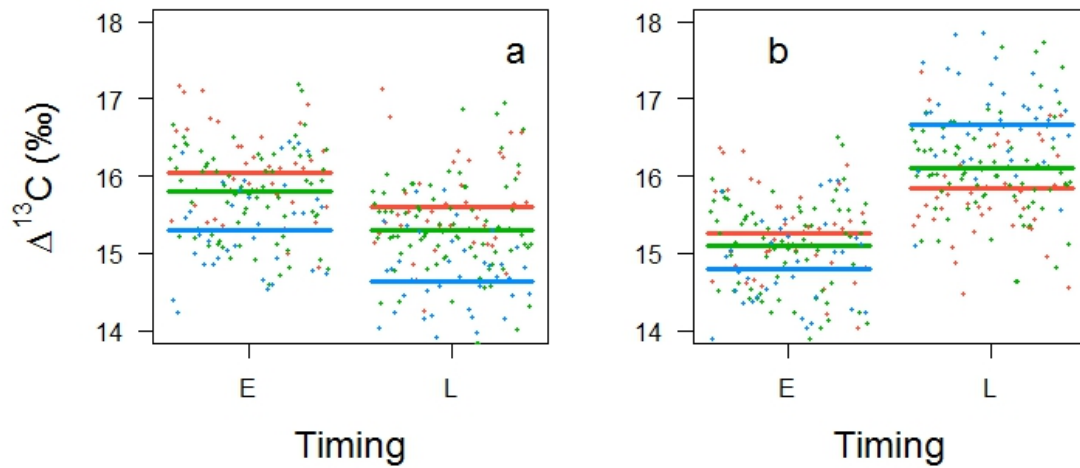
Fig. 2-4 Results of hypothesis testing model of climate sensitivity of $\Delta^{13}C$ for years where CMD is in the top two-thirds (66 %) divided by 25cm DBH (a) and 67cm DBH (b) trees and CMD for June, July, and August ($P = 0.1$). Colors indicate CMD value: Low (red, 179), moderate (green, 217), and higher (blue, 299).
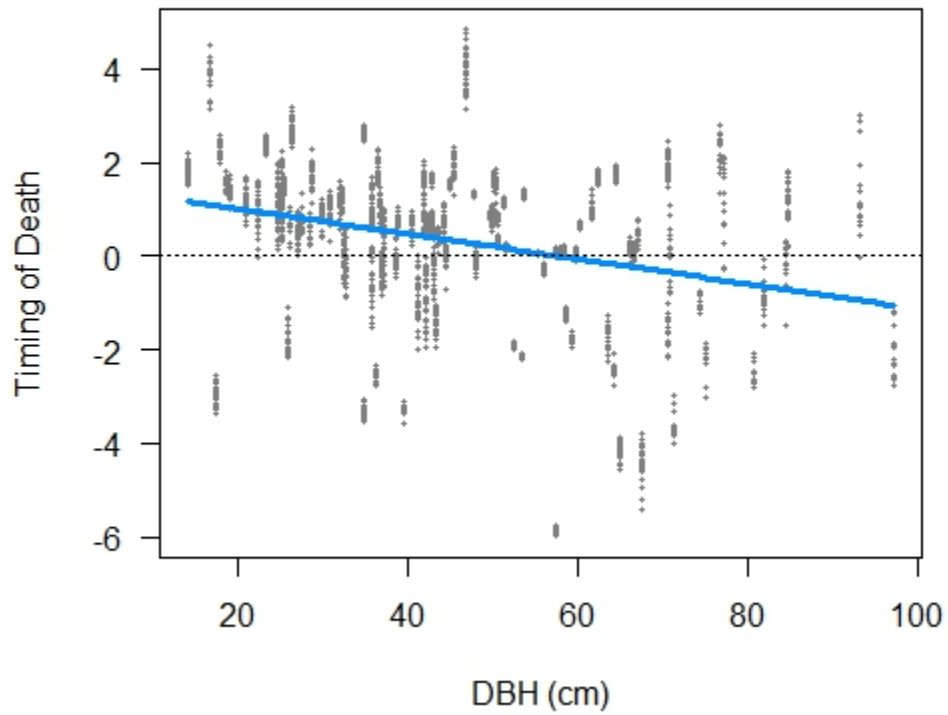
Fig. 2-5 Only significant (p<0.05) fixed effect (DBH; p<0.001) from model of timing of death (years before/after the year of highest mortality) for years where CMD was in top two-thirds (66%). Dashed black line denotes death at year of highest mortality (0).
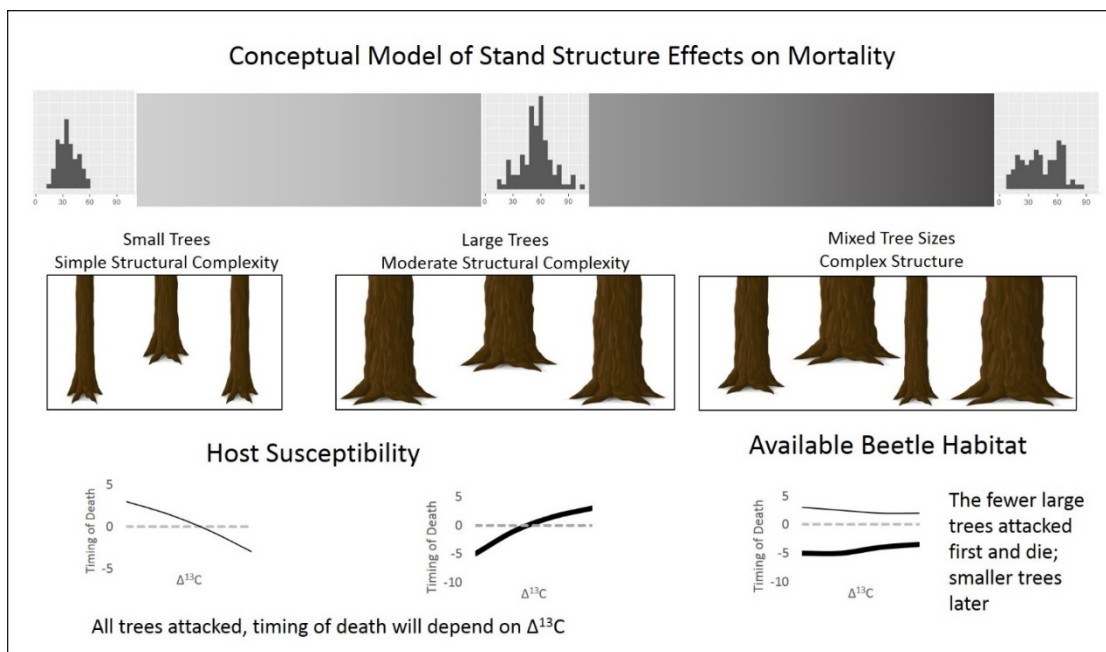
Fig. 2-6 Conceptual model of Engelmann spruce timing of death on a site-by-site basis during an epidemic spruce beetle outbreak in a continuum of stand complexity. Gray dashed line indicates year of highest mortality on each site. Line thickness denotes tree size. X-axis on graphs represents $\Delta^{13}C$ values (increasing from left to right), and y-axis are years before/after the peak of outbreak (y=0).

CHAPTER 3

AN EPIDEMIC SPRUCE BEETLE OUTBREAK CHANGES DRIVERS OF

ENGELMANN SPRUCE SEEDLING ESTABLISHMENT

Abstract. Climate change may lead to more severe disturbance regimes, and alter successional trajectories following disturbance. High elevation forests dominated by Engelmann spruce (*Picea engelmannii)* and subalpine fir (*Abies lasiocarpa*) experience epidemic spruce beetle (*Dendroctonus rufipennis*) outbreaks that alter the microclimate conditions through canopy removal, thus impacting subsequent regeneration. We examined Engelmann spruce seedling regeneration across a climate gradient on the Markagunt Plateau in southern Utah after a severe spruce beetle outbreak (90% Engelmann spruce mortality) in the 1990s. All Engelmann spruce seedlings were mapped, measured and aged, and aspects of stand structure and the microclimate (soil water content and temperature) were measured. A generalized linear multi-model approach identified factors influencing seedling regeneration that established prior to and during/after the outbreak (60% and 40% of all regeneration, respectively) at multiple scales. The pair correlation function identified the univariate and bivariate spatial relationship of spruce regeneration and canopy trees. The density of pre-outbreak seedlings was negatively related to snag basal area and early stage decay coarse woody debris (CWD), and positively related to percent understory cover and September soil water content. In contrast, post-outbreak seedling density was positively related to microclimatic climatic moisture deficit (CMD), late stage decay CWD, and July soil water content. Pre-outbreak and post-outbreak seedlings did not show significant

clumping around canopy Engelmann spruce, but post-outbreak seedlings were clumped around pre-outbreak seedlings at sites with low CMD suggesting a facilitative effect of advance regeneration. Additionally, the spatial relationship between seedlings and CWD indicated structural importance of CWD for post-outbreak seedlings. Together, these results indicate a shift in factors influencing regeneration where the density of pre-outbreak seedlings appears to have been influenced by historical competition with overstory trees, as opposed to post-outbreak seedlings which are more related to current microclimate conditions. In the context of climate change, having an abundance of advance (pre-outbreak) regeneration provides some resilience to climate-disturbance interactions. However, it is also notable that post-outbreak regeneration responded positively to CMD, suggesting that the predicted range contraction of Engelmann spruce may be more strongly limited by competition, rather than drought stress.

INTRODUCTION

Climate change is expected to alter the geographic distribution of suitable habitat for tree species (Rehfeldt et al. 1999, Davis and Shaw 2001, Rehfeldt et al. 2006, Lenoir et al. 2008, Scheller and Mladenoff 2005). Trees are long-lived, however, and range expansion and contraction may lag changes in climate (Davis 1986, HilleRisLambers et al. 2015). Warmer spring and winter temperatures allow for large population increases in bark beetles (Massey and Wygant 1954, Hansen et al. 2001, Bentz et al. 2010), in turn, overwhelming the defenses of their host species and increasing the frequency and severity of mortality events (Schmid 1981, Paine et al. 1997, Hebertson and Jenkins 2008). The significant reduction in canopy cover following these mortality events

connects the once buffered microclimate for regenerating plants to the macroclimate (De Frenne et al. 2013, Frey et al. 2016). As a result, disturbance may trigger potentially abrupt shifts in the distribution of tree species (Scheller and Mladenoff 2005, Turner 2010, Johnstone et al. 2016).

The continued success of forested systems in the face of climate-mediated disturbances depends on the patterns of future regeneration. The main biotic factors that influence seedling establishment and recruitment are seed source and competition/facilitation (Shainsky and Radosevich 1992, Baumeister and Callaway 2006, Loudermilk et al. 2016). Following an epidemic bark beetle outbreak where mature, large diameter trees are killed, there is a marked decline in seed production yet an increase in available resources. The mortality of overstory trees opens up growing space in the system for competing species in the understory to capitalize on and potentially outcompete future host regeneration (Veblen et al. 1991, DeRose and Long 2007, 2010, Dodson et al. 2014, Temperli et al. 2015).

The abiotic factors influencing regeneration include light, temperature, soil moisture, and substrate (Gray and Spies 1996). The removal of closed, continuous canopies affects abiotic factors through the elimination of the macroclimate buffering mechanism (Carlson and Groot 1997, Gray et al. 2002, Lazarus et al. 2018). Depending on gap size and position, openings in the once continuous canopy result in variable increases in solar radiation to the understory which in turn increases soil temperature extremes (Carlson and Groot 1997, Raymond et al. 2006). In addition to the loss of aboveground biomass during an epidemic outbreak, reduction in belowground biomass and associated competition for soil water in gaps may result in higher levels of soil

moisture (Gray et al. 2002, Burton et al. 2014a). Soil moisture in gaps is greater than in the continuous forest, in part due to increases in precipitation reaching the soil, as well as decreased transpiration of that moisture (Gray et al. 2002, Ritter et al. 2005). Moreover, snowpack can be higher in canopy gaps (Hardy et al. 1997) but may sublimate sooner due to increased solar radiation and wind speeds (Biederman et al. 2012, Pugh and Gordon 2013). Together, these changes in the microclimate can have significant impacts on the spatial pattern of seedling regeneration (Raymond et al. 2006).

The importance of facilitation might increase following an epidemic bark beetle outbreak as a result of changes in the microclimate (e.g., increases in the soil air temperature). Facilitation is an important driving factor in plant community structure and can coexist with competition for resources (Callaway 1995, Callaway and Walker 1997). The relative importance of the two processes can depend on the level of stress the environment holds (Bertness and Callaway 1994). On a landscape with epidemic bark beetle outbreaks, regeneration could be mediated by interspecific interactions following changes in the microclimate. As a result, we might expect to find more clumping of seedlings and saplings at sites with more extreme climatic conditions near upper and lower range limits (Callaway et al. 2002). However, if competition for resources is the limiting factor (middle elevations), the spatial arrangement of regeneration may be relatively uniform.

Here we investigate the effects of a climate mediated epidemic bark beetle disturbance in an Engelmann spruce (*Picea engelmannii*) ecosystem. Engelmann spruce do not maintain a long-lived seed bank due to seed depredation and loss of seed viability, but instead rely on variable annual seed crops for regeneration (Johnson and Fryer 1996,

Greene et al. 1999). The main coniferous competitor of Engelmann spruce is subalpine fir (*Abies lasiocarpa*). These two species can co-dominate subalpine ecosystems throughout the western United States. Although Engelmann spruce is longer lived, and comes to dominate the canopy, the mid- and understory typically include an abundance of subalpine fir that has the potential to reduce suitable habitat for future Engelmann spruce cohorts (Knapp and Smith 1982). Due to their slow development of a long taproot, Engelmann spruce seedlings are sensitive to changes in soil moisture (Lazarus et al. 2018), and they have smaller seeds that germinate faster and at lower temperatures compared to other competitors (Noble and Alexander 1977). Substrate type is therefore considered an important factor that can mediate the effects of soil moisture/drought stress as indicated by the high levels of survival of *Picea (spp.)* seedlings on CWD (Macek et al. 2017), which holds moisture longer than soils with a thick litter layer (Knapp and Smith 1982). However, because significant seed production by Engelmann spruce does not begin until individuals are large (Alexander and Shepperd 1984), regeneration following an epidemic outbreak could be limited.

Our objectives were to identify how: 1) the factors influencing Engelmann spruce seedling density, and 2) their facilitation with snags, other seedlings, and/or CWD vary based on timing of establishment (i.e., pre- or during/post-outbreak regeneration). For the first objective, we expected the distribution of post-outbreak seedlings to be more sensitive to climatic factors than pre-outbreak seedlings with less regeneration occurring on more stressful sites (e.g. high climatic moisture deficit; CMD). However, at these more stressful sites, we expected to find a substantial effect of facilitation on post-outbreak seedling establishment (Obj. 2). Specifically, we expected post-outbreak

seedlings to be clustered around Engelmann spruce snags, and more prevalent on the north side of down logs; an area that could act as a replacement of the buffering effect that the canopy once exerted.

METHODS

Study area

The Markagunt Plateau is located in the Dixie National Forest in southwestern Utah (Fig. 3-1). Part of the Colorado Plateau, this high elevation area experienced an epidemic spruce beetle outbreak in the 1990s with 90% mortality of mature Engelmann spruce across the landscape (DeRose and Long 2007). Prior to the outbreak, forests ranging from about 2700-3400 m asl were dominated by Engelmann spruce with common associates of subalpine fir, aspen (*Populus tremuloides*), Douglas-fir (*Pseudotsuga menziesii*), and limber pine (*Pinus flexilis*). The Markagunt Plateau is near the southern end of the species distributional range of Engelmann spruce: an area where future projections indicate the loss of suitable habitat for the species based on bioclimatic envelopes (Rehfeldt et al. 2006; Fig. 3-1 inset map). Climate on the Markagunt Plateau is characterized as Humid Continental (Gillies and Ramsey 2009) with mean summer (JJA) temperatures ranging from 8.5 to 14.8 °C and winters (DJF) from -3.0 to -8.0 °C from 1986-2016 across all study sites (Wang et al. 2016). Average annual precipitation on the plateau across all study sites from 1986-2016 was 760 mm with an average of 54% falling as snow (Wang et al. 2016). Precipitation on the plateau is bimodal with monsoonal rain from the southwest in the summer and snowfall from the Pacific in the winter (Mock 1996). Climatic moisture deficit (CMD), defined as potential

evapotranspiration minus precipitation ranges from 179 mm to 416 mm across our sites (Wang et al. 2016).

Data collection

We collected vegetation data from sixteen plots following the design of the Forest Inventory and Analysis (FIA; Field manual USDA Forest Service 2016) in once Engelmann spruce-dominated stands (either live or dead) across an elevation gradient of 2708 to 3307 m that corresponded to a gradient in CMD of 179 to 416 mm (Table B-1). Each plot consisted of four, circular subplots (168 m², 7.31 m radius) where all trees (≥12.7 cm diameter at breast height, DBH) were measured for species, status, DBH, and height, and mapped to the subplot center.

In addition to the FIA protocol, we measured and mapped Engelmann spruce seedlings (<2.54 cm DBH) across the subplot. We recorded height and basal diameter of each seedling and estimated age to the decade by counting bud scars (Niklasson 2002, Zielonka 2006, Bace et al. 2011). We also recorded the substrate type the seedling was on based on four major groups (duff, log, mineral soil, rock). An additional microplot (13.5 m², 2.07 m radius) was established around each seedling, where we mapped and measured all saplings, CWD, and any trees that fell outside of the subplot, as well as tallied all seedlings by species. Decay classes were recorded for each log following FIA protocol (USDA Forest Service 2016), and percent cover by vegetation, early stage decay wood, and late stage decay wood was estimated (percent categories: 0, 1, 5, 15, 25, 50, 75, 85, 95, 99, 100).

To quantify microclimate variability among plots, we measured temperature and volumetric soil water content (SWC) using Thermochron iButtons and a FieldScout portable time domain reflectometer (TDR), respectively. iButtons were deployed in the center of each subplot 30 cm above the ground on a PVC pipe using reflective tape and insulation, and were left on site for three months (July-Sept). SWC was measured in nine places in each subplot (in the subplot center and 4 m away in the cardinal and intercardinal directions) and repeated every month for three months (July-Sept).

Six additional plots were added at the sites with the most extreme environments (highest and lowest CMD, 22 plots total; Fig. 3-1) at least 50 m away from the original plot at that location. In addition to the FIA protocol, mapped Engelmann spruce seedling data (no micro-climate data) were collected on these sites. They were used to increase the sample depth for the spatial analysis (for complete field methods see Appendix E).

Soil moisture and microclimate

In many forests of the Western U.S., soil water content typically declines over the course of the growing season as water accumulated during winter is depleted by transpiring vegetation without being replenished by precipitation and/or snowmelt (e.g., Gray and Spies 1996). However, in the southwestern US, summer precipitation in the form of monsoon rains make this pattern less predictable. Additionally, SWC can vary spatially with gap size, within gap position, and substrate type (Gray et al. 2002, Raymond et al. 2006, Burton et al. 2014a). To account for spatio-temporal trends in SWC, we created a model of SWC with site, Julian day, time since last rain, and time of day as predictors (Fig. F-1). We then characterized site-to-site variation in SWC with

model estimates at each site at the beginning and end of the measurement period when differences across sites were the largest (day 187 and day 265; Fig. F-1).

From the iButton temperature data, we calculated climatic moisture deficit (CMD), by subtracting precipitation from potential evapotranspiration, for July, August and September for each subplot (Fig. B-2). Potential evapotranspiration was estimated following the Hargreaves method (Yates and Strzepek 1994). Downscaled monthly radiation and precipitation values were obtained from ClimateWNA for each plot center (Wang et al. 2016).

Models of seedling density

We developed models of Engelmann spruce regeneration density (seedlings and saplings) in five steps accounting for a hierarchy of controls (Table 3-1; Burton et al. 2014b). In the first step, we assessed alternative models of fine scale abiotic variables (1a) including the microclimate conditions of each subplot, followed by the subplot average of biotic measurements (1b) recorded in the 2.07 m radius plots around each seedling (Table 3-1). In step two, we expanded the scope to include understory (2a) and overstory (2b) plot-level metrics characterizing forest structure (Table 3-1). Finally, we included landscape-level variables (3) accounting for the impact of the macroclimate (Table 3-1). In each step, we included all possible biological interactions within that level. We then selected the best model based on Akaike information criterion (AIC) from each step before proceeding to the next step where alternative models with additional variables and interactions were added to the model selected in the previous step (Burnham and Anderson 2002). Interactions across levels were only tested if the main

effect from the previous step was already present in the best-selected model. Since we treated each 7.31 m radius subplot as its own sampling unit (n=88), we also tested for the significance of the random effect of site due to our nested study design by comparing AIC from models with and without the random effect (holding all fixed effects constant). Seedlings were retrospectively divided into two categories based on age estimations at a decadal resolution: pre-outbreak (established prior to 1987) and during/post-outbreak (established 1987-2017). Saplings (>2.54 cm and <12.7 cm DBH) were assumed to have originated prior to the outbreak. We developed models for 1) total Engelmann spruce seedling and sapling density (Table C-1), 2) the density of Engelmann spruce seedlings and saplings that established prior to the beetle outbreak (Table C-2), and 3) the density of Engelmann spruce seedlings that established during or after the beetle outbreak (Table C-3). For all three models we used a negative binomial generalized linear model due to detected overdispersion when fitting a Poisson distribution model.

Spatial analysis

The importance of facilitation can be indicated by spatial clumping of individual seedlings and spatial associations between individual seedlings and biological legacies such as snags. Snags, if killed in the outbreak, could have functioned as competitors for pre-outbreak seedlings, whereas for post-outbreak seedlings they can moderate the harsh microclimate following the death of the live canopy. To examine where seedlings were spatially random, clustered, or uniform, we analyzed univariate and bivariate versions of the pair correlation function, *g(r)*, on the point patterns of seedlings and Engelmann spruce trees at all sites together and divided into three CMD categories: High (304-418

mm), Moderate (243-275 mm), and Low (179-205 mm) to test for differences between categories. The pair correlation function computes the average number of points lying within a certain distance (r) of each data point compared to a null model of complete spatial randomness, where $g(r) = 1$ (Baddeley et al. 2016). Values larger than one indicate more points at that distance than random (i.e., clumped), and values less than one indicate a more uniform distribution. The pair correlation function is similar to Ripley's K but distinguishes between specific interpoint distances instead of computing a cumulative average, making it a more robust analysis especially at close distances (Wiegand and Moloney 2004, Perry et al. 2006, Law et al. 2009, Wild et al. 2014).

We first analyzed the univariate version of the pair correlation function to determine the relationships of seedlings and of Engelmann spruce snags separately. To compare the spatial relationship of seedlings to Engelmann spruce snags, we used a bivariate version of the pair correlation function. Both univariate and bivariate point pattern analyses were analyzed using the spatstat package (Baddeley and Turner 2005) in *R* (R Core Team 2016) with confidence envelopes based on 99 simulations of complete spatial randomness (Appendix D). Because of the small area encompassed by each FIA subplot and due to their stratified random sampling design, all four subplots at one site were combined into one larger plot by truncating the edges of each circular plot and combining the four, smaller, square plots into one larger plot 20.85 m x 20.85 m (Woodall and Graham 2004). Seedlings established pre- and post-outbreak were modeled together and also independently to test for differences associated with the outbreak. Bivariate and univariate pair correlation analyses were pooled for all sites and for sites by CMD categories. Pooling allows for comparison of replicated spatial point patterns

created as a result of the same spatial process. It takes the weighted average of each

individual analysis and accounts for within group variation by calculating confidence

intervals (Baddeley et al. 2016).

Direction from coarse woody debris

To assess the directional relationship of seedlings from down logs, we created

circular histograms (rose diagrams) matching the cardinal directions. We made separate

rose diagrams for all seedlings together, as well as pre-outbreak and post-outbreak

seedlings individually. For each diagram, the data were subdivided to only include

seedlings on subplots with a slope ≥10%. Additionally, only logs that would have been

down before the seedling established, as indicated by decay class and age of individual

seedlings, were included.

RESULTS

A total of 505 Engelmann spruce seedlings and saplings were documented across

all 16 plots; 302 from before the outbreak and 203 during/after the outbreak (60% and

40%, respectively; Table 3-2). The greatest number of spruce seedlings (144 seedlings)

was found on the SNO site and the least at SPC (3 seedlings; Table 3-2). Most seedlings

were found growing on mineral soil, however, when dividing by regeneration timing, a

large proportion of post-outbreak seedlings were found on downed logs compared to pre-

outbreak (Table 3-2).

The final model of all spruce regeneration density (explained deviance, D-squared

= 49%; Fig. 3-2, Table 3-3) included basal area of snags (Fig. 3-2b) as well as SWC on

Julian day 265 (September 22nd), percent understory cover, and their two-way interaction (Fig. 3-2a) as fixed effects (Table 3-3). Regeneration density was positively related to SWC at high percent understory cover (90%), but negatively related to SWC at low percent understory cover (5%; Fig. 3-2a). The model of pre-outbreak seedling density (D-squared = 52%, Fig. 3-3, Table 3-3) indicated a negative relationship of seedling density to basal area of snags (Fig. 3-3a), and percent cover by early stage decay CWD (Fig. 3-3b), and a positive relationship to percent understory cover (Fig. 3-3c), and SWC on Julian day 265 (September 22nd; Fig. 3-3d). The model of post-outbreak regeneration (D-squared = 27%; Fig. 3-4) indicated a positive relationship of seedling density to microclimate CMD (Fig. 3-4a), percent cover by late stage decay CWD (Fig. 3-4b), and SWC on Julian day 187 (July 6th; Fig. 3-4c).

The univariate *g(r)* for all seedlings indicated clumping was most pronounced at high and low CMD (Fig. 3-5). The bivariate *g(r)* for all seedlings indicated uniformity at close distances, mainly driven by the pre-outbreak seedlings (Figs. 3-6a and 3-6b). The pre-outbreak seedlings had a uniform arrangement from Engelmann spruce trees at close distances (<3 m) with clumping at larger distances (3-4 m; Fig. 3-6b). Post-outbreak seedlings were randomly spaced from Engelmann spruce trees at all distances (Fig. 3-6c). When the bivariate relationship of post-outbreak seedlings to Engelmann spruce trees was grouped by CMD, there was a uniform arrangement at high and mid CMD sites, but random at low CMD sites (Fig. 3-7a). The bivariate relationship between post-outbreak seedlings and pre-outbreak seedlings indicated clumping at low CMD sites (Fig. 3-7b).

The rose diagrams for pre- and post-outbreak seedlings in relation to CWD indicate pre-outbreak seedlings distributed on all sides of down logs, with a slight peak

on the NE side, whereas post-outbreak seedlings were found predominately on the SW side (Fig. 3-8).

DISCUSSION

We detected a strong shift in the patterns of Engelmann spruce regeneration based on timing (pre versus post) of establishment using multiple lines of evidence. Pre-outbreak regeneration was largely influenced by historical competition with Engelmann spruce as indicated by their negative relationship to snag basal area and early stage decay CWD (Figs. 3-3c and 3-3d), and their spatial dispersion from snags (Fig. 3-6b). In contrast, post-outbreak seedlings were more sensitive to current climatic conditions; positively responding to where it was warmer and sunnier, as indicated by our density models (Figs. 3-4a and 3-4b), spatial analysis (Fig. 3-6c), and their relationship with CWD (Fig. 3-8b). The importance of warmer, sunnier conditions and the increase in the number of post-outbreak seedlings at lower elevations suggests that their lower range limit is more influenced by competition and/or the historic fire frequency than drought stress.

Pre-outbreak regeneration was most likely limited by historical competition. When these seedlings established, sites that had more standing live trees, particularly Engelmann spruce, now have less surviving regeneration (Fig. 3-3). Additionally, the distribution of pre-outbreak saplings and seedlings was likely controlled more by competition with extant Engelmann spruce, rather than being facilitated by Engelmann spruce snags (Fig. 3-6b). This is consistent with the spatial patterns expected for trees of the same cohort driven by density-dependent mortality in other Picea spp. (e.g., Svoboda

et al. 2010). The only climatic factor that was important for prediction of pre-outbreak seedling density was late September soil moisture, which marks the precipitation transition from rain to snow on the Markagunt Plateau (Fig. B-1), consistent with the findings of other studies (e.g., Andrus et al. 2018).

Alternatively, post-outbreak seedlings were more limited by microsite climatic factors. Contrary to expectations, post-outbreak regeneration was surprisingly not limited by high CMD (Fig. 3-4b). Instead, the sites with high CMD that were less favorable to pre-outbreak regeneration had a greater number of post-outbreak seedlings. This finding was surprising given the sensitivity of Engelmann spruce seedlings to drought (Knapp and Smith 1982, Lazarus et al. 2018). To help compensate for this drought sensitivity, establishment of seedlings on late-stage decay CWD is a well-documented strategy given the increased water holding capacity of decayed logs (Knapp and Smith 1982, Zielonka 2006, Macek et al. 2017) which is consistent with the increased use of CWD as a substrate for post-outbreak seedlings (Table 3-2). Together, this suggests that these high CMD sites contained enough water for seedlings to establish either through higher soil moisture levels (our model controlled for variation in %SWC) and/or establishment on CWD. Perhaps the reason these sites have a higher moisture deficit is not due to a complete lack of soil moisture, but instead to an abundance of potential evapotranspiration (or solar radiation) which created these more productive sites that promoted Engelmann spruce seedling establishment. However, it is important to note that while the post-outbreak seedling model suggests high CMD had a positive effect on seedling density, the explained deviance was relatively low and we ultimately recorded the highest density of post-outbreak seedlings on a low CMD site (SNO; Table 3-2).

The relationship of post-outbreak seedlings to the structure provided by CWD is also suggestive of their success in warmer, sunnier microsites. Post-outbreak seedlings were consistently found on the SW side of down logs on relatively steep slopes (Fig. 3-8). The north side of down logs on our predominately north facing slopes provide shade, and wetter micro-environments for regeneration. Given the significant disturbance and loss of the canopy, it was then surprising that post-outbreak seedlings were not regenerating on the north side of down logs to offset the high solar radiation and temperature fluctuations in gaps (Carlson and Groot 1997, Raymond et al. 2006). Instead, their presence on the sunnier, warmer SW side is consistent with our density model results, suggestive of the benefit derived from more productive microsites given adequate soil moisture.

Additionally, the spatial arrangement of post-outbreak seedlings supports the suitable habitat found at high CMD sites. Although seedlings were found in clusters around themselves (Fig. 3-5)—suggestive of microsite limitations across sites—contrary to expectations, these clusters of post-outbreak seedlings were not found around Engelmann spruce snags (Figs. 3-6c and 3-7a). The lack of facilitation, especially at the high CMD sites suggests that these sites already have a favorable microclimate for seedlings, consistent with our density model. Our results, in stands consisting of two to four species, appear to contradict other studies conducted in monospecific stands of Norway spruce (*Picea abies*) in central Europe, where spruce seedlings were found tightly clustered around canopy trees (Bace et al. 2011, Wild et al. 2014). Perhaps this difference in the clustering behavior of seedlings is because on our sites subalpine fir seedlings formed tight clusters around Engelmann spruce snags and thereby outcompeted

Engelmann spruce seedlings for that specific growing space (Fig. B-3; DeRose and Long 2010).

The increased presence of post-outbreak seedlings in warmer, sunnier conditions (high CMD sites, SW side of down logs, no facilitation at high CMD) could indicate their success on more productive microsites. Conversely, when taken with the shift in timing of importance of soil moisture (Table 3-3), post-outbreak seedlings could also be avoiding colder microsites, specifically through the avoidance of excessive snowpack (e.g., Peterson and Peterson 2001). The lack of importance of early fall soil moisture, which marks the beginning of the transition to snow (Fig. B-1), for post-outbreak seedlings suggests that the increased snowpack in gaps formed during the outbreak does not contribute to seedling survival, as it once did before the mortality associated with the beetle outbreak (e.g., Andrus et al. 2018). The mechanism for facilitation by snags in central Europe is the earlier snowmelt found around tree wells (Pomeroy et al. 2009) that traps seeds and allows for subsequent regeneration (Wild et al. 2014). On the landscape scale, the higher density of seedlings on high CMD sites could be due to the earlier snow melt in these low elevation areas. At small scales, this facilitation could also be afforded by the abundant CWD, where establishment of seedlings on the SW side of down logs is driven by an avoidance of the snowpack on their north side. Additionally, on high elevation, low CMD sites where snowpack would be deepest and persist longest, we found post-outbreak seedlings clustered around pre-outbreak seedlings suggestive of the importance of advance regeneration that may be providing the same snow buffering properties as snags in other systems or as canopy trees were before the outbreak.

Our study analyzes the current density of Engelmann spruce regeneration, and therefore, has life-history stage limitations. Without the presence of a large disturbance, pre-outbreak seedlings could be an indicator of where future post-outbreak seedlings may be expected to survive, and the difference in factors driving density patterns between the two groups could indicate how factors change throughout the development of seedlings. However, because of the impact of the beetle outbreak, we do not expect pre-outbreak seedlings to be an indicator of future post-outbreak seedlings due to the differences in habitat during establishment. Our study instead suggests that there are differences in seedling establishment created by an epidemic beetle outbreak. However, further research is needed to expand on our findings for the future recruitment and success of these seedlings. We measured current seedling density across all sites and the characteristics that account for their distribution. The continued presence of Engelmann spruce in this ecosystem depends on the future survival and growth of these seedlings to reproductive maturity. Although other studies suggest increased survival of post-outbreak seedlings on CWD (e.g., Macek et al. 2017), we do not know which of our sites/individuals will see continued success in the future.

Because previous research has predicted that Engelmann spruce in ecosystems similar to the Markagunt Plateau may be at risk of extirpation based on climate predictions (Rehfeldt et al. 2006), our research showing spruce establishment across a range of environmental conditions is of great management concern. Given the lack of resistance that mature Engelmann spruce stands have to epidemic beetle outbreaks, management practices should be focused on creating resilience in terms of promoting the future regeneration (i.e., through silvicultural treatments; Windmuller-Campione and

Long 2015, Windmuller-Campione et al. 2017). Due to the widespread presence of

spruce regeneration across our study sites, it appears that even though this system was not

resistant to an epidemic outbreak it does appear to have been more resilient to the last

outbreak than we originally predicted, at least in the 20 years immediately following the

disturbance.

LITERATURE CITED

Alexander, R. R., and W. D. Shepperd. 1984. Silvicultural characteristics of Engelmann

    spruce. Rocky Mountain Research Station Publications 4:412-417.

Andrus, R. A., B. J. Harvey, K. C. Rodman, S. J. Hart, and T. T. Veblen. 2018. Moisture

    availability limits subalpine tree establishment. Ecology 99:567-575.

Bace, R., M. Svoboda, and P. Janda. 2011. Density and height structure of seedlings in

    subalpine spruce forests of central Europe: logs vs. stumps as a favourable

    substrate. Silva Fennica 45:1065-1078.

Baddeley, A., and R. Turner. 2005. Spatstat: an R package for analyzing spatial point

    patterns. Journal of statistical software 12:1-42.

Baddeley, A., E. Rubak, and R. Turner. 2016. Spatial point patterns: methodology and

    applications with R. Boca Ranton, FL: CRC Press.

Baumeister, D., and R. M. Callaway. 2006. Facilitation by *Pinus flexilis* during

    succession: a hierarchy of mechanisms benefits other plant species. Ecology

    87:1816-1830.

Bentz, B. J., J. Régnière, C. J. Fettig, M. Hansen, J. L. Hayes, J. A. Hicke, R. G. Kelsey,

    J. F. Negrón, and S. J. Seybold. 2010. Climate change and bark beetles of the

western United States and Canada: direct and indirect effects. BioScience 60:602-613.

Bertness, M. D., and R. Callaway. 1994. Positive interactions in communities. Trends in Ecology & Evolution 9:187-191.

Biederman, J. A., P. D. Brooks, A. A. Harpold, D. J. Gochis, E. Gutmann, D. E. Reed, E. Pendall, and B. E. Ewers. 2012. Multiscale observations of snow accumulation and peak snowpack following widespread, insect-induced lodgepole pine mortality. Ecohydrology 7:150-162.

Burnham, K. P., and D. R. Anderson. 2002. Model selection and multimodel inference: a practical information-theoretic approach. Second. New York, NY: Springer Science + Business Media, LLC.

Burton, J. I., D. J. Mladenoff, J. A. Forrester, and M. K. Clayton. 2014a. Experimentally linking disturbance, resources and productivity to diversity in forest ground-layer plant communities. Edited by Frank Gilliam. Journal of Ecology 102:1634-1648.

Burton, J. I., L. M. Ganio, and K. J. Puettmann. 2014b. Multi-scale spatial controls of understory vegetation in Douglas-fir–western hemlock forests of western Oregon, USA. Ecosphere 5:1-34.

Callaway, R. M. 1995. Positive interactions among plants. Botanical Review 61:306-349.

Callaway, R. M., et al. 2002. Positive interactions among alpine plants increase with stress. Nature 417:844-848.

Callaway, R. M., and L. R. Walker. 1997. Competition and facilitation: a synthetic approach to interactions in plant communities. Ecology 78:1958-1965.

Carlson, D. W., and A. Groot. 1997. Microclimate of clear-cut, forest interior, and small openings in trembling aspen forest. Agricultural and Forest Meteorology 87:313-329.

Davis, M. B. 1986. Climatic instability, time, lags, and community disequilibrium. Edited by Jared M. Diamond and Ted J. Case. Community Ecology. New York: Harper and Row.

Davis, M. B., and R. G. Shaw. 2001. Range shifts and adaptive responses to Quaternary climate change. Science 292:673-679.

De Frenne, P., et al. 2013. Microclimate moderates plant responses to macroclimate warming. Proceedings of the National Academy of Sciences 110:18561-18565.

DeRose, R. J., and J. N. Long. 2007. Disturbance, structure, and composition: spruce beetle and Engelmann spruce forests on the Markagunt Plateau, Utah. Forest Ecology and Management 244:16-23.

DeRose, R. J., and J. N. Long. 2010. Regeneration response and seedling bank dynamics on a *Dendroctonus rufipennis*-killed *Picea engelmannii* landscape. Journal of Vegetation Science 21:377-387.

Dodson, E.K., J. I. Burton, and K. J. Puettmann. 2014. Multiscale controls on natural regeneration dynamics after partial overstory removal in Douglas-fir forests in western Oregon, USA. Forest Science 60:953-961.

Frey, S. J. K., A. S. Hadley, S. L. Johnson, M. Schulze, J. A. Jones, and M. G. Betts. 2016. Spatial models reveal the microclimatic buffering capacity of old-growth forests. Science Advances 2:1-9.

Gillies, R. R., and R. D. Ramsey. 2009. Climate of Utah. In Rangeland Resources of Utah, edited by R. E. Banner, B. D. Baldwin, and E. I. L. McGinty, 2nd ed.

Gray, A. N., and T. A. Spies. 1996. Gap size, within-gap position and canopy structure effects on conifer seedling establishment. Journal of Ecology 84:635-645.

Gray, A. N., T. A. Spies, and M. J. Easter. 2002. Microclimatic and soil moisture responses to gap formation in coastal Douglas-fir forests. Canadian Journal of Forest Research 32:332-343.

Greene, D. F., J. C. Zasada, L. Sirois, D. Kneeshaw, H. Morin, I. Charron, and M. J. Simard. 1999. A review of the regeneration dynamics of North American boreal forest tree species. Canadian Journal of Forest Research 29:824-839.

Hansen, E. M., B. J. Bentz, and D. L. Turner. 2001. Temperature-based model for predicting univoltine brood proportions in spruce beetle (Coleoptera : Scolytidae). Canadian Entomologist 133:827-841.

Hardy, J. P., R. E. Davis, R. Jordan, X. Li, C. Woodcock, W. Ni, and J. C. McKenzie. 1997. Snow ablation modeling at the stand scale in a boreal jack pine forest. Journal of Geophysical Research 102:29,397-29,405.

Hebertson, E. G., and M. J. Jenkins. 2008. Climate factors associated with historic spruce beetle (Coleoptera: Curculionidae) outbreaks in Utah and Colorado. Environmental Entomology 37:281-292.

HilleRisLambers, J., L. D. L. Anderegg, I. Breckheimer, K. M. Burns, A. K. Ettinger, J. F. Franklin, J. A. Freund, K. R. Ford, and S. J. Krolss. 2015. Implications of climate change for turnover in forest composition. Northwest Science 89:201-218.

Johnson, E. A., and G. I. Fryer. 1996. Why Engelmann spruce does not have a persistent seed bank. Canadian Journal of Forest Research 26:872-878.

Johnstone, J. F., C. D. Allen, J. F. Franklin, L. E. Frelich, B. J. Harvey, P. E. Higuera, M. C. Mack, R. K. Meentemeyer, M. R. Metz, G. L. W. Perry, T. Schoennagel, and M. G. Turner. 2016. Changing disturbance regimes, ecological memory, and forest resilience. Frontiers in Ecology and the Environment 14:369-378.

Knapp, A. K., and W. K. Smith. 1982. Factors influencing understory seedling establishment of Engelmann spruce (*Picea engelmannii*) and subalpine fir (*Abies lasiocarpa*) in southeast Wyoming. Canadian Journal of Botany 60:2753-2761.

Law, R., J. Illian, D. F. R. P. Burslem, G. Gratzer, C. V. S. Gunatilleke, and I. A. U. N. Gunatilleke. 2009. Ecological information from spatial patterns of plants: insights from point process theory. Journal of Ecology 97:616-628.

Lazarus, B. E., C. Castanha, M. J. Germino, L. M. Kueppers, and A. B. Moyes. 2018. Growth strategies and threshold responses to water deficit modulate effects of warming on tree seedlings from forest to alpine. Journal of Ecology 106: 571-585.

Lenoir, J., J. C. Gegout, P. A. Marquet, P. de Ruffray, and H. Brisse. 2008. A significant upward shift in plant species optimum elevation during the 20th century. Science 320:1768-1771.

Loudermilk, L. E., J. K. Hiers, S. Pokswinski, J. J. O'Brien, A. Barnett, and R. J. Mitchell. 2016. The path back: oaks (*Quercus* spp.) facilitate longleaf pine (*Pinus palustris*) seedling establishment in xeric sites. Ecosphere 7:1-14.

Macek, M., J. Wild, M. Kopeckỳ, J. Červenka, M. Svoboda, J. Zenáhlíková, J. Brŭna, R. Mosandl, and A. Fischer. 2017. Life and death of *Picea abies* after bark-beetle

outbreak: Ecological processes driving seedling recruitment. Ecological Applications 27:156-167.

Massey, C. L., and N. D. Wygant. 1954. Biology and control of the Engelmann spruce beetle in Colorado. USDA Forest Service, Circular no. 944, Washington DC.

Mock, C. J. 1996. Climatic controls and spatial variations of precipitation in the western United States. Journal of Climate 9:1111-1125.

Niklasson, M. 2002. A comparison of three age determination methods for suppressed Norway spruce: implications for age structure analysis. Forest Ecology and Management 161:279-288.

Noble, D. L., and R. R. Alexander. 1977. Environmental factors affecting natural regeneration of Engelmann spruce in the central Rocky Mountains. Forest Science 23:420-429.

Paine, T. D., K. F. Raffa, and T. C. Harrington. 1997. Interactions among scolytid bark beetles, their associated fungi, and live host conifers. Annual Review of Entomology 42:179-206.

Perry, G. L. W, B. P. Miller, and N. J. Enright. 2006. A comparison of methods for the statistical analysis of spatial point patterns in plant ecology. Plant Ecology 187:59-82.

Peterson, D. W., and D. L. Peterson. 2001. Mountain hemlock growth responds to climatic variability at annual and decadal time scales. Ecology 82: 3330-3345.

Pomeroy, J., D. Marks, and T. Link. 2009. The impact of coniferous forest temperature on incoming longwave radiation to melting snow. Hydrological Processes 23:2513-2525.

Pugh, E., and E. Gordon. 2013. A conceptual model of water yield effects from beetle-induced tree death in snow-dominated lodgepole pine forests. Hydrological Processes 27:2048-2060.

R Core Team. 2016. R: a language and environment for statistical computing. R Foundation for Statistical Computing, Vienna, Austria.

Raymond, P., A. D. Munsun, J.-C. Ruel, and K. D. Coates. 2006. Spatial patterns of soil microclimate, light, regeneration, and growth within silvicultural Gaps of mixed tolerant hardwood - white pine stands. Canadian Journal of Forest Research 36:639-651.

Rehfeldt, G. E., N. L. Crookston, M. V. Warwell, and J. S. Evans. 2006. Empirical analyses of plant-climate relationships for the western United States. International Journal of Plant Sciences 167:1123-1150.

Rehfeldt, G. E., C. C. Ying, D. L. Spittlehouse, and D. A. Hamilton. 1999. Genetic responses to climate in *Pinus contorta*: niche Breadth, Climate Change, and Reforestation. Ecological Monographs 69:375-407.

Ritter, E., L. Dalsgaard, and K. S. Einhorn. 2005. Light, temperature and soil moisture regimes following gap formation in a semi-natural beech-dominated forest in Denmark. Forest Ecology and Management 206:15-33.

Scheller, R. M., and D. J. Mladenoff. 2005. A spatially interactive simulation of climate change, harvesting, wind, and tree species migration and projected changes to forest composition and biomass in northern Wisconsin, USA. Global Change Biology 11:307-321.

Schmid, J. M. 1981. Spruce beetles in blowdown. USDA Forest Service, Rocky
    Mountain Forest and Range Experiment Station Research Note RM-411.

Shainsky, L. J., and S. R. Radosevich. 1992. Mechanisms of competition between
    Douglas-fir and red alder seedlings. Ecology 73:30-45.

Svoboda, M., S. Fraver, P. Janda, R. Bače, and J. Zenáhlíková. 2010. Natural
    development and regeneration of a central European montane spruce forest.
    Forest Ecology and Management 260:707-714.

Temperli, C., T. T. Veblen, S. J. Hart, D. Kulakowski, and A. J. Tepley. 2015.
    Interactions among spruce beetle disturbance, climate change and forest dynamics
    captured by a forest landscape model. Ecosphere 6:1-20.

Turner, M. G. 2010. Disturbance and landscape dynamics in a changing world. Ecology
    91:2833-2849.

USDA Forest Service. 2016. Forest inventory and analysis national core field guide.
    Volume I: Field Data Collection Procedures for Phase 2 Plots, Version 7.1.

Veblen, T. T., K. S. Hadley, M. S. Reid, and A. J. Rebertus. 1991. The response of
    subalpine forests to spruce beetle outbreak in Colorado. Ecology 72:213-231.

Wang, T., A. Hamann, D. Spittlehouse, and C. Carroll. 2016. Locally downscaled and
    spatially customizable climate data for historical and future periods for North
    America. PloS ONE 116.

Wiegand, T., and K. A. Moloney. 2004. Rings, circles, and null-models for point pattern
    analysis in ecology. Oikos 104:209-229.

Wild, J., M. Kopecký, M. Svoboda, J. Zenáhlíková, M. Edwards-Jonášová, and T.
    Herben. 2014. Spatial patterns with memory: Tree regeneration after stand-

replacing disturbance in *Picea abies* mountain forests. Journal of Vegetation
Science 25:1327-1340.

Windmuller-Campione, M., and J. Long. 2015. If long-term resistance to a spruce beetle
epidemic is futile, can silvicultural treatments increase resilience in spruce-fir
forests in the central Rocky Mountains? Forests 6:1157-1178.

Windmuller-Campione, M., D. H. Page, and J. Long. 2017. Does the practice of
silviculture build resilience to the spruce beetle? A case study of treated and
untreated spruce-fir stands in northern Utah. Journal of Forestry 115:559-567.

Woodall, C.W., and J.M. Graham. 2004. A technique for conducting point pattern
analysis of cluster plot stem-maps. Forest Ecology and Management 198:31-37.

Yates, D., and K. M. Strzepek. 1994. Potential evapotranspiration methods and their
impact on the assessment of river basin runoff under climate change. IIASA
Working Paper. IIASA, Laxenburg, Austria, WP-94-046.

Zielonka, T. 2006. When does dead wood turn into a substrate for spruce replacement?
Journal of Vegetation Science 17:739-746.

TABLES AND FIGURES

TABLE 3-1. Scale of characteristics measured at each site and used in the model selection process describing Engelmann spruce regeneration. Soil water content was modeled for Julian days 187 and 265 (SWC.187 and SWC.265, respectively). Fine scale biotic measurements were taken in a 2.07m microplot around Engelmann spruce seedlings. Microclimate CMD was calculated from iButton temperature data and macroclimate CMD was used from ClimateWNA for each site (Wang et al. 2016).

1. Fine		2. Plot		3. Landscape
a. Abiotic	b. Biotic	a. Understory	b. Overstory	
SWC.187	#ABLA seedlings	%understory cover	%canopy cover	Slope
SWC.265	%early-stage decay CWD	#ABLA saplings	QMD* of dead trees	Aspect
Microclimate CMD	%late-stage decay CWD		Min. tree height	Elevation
	%understory cover		BA** ABLA	Macroclimate CMD
			BA live PIEN	
			BA dead trees	

*QMD is quadratic mean diameter
**BA is basal area of live and dead trees

TABLE 3-2. Summary statistics on total number of seedlings and saplings, pre-outbreak seedlings and saplings, and during/post-outbreak seedlings per site. Proportion of seedlings on duff, down logs, mineral soil (m.soil), and rock also included. Bolded numbers indicate substrate with highest proportion of seedlings from the site.

				Substrate Type			
Site	Total	Pre	Post	duff	log	m.soil	rock
ASH	12	8	4	14.3	14.3	**71.4**	0
BHF	41	31	10	0	0	**100**	0
BPT	14	13	1	**75**	25	0	0
CEB	23	12	11	**57.1**	0	42.9	0
DCK	38	25	13	4.5	13.6	**68.2**	13.6
DCS	21	11	10	25	16.6	**58.3**	0
HCK	67	35	32	25	**48.1**	26.9	0
HPT	34	23	11	11.8	23.5	**64.7**	0
LC	9	1	8	22.2	0	**77.8**	0
MTH	28	10	18	27.3	4.5	**63.6**	4.5
NLS	9	2	7	25	**37.5**	**37.5**	0
RBW	22	19	3	**42.9**	28.6	28.6	0
SNO	144	98	46	29	11	**59**	1
SPC	3	2	1	0	0	**100**	0
TCC	13	6	7	0	28.6	**71.4**	0
TIP	27	6	21	19.2	30.8	**50**	0
TOTAL	*505*	*302*	*203*	*23.7*	*18.7*	***56.1***	*1.5*
Pre	*302*			*28.1*	*2.9*	***67.0***	*1.9*
Post	*203*			*19.7*	*30*	***49.8***	*0.5*

TABLE 3-3. Final models of seedling and sapling density by response variable (all seedlings and saplings, pre-outbreak seedlings and saplings, post-outbreak seedlings). Soil water content in September and July (SWC.265 & SWC.187), percent understory cover, percent cover by early stage decay coarse woody debris (CWD), percent cover by late stage decay CWD, snag basal area (BA.D), and microclimate climatic moisture deficit (CMD). For full model selection process see Appendix C.

Response Variable	Final Model	Explained Deviance
All seedlings & saplings	SWC.265 + %understory cover + BA.D + SWC.265*%understory cover	49%
Pre-outbreak seedlings & saplings	SWC.265 + %understory cover + BA.D + %Early stage decay CWD	52%
Post-outbreak seedlings	SWC.187 + Microclimate CMD + %Late stage decay CWD	27%
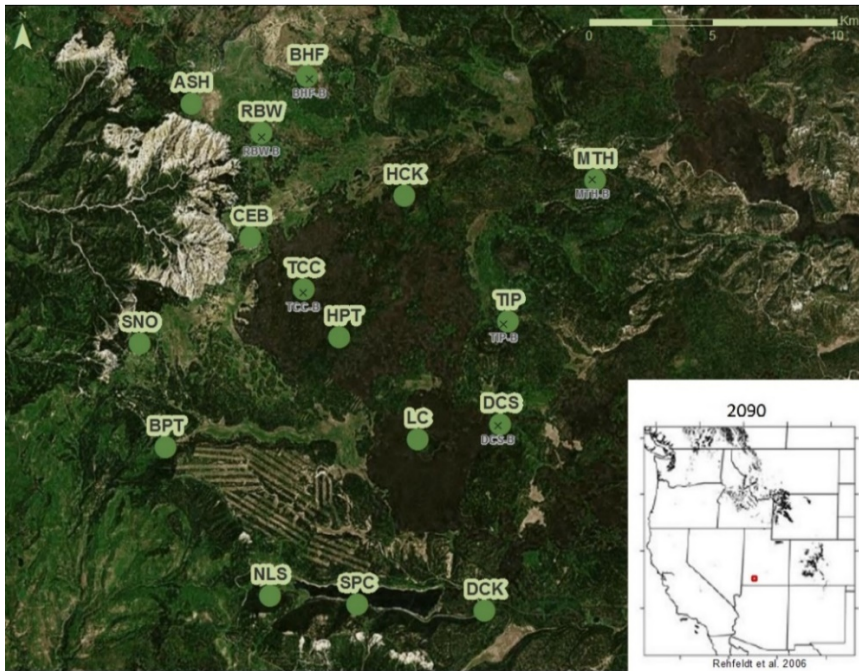
FIG. 3-1. Map of Engelmann spruce seedling regeneration study plots on the Markagunt Plateau in southern Utah. Each site consists of 4 subplots following FIA protocol (USDA Forest Service 2016). Inset map shows the forecasted range of Engelmann spruce in 2090 using climate models (Rehfeldt et al. 2006). Red box denotes extent of site map. Sites with an X mark where six plots were added for the point pattern analysis.
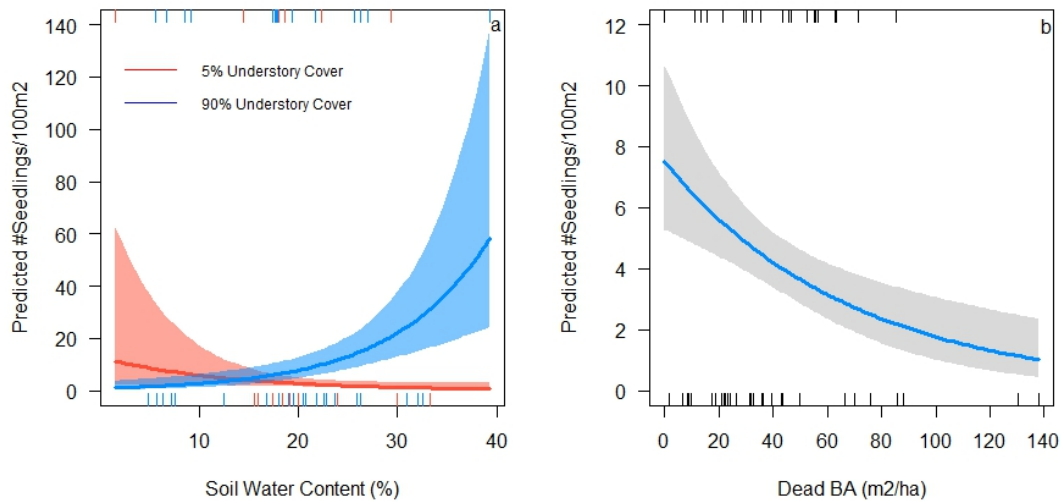
FIG. 3-2. Predicted number of all seedlings and saplings per 100 m2 by soil water content on Julian day 265 and percent understory cover around each seedling (a); basal area (BA) of snags (m2/ha; b). Note difference in y-axis scale.
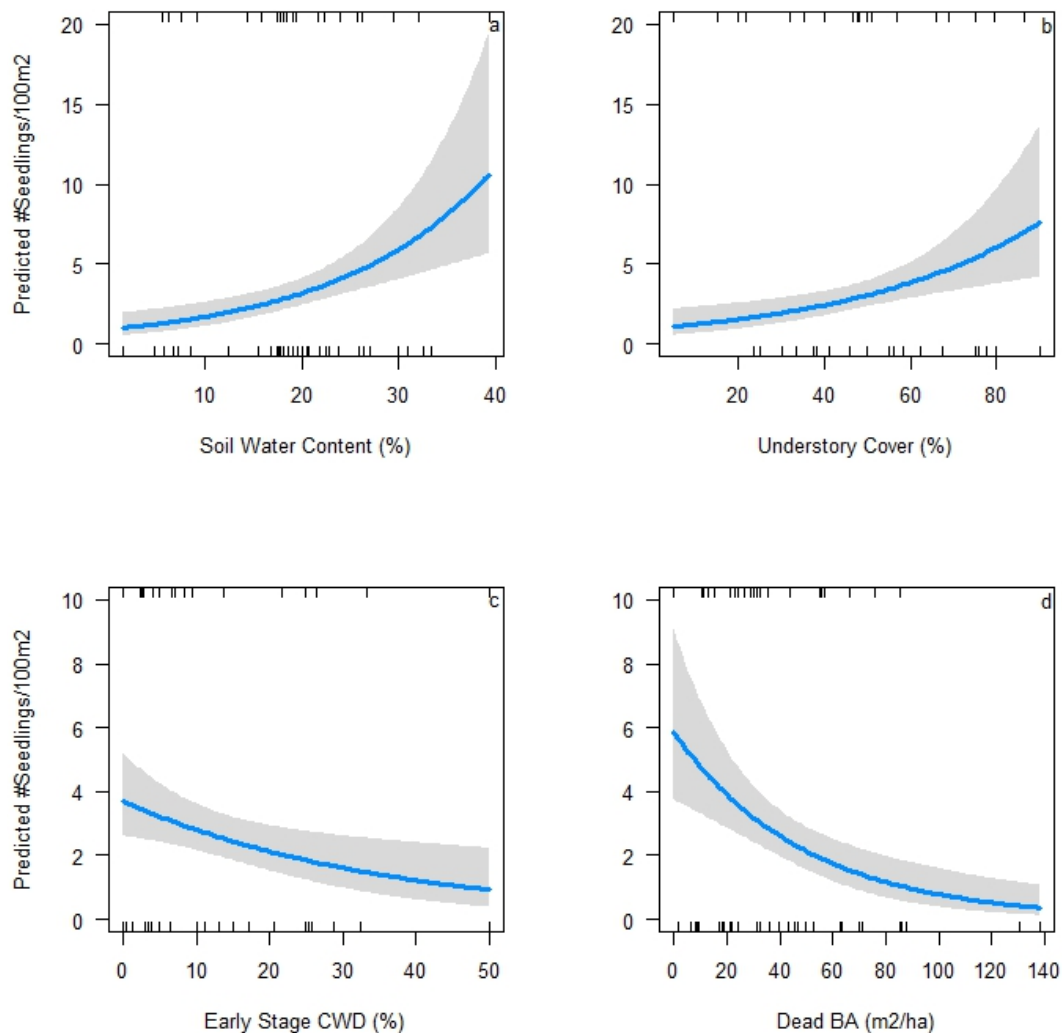
FIG. 3-3. Predicted number of pre-outbreak seedlings and saplings per 100 m2 by soil water content on Julian day 265 (a); percent understory cover around each seedling (b); percent early stage decay coarse woody debris (CWD; c); and basal area (BA) of snags (m2/ha; d). Note difference in y-axis scale from top row to bottom.
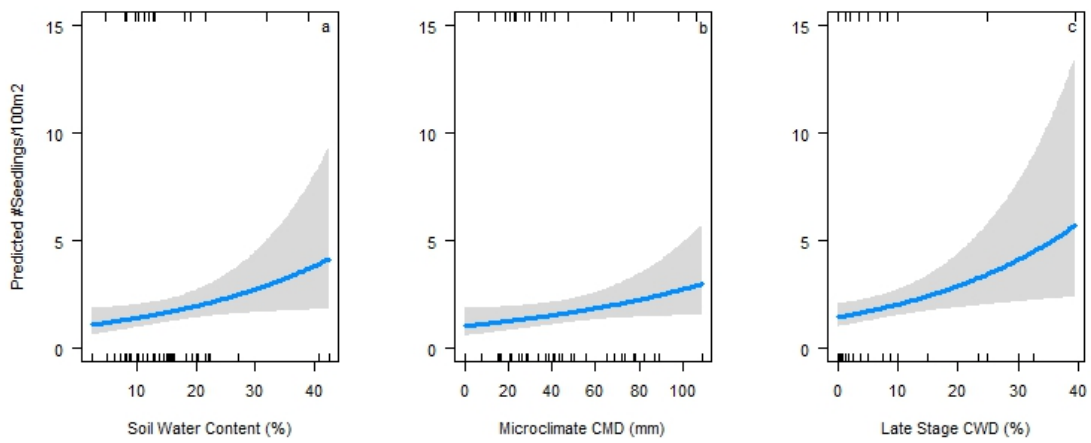
FIG. 3-4. Predicted number of during/post-outbreak seedlings per 100 m2 by soil water content on Julian day 187 (a); summer (July-September) microclimate climatic moisture deficit (b); and percent late stage decay coarse woody debris (CWD; c).
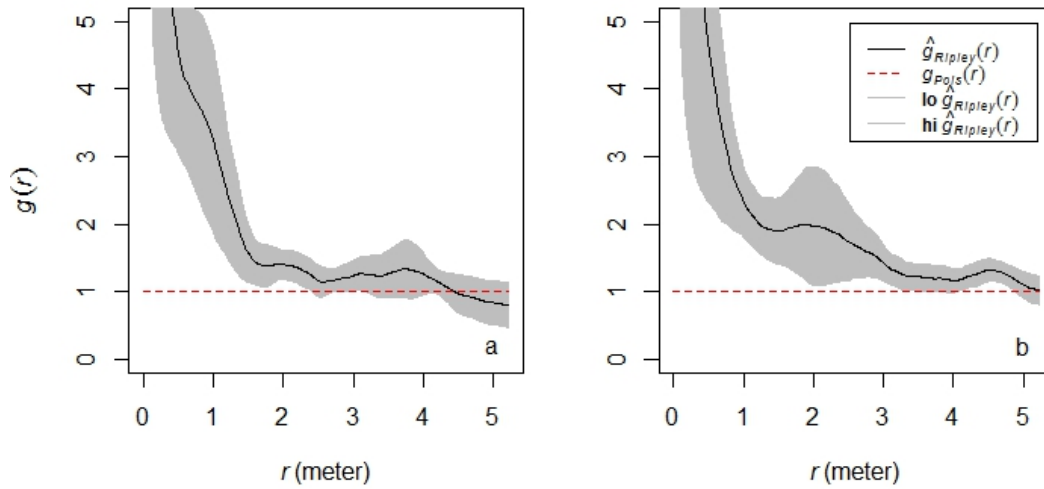
FIG. 3-5. Univariate point pattern analysis of pre-outbreak seedlings (a) and post-outbreak seedlings (b). Black solid line is the pooled isotropic-corrected estimate of g(r). Red dashed line represents the pooled theoretical Poisson g(r). Gray bands indicate the upper and lower limits of two-sigma CI based on isotropic-corrected estimate of g(r).
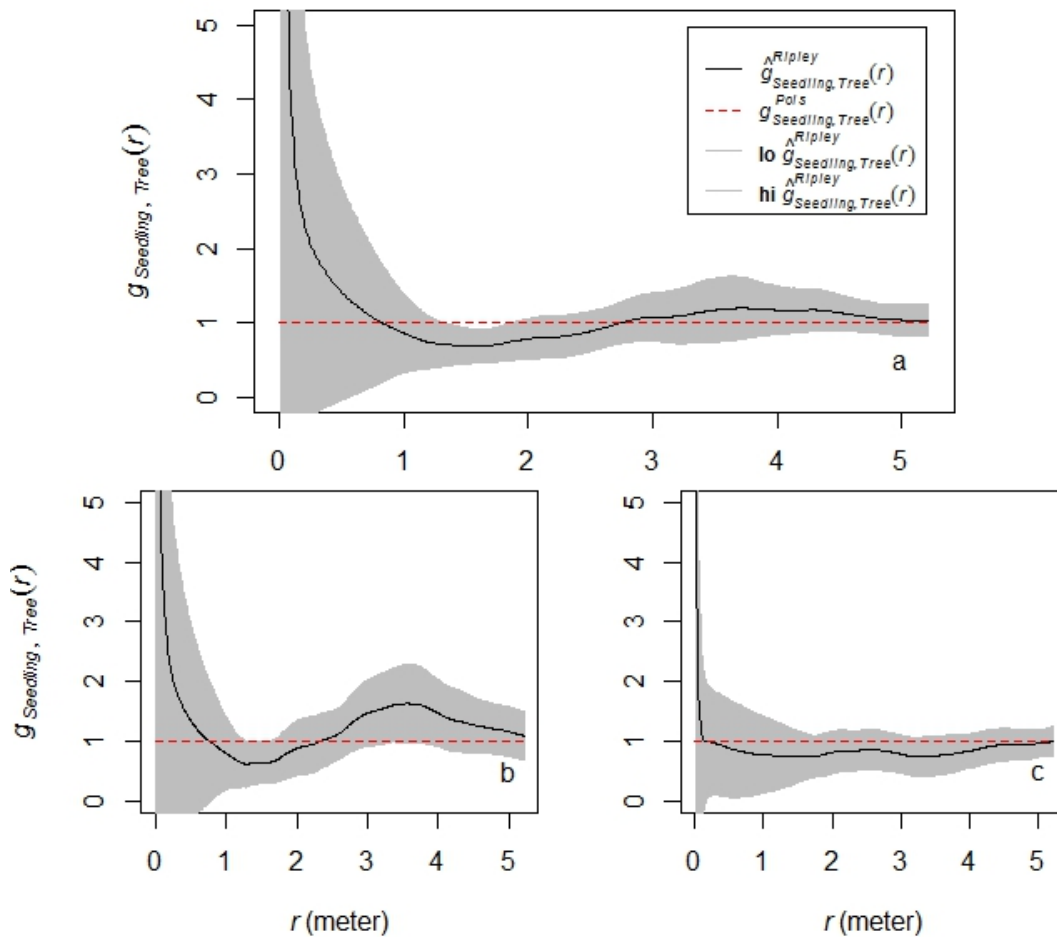
FIG. 3-6. Bivariate point pattern analysis for all (a), pre (b), and post outbreak (c) to Engelmann spruce trees. Black solid line is the bivariate (seedling, tree) pooled isotropic-corrected estimate of $g(r)$. Red dashed line represents the bivariate (seedling, tree) pooled theoretical Poisson $g(r)$. Gray bands indicate the bivariate (seedling, tree) upper and lower limits of two-sigma CI based on isotropic-corrected estimate of $g(r)$.
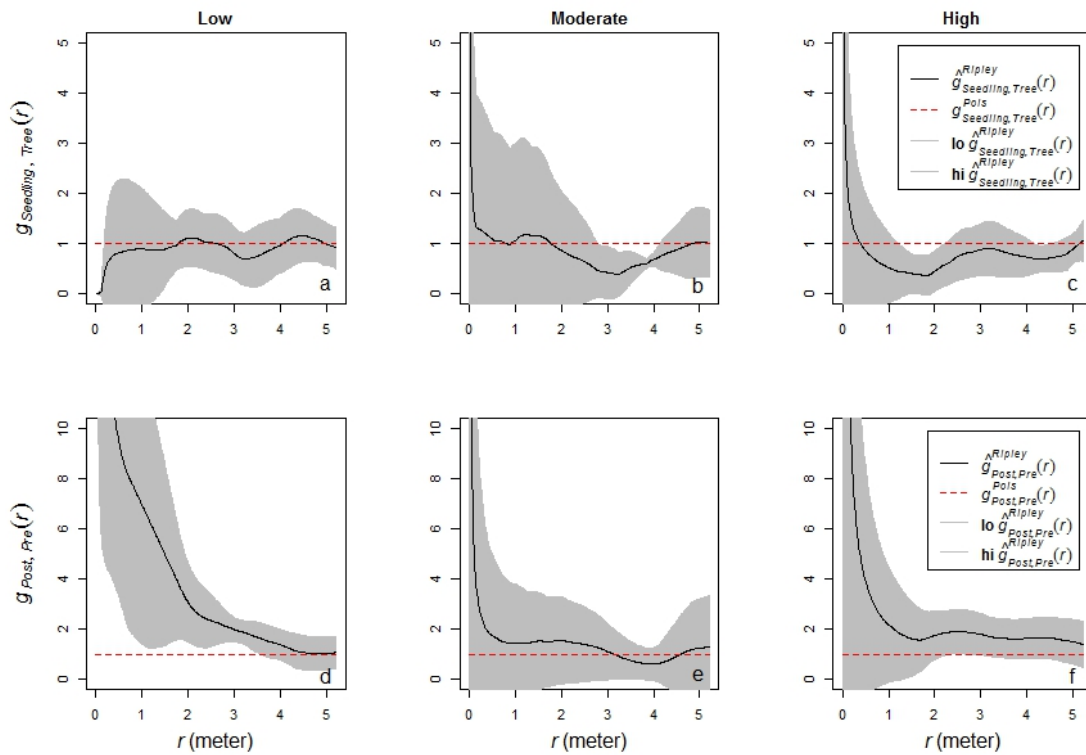
FIG. 3-7. Bivariate point pattern analysis for post-outbreak seedlings to Engelmann spruce snags (a-c) and post-outbreak to pre-outbreak seedlings (d-f). Spatial patterns are divided by categorical CMD values: Low: (179-205 mm; a & d), Moderate (243-275 mm; b & e), and High (304-418 mm; c & f). Black solid line is the bivariate (seedling, tree and pre, post-outbreak seedlings) pooled isotropic-corrected estimate of $g(r)$. Red dashed line represents the bivariate (seedling, tree and pre, post-outbreak seedlings) pooled theoretical Poisson $g(r)$. Gray bands indicate the bivariate (seedling, tree and pre, post-outbreak seedlings) upper and lower limits of two-sigma CI based on isotropic-corrected estimate of $g(r)$. Note the difference in y-axis scale from top row to bottom.
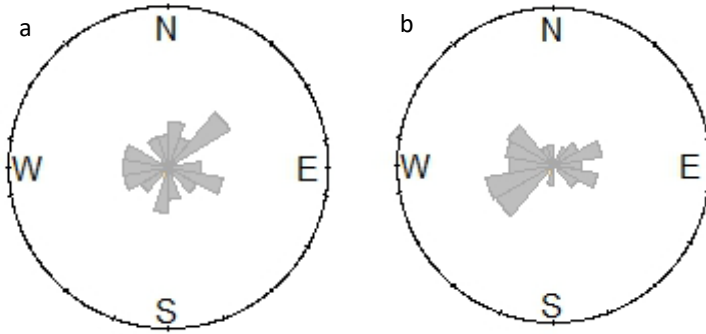
FIG. 3-8. Spatial histogram of pre-outbreak (a) versus post-outbreak (b) seedlings from closest piece of coarse woody debris (CWD) on slopes ≥10%.

CHAPTER 4

SUMMARY AND CONCLUSIONS

When disturbances interact with climate change, it can lead to new disturbance regimes outside the range of historical variability. These climate-mediated disturbances can result in new ecosystems and not return to the original steady-state system. The Markagunt Plateau experienced an epidemic spruce beetle outbreak in the 1990s during a prolonged drought. Our research dealt with two aspects of this climate-mediated disturbance: the mortality during the outbreak and the subsequent regeneration.

Warmer temperatures have been well-documented in amplifying beetle outbreaks through their direct effects on the beetle lifecycle. However, we were also interested in the effect that warmer temperatures, leading to droughts, has on host susceptibility. Specifically, we were interested in whether tree drought stress contributes to the shift from an endemic to epidemic level beetle outbreak. From our carbon isotope analysis, we found that large trees that died during endemic beetle populations were significantly more sensitive to drought than large trees that succumbed to death during epidemic population levels. The difference in drought sensitivity of these large trees helped transition an endemic level outbreak into an epidemic one, in addition to the direct effects on beetles. Smaller trees did not show as distinct of a difference in drought sensitivity. Small trees that died during endemic population levels were most likely growing in the shade, compared to small sun-grown trees that died during epidemic population levels. This difference in drought sensitivity mediated by tree size reflects the difference in stand structure during the landscape level progression of a beetle outbreak. Stands with an

abundance of large trees are generally attacked first during an outbreak and in these stands, host susceptibility played an important role. However, later in a landscape outbreak, stands with smaller trees would be attacked and drought sensitivity would become less important.

Given the high levels of mortality among mature Engelmann spruce on the Markagunt Plateau, we were also interested in the future recovery of the ecosystem in terms of its regeneration. Engelmann spruce do not maintain a long-lived seed bank, and thus the 95% mortality rate across the landscape has consequences for future establishment. We sampled Engelmann spruce seedlings and saplings across a climate gradient on the Plateau to identify where regeneration was occurring and if the patterns of regeneration had changed following the outbreak. We found that the density of regeneration that established prior to the outbreak was responding to historical competition with Engelmann spruce. The density of regeneration that established during and since the outbreak, however, was responding to microclimate factors. These seedlings were generally on lower elevation sites, perhaps in an avoidance of excessive snowpack or in favor of the higher productivity found there. Post-outbreak seedlings that did establish at high elevations were found clustered around pre-outbreak seedlings suggesting their reliance on facilitation in the form of earlier snowmelt around these older seedlings. Overall, there were limited Engelmann spruce seedlings, especially when compared to the abundance of other species (e.g. subalpine fir), and the persistence of seedlings at lower elevations suggests their lower range limit is not limited by drought stress but perhaps by competition instead.

This climate-mediated disturbance on the Markagunt Plateau has not only affected the progression of the beetle outbreak, but also the subsequent regeneration. Increased host susceptibility through drought stress aided in the transition from the endemic level outbreak to a massive epidemic outbreak with 95% mortality among mature Engelmann spruce. Regeneration following the outbreak seems to be found in areas with less snowpack and higher productivity compared to regeneration before the outbreak. Despite the limited spruce regeneration, this system does appear to have been more resilient to the last outbreak than we originally predicted, at least in the 20 years immediately following the disturbance. However, the continued presence of Engelmann spruce in this ecosystem depends on the future survival and growth of these seedlings to reproductive maturity.

APPENDICES

APPENDIX A: CHAPTER 2 SUPPLEMENTARY TABLES AND FIGURES

Table A-1. Correlation between various tree measurements and climate variables. Tree measurements included $\Delta^{13}C$, ring width (RW), latewood width (LW), and earlywood width (EW). Climate variables included current year summer (June, July, August) maximum temperature (Tmax), climatic moisture deficit (CMD), and Palmer-Drought Severity Index (PDSI; PRISM; Climate WNA).

Site	Timing	Variable	Correlation		
			Tmax	CMD	PDSI
ASH	E	$\Delta^{13}C$	-0.52	-0.60	0.34
ASH	E	RW	-0.11	-0.31	0.17
ASH	E	LW	0.14	-0.031	0.0092
ASH	E	EW	-0.14	-0.36	0.19
ASH	L	$\Delta^{13}C$	-0.24	-0.53	0.26
ASH	L	RW	-0.16	-0.10	0.12
ASH	L	LW	-0.0022	-0.0073	-0.028
ASH	L	EW	-0.17	-0.14	0.13
HCK	E	$\Delta^{13}C$	-0.54	-0.67	0.43
HCK	E	RW	-0.073	-0.062	0.11
HCK	E	LW	0.046	-0.098	0.14
HCK	E	EW	-0.061	-0.060	0.070
HCK	L	$\Delta^{13}C$	-0.33	-0.45	0.44
HCK	L	RW	-0.19	-0.18	0.12
HCK	L	LW	-0.091	0.028	0.023
HCK	L	EW	-0.17	-0.19	0.091
HPT	E	$\Delta^{13}C$	-0.35	-0.53	0.42
HPT	E	RW	0.066	0.027	0.0028
HPT	E	LW	0.099	0.11	-0.035
HPT	E	EW	0.074	-0.023	0.0073
HPT	L	$\Delta^{13}C$	-0.26	-0.049	0.21
HPT	L	RW	-0.30	-0.29	0.37
HPT	L	LW	-0.25	-0.21	0.25
HPT	L	EW	-0.37	-0.37	0.44
MID	E	$\Delta^{13}C$	-0.52	-0.57	0.55
MID	E	RW	-0.17	-0.048	0.18
MID	E	LW	0.055	0.024	-0.030
MID	E	EW	-0.22	-0.084	0.26
MID	L	$\Delta^{13}C$	-0.51	-0.59	0.55
MID	L	RW	-0.086	0.0068	0.081

MID	L	LW	0.024	0.090	-0.096
MID	L	EW	-0.14	-0.056	0.14
NLS	E	$\Delta^{13}C$	-0.35	-0.25	0.23
NLS	E	RW	0.096	0.051	-0.035
NLS	E	LW	-0.058	0.11	-0.14
NLS	E	EW	0.20	0.082	-0.098
NLS	L	$\Delta^{13}C$	-0.50	-0.43	0.59
NLS	L	RW	0.087	0.026	0.0075
NLS	L	LW	0.019	-0.11	0.18
NLS	L	EW	0.062	0.026	0.013
SNO	E	$\Delta^{13}C$	-0.47	-0.55	0.29
SNO	E	RW	0.038	0.022	-0.16
SNO	E	LW	0.060	0.12	-0.15
SNO	E	EW	-0.033	-0.017	-0.15
SNO	L	$\Delta^{13}C$	-0.0068	-0.12	0.058
SNO	L	RW	0.023	0.066	0.091
SNO	L	LW	0.22	-0.0096	-0.020
SNO	L	EW	-0.012	0.036	0.10
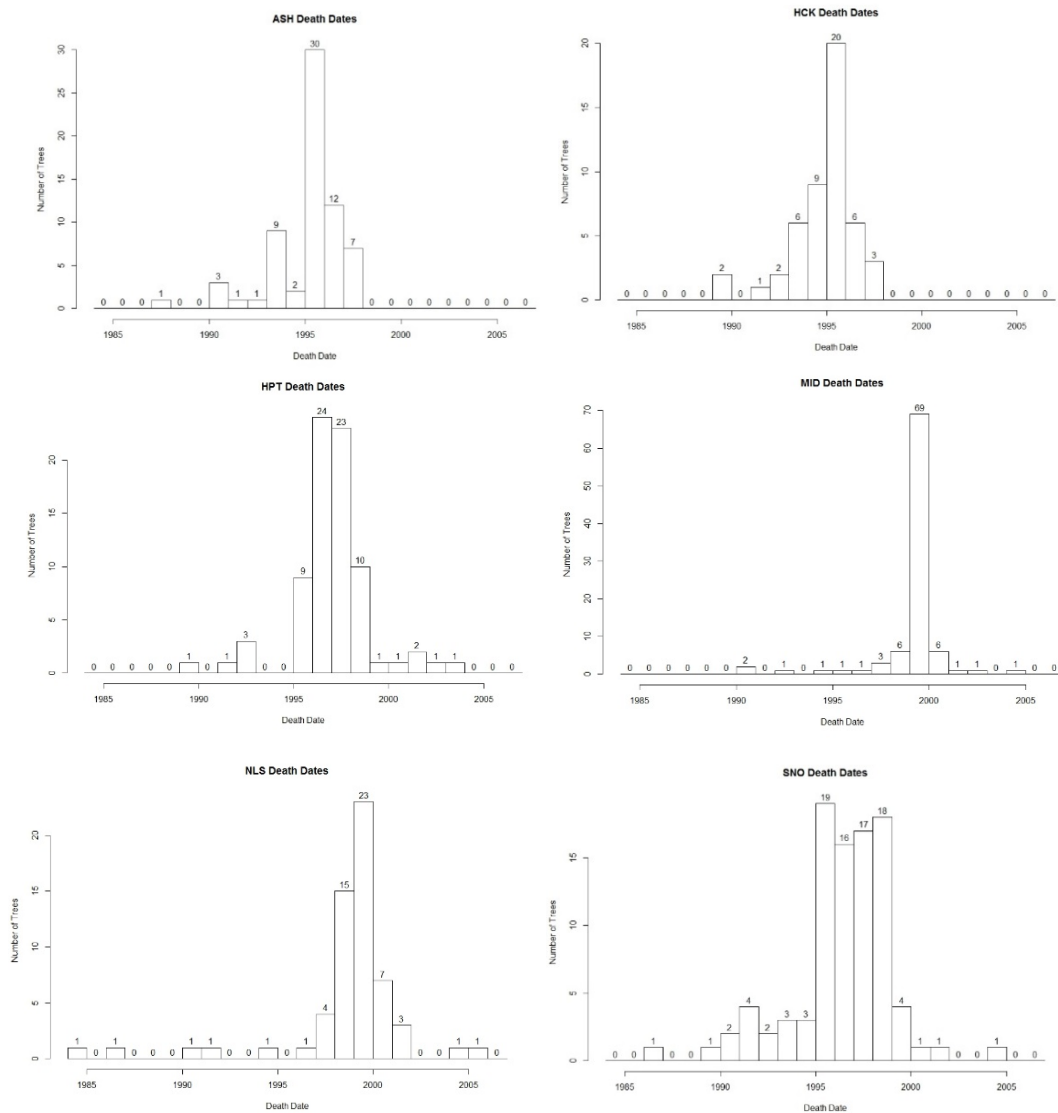
Fig. A-1. Histogram of death dates per site used in the isotope analysis. Cores before and after the peak of death dates per site were isolated for further analyses. Note: x-axis tick marks denote bar to the left.
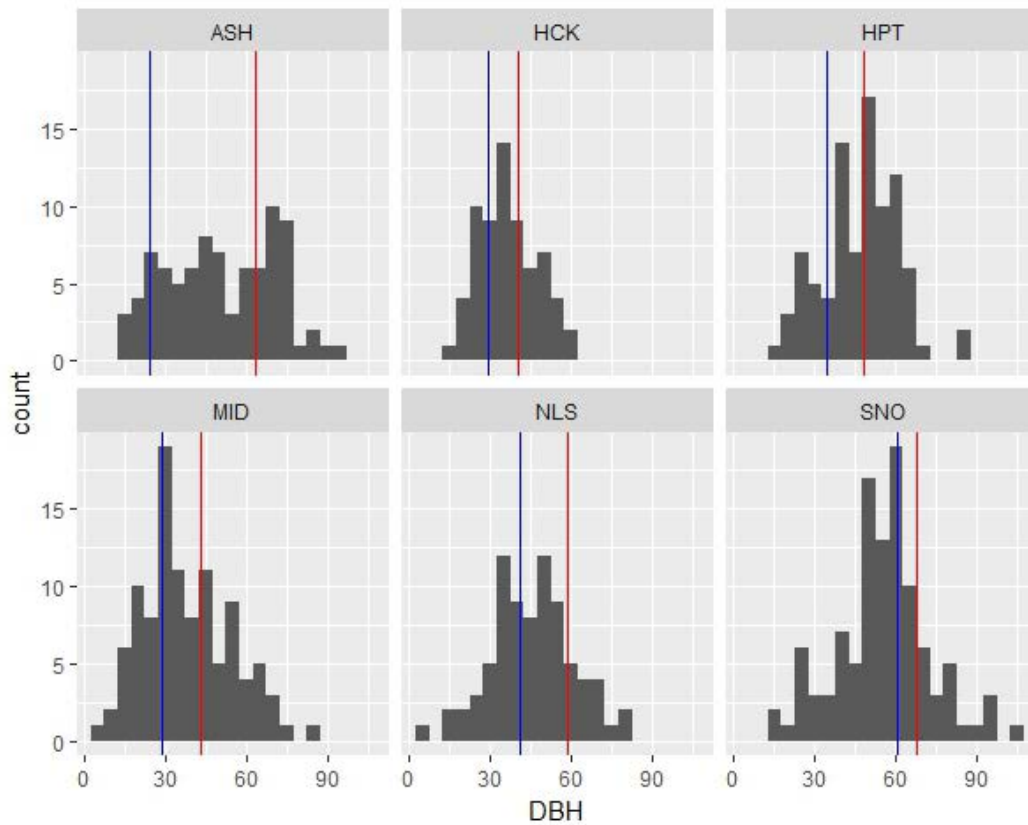
Fig. A-2. Diameter distributions of all Engelmann spruce trees (DBH > 5 cm) in the stand at each site. Blue line denotes the average DBH of early-dying trees per site, and the red line denotes the average DBH of late-dying trees per site. From the t-test results, significant differences in DBH ($P < 0.05$) occurred at ASH, HCK, NLS with a marginally significant difference ($P < 0.1$) at MID.
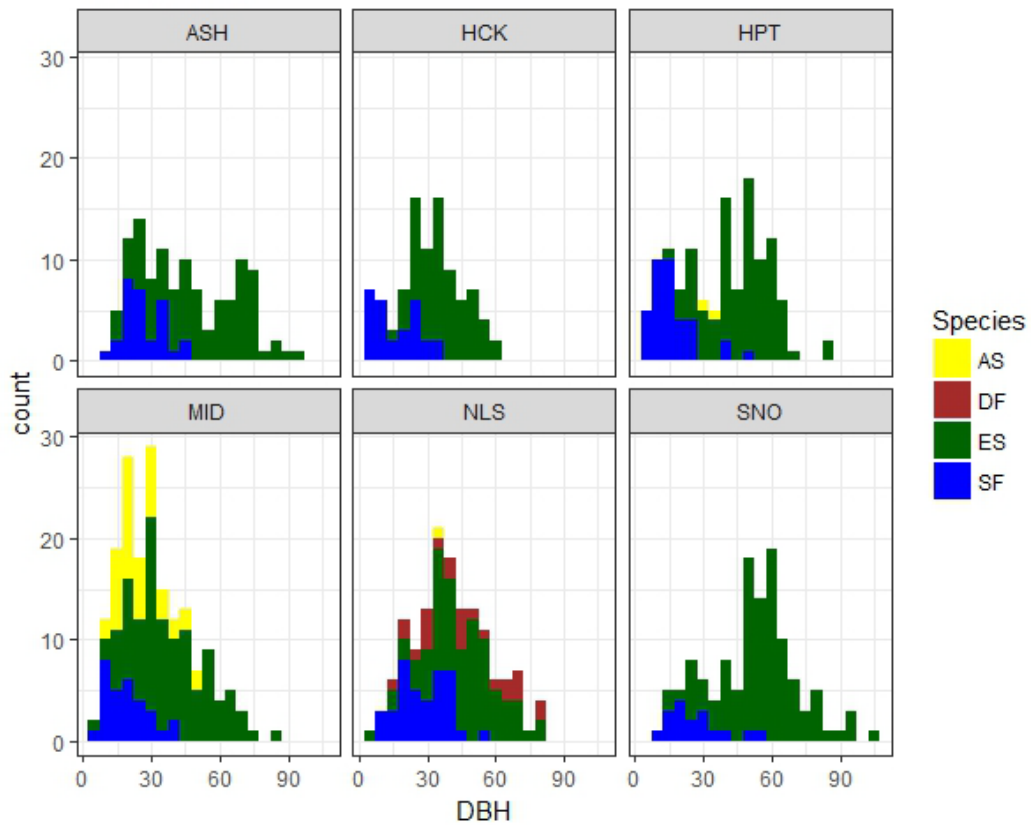
Fig. A-3. Species composition of all trees (DBH > 5 cm) in the stand at each site color coded by species. Aspen (AS; yellow), Douglas-fir (DF; brown), Engelmann spruce (ES; green), and subalpine fir (SF; blue).

APPENDIX B: CHAPTER 3 SUPPLEMENTARY TABLES AND FIGURES

Table B-1. Site summary information calculated as averages from all subplots at each site. Including elevation, slope, aspect, climatic moisture deficit (CMD), basal area of dead Engelmann spruce (BA D ES), and tree species richness (Spp richness).

Site	Elevation (m)	Slope (%)	Aspect (°)	CMD (mm)	BA D ES (m2/ha)	Spp Richness
ASH	3182	6.5	8	188	0.34	2
BHF	3301	7.5	126	179	1.00	2
BPT	3005	41	299	243	0.26	3
CEB	3190	9	114	205	0.67	2
DCK	2763	12	237	355	0.58	3
DCS	2841	4.5	24	336	0.13	4
HCK	3090	17	320	261	0.32	2
HPT	3053	0	NA	248	0.53	3
LC	2985	9	176	275	0.83	3
MTH	2719	24	105	416	0.03	3
NLS	2821	27	360	304	0.63	3
RBW	3211	8	178	187	0.25	3
SNO	3188	39	342	204	0.6	2
SPC	2800	28	89	321	0.2	3
TCC	3238	7	240	186	1.4	2
TIP	2790	29	264	369	0.13	3
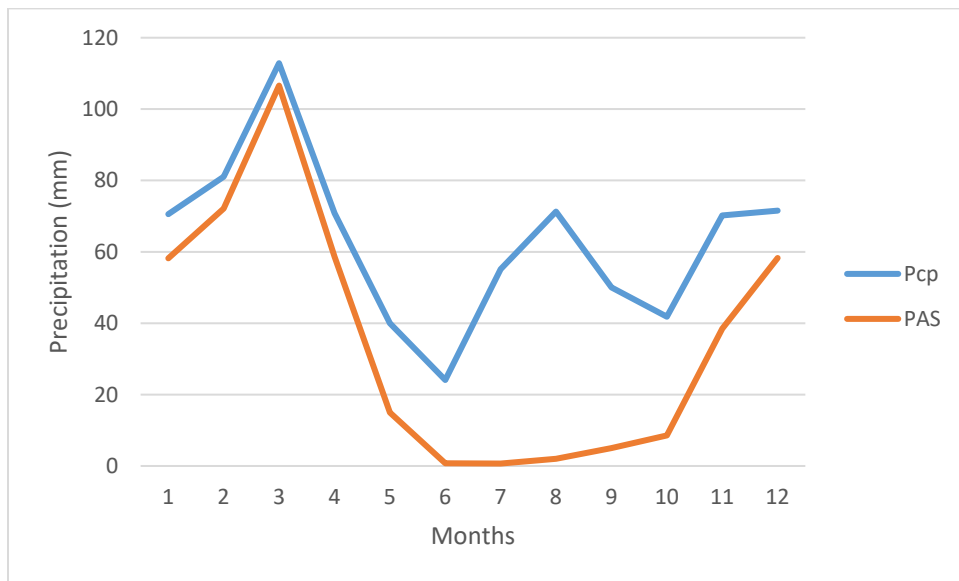
Fig. B-1. Monthly precipitation (Pcp) and precipitation as snow (PAS) from 30yr normals averaged for all sites (Wang et al. 2016).
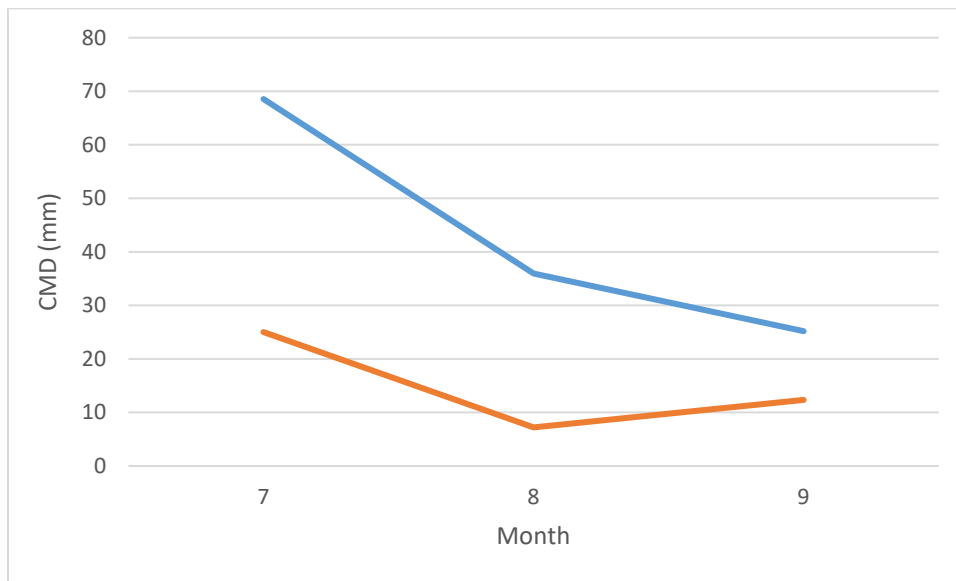
Fig. B-2. Monthly July, August, and September climatic moisture deficit (CMD) for the macroclimate (blue) compared to the microclimate (red) averaged for all sites. Macroclimate CMD from 30yr normals (Wang et al. 2016). Microclimate CMD calculated from iButton temperature data.

Fig. B-3. Example of a cluster of subalpine fir seedlings around an Engelmann spruce snag at one of our high elevation sites (BHF).

APPENDIX C: CHAPTER 3 MODEL SELECTION PROCESS FOR ALL

SEEDLINGS, PRE-OUTBREAK SEEDLINGS, AND POST-

OUTBREAK SEEDLINGS

Table C-1. Full model selection process from model using all seedlings and saplings as
response variable. Selected models from each step are highlighted in bold text.

Level	Step	Variables	AIC	K
	1	Intercept	562	0
1a. Abiotic	2.01	SWC.187	397	1
	2.02	**SWC.265**	**393**	**1**
	2.03	CMD.calc	405	1
	2.04	SWC.187, SWC.265	392	2
	2.05	SWC.187, CMD.calc	399	2
	2.06	SWC.265, CMD.calc	394	2
	2.07	SWC.187, SWC.265,CMD.calc	394	3
	2.08	SWC.187,SWC.265,CMD, SWC.187*CMD	396	4
	2.09	SWC.187,SWC.265,CMD, SWC.265*CMD	396	4
1b. Biotic	3.01	SWC.265, sf seedling	342	2
	3.02	SWC.265, %EW	341	2
	3.03	SWC.265, %LW	342	2
	3.04	SWC.265, %under	337	2
	3.05	SWC.265, sfseedling, %EW	343	3
	3.06	SWC.265, sfseedling, %LW	344	3
	3.07	SWC.265, sfseedling, %under	339	3
	3.08	SWC.265, %EW, %LW	343	3
	3.09	SWC.265, %EW, %under	337	3
	3.10	SWC.265, %LW, %under	338	3
	3.11	SWC.265, sfseedling, %EW, %LW	345	4
	3.12	SWC.265, sfseedling, %EW, %under	338	4
	3.13	SWC.265, sfseedling, %LW, %under	340	4
	3.14	SWC.265, %EW, %LW, %under	339	4
	3.15	SWC.265,sfseedling,%EW,%LW,%under	340	5
	3.16	**SWC.265, %under, SWC.265*%under**	**333**	**3**
	3.17	SWC.265, %under, %LW, SWC.265*%under, %LW*%under	335	5
	3.18	SWC.265, %under, %LW, SWC.265*%under, %LW*SWC.265	334	5
	3.19	SWC.265, %under, %LW, SWC.265*%LW	338	4

	3.20	SWC.265, %under, %LW, sfseedling, SWC.265*%under, %LW*SWC.265, Sf*SWC.265	338	7
	3.21	SWC.265, %under, sfseedling, SWC.265*%under, Sf*SWC.265	337	5
	3.22	SWC.265, %under, %LW, sfseedling, %LW*SWC.265, Sf*SWC.265	341	6
	3.23	SWC.265, %under, %LW, SWC.265*%under, %LW*SWC.265, %under*%LW	336	6
	3.24	SWC.265, %under, %LW, SWC.265*%under, %LW*SWC.265, %EW	336	6
2a.Understory	4.01	SWC.265,%under, SWC.265*%under, sfsapling	335	4
	4.02	SWC.265,%under, SWC.265*%under, sfsapling, sfsapling*SWC.265	336	5
2b. Overstory	5.01	SWC.265,%under, SWC.265*%under, %cover	335	4
	5.02	SWC.265,%under, SWC.265*%under, QMD	330	4
	5.03	SWC.265,%under, SWC.265*%under, Ht	334	4
	5.04	SWC.265,%under, SWC.265*%under, BA.SF	335	4
	5.05	SWC.265,%under, SWC.265*%under, BA.ES.L	335	4
	5.06	**SWC.265,%under, SWC.265*%under, BA.D**	**324**	**4**
	5.07	SWC.265,%under, SWC.265*%under, %cover, QMD	332	5
	5.08	SWC.265,%under, SWC.265*%under, %cover, Ht	336	5
	5.09	SWC.265,%under, SWC.265*%under, %cover,BA.SF	336	5
	5.10	SWC.265,%under, SWC.265*%under, %cover, BA.ES.L	337	5
	5.11	SWC.265,%under, SWC.265*%under, %cover, BA.D	325	5
	5.12	SWC.265,%under, SWC.265*%under, QMD, Ht	330	5
	5.13	SWC.265,%under, SWC.265*%under, QMD, BA.SF	331	5
	5.14	SWC.265,%under, SWC.265*%under, QMD, BA.ES.L	332	5

	5.15	SWC.265,%under, SWC.265*%under, QMD, BA.D	325	5
	5.16	SWC.265,%under, SWC.265*%under, Ht, BA.SF	336	5
	5.17	SWC.265,%under, SWC.265*%under, Ht, BA.ES.L	336	5
	5.18	SWC.265,%under, SWC.265*%under, Ht, BA.D	325	5
	5.19	SWC.265,%under, SWC.265*%under, BA.SF, BA.ES.L	337	5
	5.20	SWC.265,%under, SWC.265*%under, BA.SF, BA.D	324	5
	5.21	SWC.265,%under, SWC.265*%under, BA.ES.L, BA.D	325	5
	5.22	SWC.265,%under, SWC.265*%under, %cover, QMD, Ht	331	6
	5.23	SWC.265,%under, SWC.265*%under, %cover, QMD, BA.SF	332	6
	5.24	SWC.265,%under, SWC.265*%under, %cover, QMD, BA.ES.L	334	6
	5.25	SWC.265,%under, SWC.265*%under, %cover, QMD, BA.D	327	6
	5.26	SWC.265,%under, SWC.265*%under, %cover, Ht, BA.SF	337	6
	5.27	SWC.265,%under, SWC.265*%under, %cover, Ht, BA.ES.L	338	6
	5.28	SWC.265,%under, SWC.265*%under, %cover, Ht, BA.D	327	6
	5.29	SWC.265,%under, SWC.265*%under, %cover, BA.SF, BA.ES.L	338	6
	5.30	SWC.265,%under, SWC.265*%under, %cover, BA.SF, BA.D	325	6
	5.31	SWC.265,%under, SWC.265*%under, %cover, BA.ES.L, BA.D	327	6
	5.32	SWC.265,%under, SWC.265*%under, QMD, Ht, BA.SF	331	6
	5.33	SWC.265,%under, SWC.265*%under, QMD, Ht, BA.ES.L	332	6
	5.34	SWC.265,%under, SWC.265*%under, QMD, Ht, BA.D	327	6
	5.35	SWC.265,%under, SWC.265*%under, QMD, BA.SF, BA.ES.L	333	6
	5.36	SWC.265,%under, SWC.265*%under, QMD, BA.SF, BA.D	325	6

	5.37	SWC.265,%under, SWC.265*%under, QMD, BA.ES.L, BA.D	327	6
	5.38	SWC.265,%under, SWC.265*%under, Ht, BA.SF, BA.ES.L	338	6
	5.39	SWC.265,%under, SWC.265*%under, Ht, BA.SF, BA.D	326	6
	5.40	SWC.265,%under, SWC.265*%under, BA.SF, BA.ES.L, BA.D	326	6
	5.41	SWC.265,%under, SWC.265*%under, %cover, QMD, Ht, BA.SF	332	7
	5.42	SWC.265,%under, SWC.265*%under, %cover, QMD, Ht, BA.ES.L	333	7
	5.43	SWC.265,%under, SWC.265*%under, %cover, QMD, Ht, BA.D	328	7
	5.44	SWC.265,%under, SWC.265*%under, %cover, QMD, BA.SF, BA.ES.L	334	7
	5.45	SWC.265,%under, SWC.265*%under, %cover, QMD, BA.SF, BA.D	327	7
	5.46	SWC.265,%under, SWC.265*%under, %cover, QMD, BA.ES.L, BA.D	329	7
	5.47	SWC.265,%under, SWC.265*%under, QMD, Ht, BA.SF, BA.ES.L	332	7
	5.48	SWC.265,%under, SWC.265*%under, QMD, Ht, BA.SF, BA.D	327	7
	5.49	SWC.265,%under, SWC.265*%under, QMD, Ht, BA.ES.L,BA.D	329	7
	5.50	SWC.265,%under, SWC.265*%under, QMD, BA.SF, BA.ES.L, BA.D	327	7
	5.51	SWC.265,%under, SWC.265*%under, Ht, BA.SF, BA.ES.L, BA.D	328	7
	5.52	SWC.265,%under, SWC.265*%under, %cover, QMD, Ht, BA.SF, BA.ES.L	334	8
	5.53	SWC.265,%under, SWC.265*%under, %cover, QMD, Ht, BA.SF, BA.D	328	8
	5.54	SWC.265,%under, SWC.265*%under, %cover, QMD, Ht, BA.ES.L, BA.D	330	8
	5.55	SWC.265,%under, SWC.265*%under, QMD, Ht, BA.SF, BA.ES.L, BA.D	329	8
	5.56	SWC.265,%under, SWC.265*%under, %cover, QMD, Ht, BA.SF, BA.ES.L, BA.D	330	9
	5.57	SWC.265,%under, SWC.265*%under, %cover, %cover*SWC.265	337	5
	5.58	SWC.265,%under, SWC.265*%under, QMD, QMD*SWC.265	332	5

	5.59	SWC.265,%under, SWC.265*%under, QMD, LW, QMD*LW	332	6
	5.60	SWC.265,%under, SWC.265*%under, BA.D, BA.D*SWC.265	325	5
	5.61	SWC.265,%under, SWC.265*%under, BA.D, Per.Under.ave, BA.D*Per.Under.ave	324	6
3. Landscape	6.01	SWC.265,%under, SWC.265*%under, BA.D, CMD	322	5
	6.02	SWC.265,%under, SWC.265*%under, BA.D, slope	326	5
	6.03	SWC.265,%under, SWC.265*%under, BA.D, aspect	325	5
	6.04	SWC.265,%under, SWC.265*%under, BA.D, elevation	324	5
	6.05	SWC.265,%under, SWC.265*%under, BA.D, CMD, slope	324	6
	6.06	SWC.265,%under, SWC.265*%under, BA.D, CMD, aspect	324	6
	6.07	SWC.265,%under, SWC.265*%under, BA.D, slope, aspect	327	6
	6.08	SWC.265,%under, SWC.265*%under, BA.D, slope, elevation	326	6
	6.09	SWC.265,%under, SWC.265*%under, BA.D, aspect, elevation	326	6
	6.10	SWC.265,%under, SWC.265*%under, BA.D, CMD, slope, aspect	326	7
	6.11	SWC.265,%under, SWC.265*%under, BA.D, slope, aspect, elevation	328	7
	6.12	SWC.265,%under, SWC.265*%under, BA.D, CMD, CMD*SWC.265	324	6
	6.13	SWC.265,%under, SWC.265*%under, BA.D, aspect, aspect*%under	325	6
	6.14	SWC.265,%under, SWC.265*%under, BA.D, aspect, per.under.ave, aspect*%under.ave	326	7
	6.15	SWC.265,%under, SWC.265*%under, BA.D, aspect, aspect*SWC.265	326	6

Table C-2. Full model selection process from model using pre-outbreak seedlings and saplings as response variable. Selected models from each step are highlighted in bold text.

	Step	Variables	AIC	K
	1	Intercept	468	0
1a. Abiotic	2.01	SWC.187	330	1
	2.02	**SWC.265**	**322**	**1**
	2.03	CMD.calc	337	1
	2.04	SWC.187, SWC.265	322	2
	2.05	SWC.187, CMD.calc	329	2
	2.06	SWC.265, CMD.calc	324	2
	2.07	SWC.187, SWC.265,CMD.calc	323	3
	2.08	SWC.187,SWC.265,CMD, SWC.187*CMD	324	4
	2.09	SWC.187,SWC.265,CMD, SWC.265*CMD	325	4
	2.10	SWC.265, CMD, SWC.265*CMD	326	3
1b. Biotic	3.01	SWC.265, sf seedling	287	2
	3.02	SWC.265, %EW	285	2
	3.03	SWC.265, %LW	287	2
	3.04	SWC.265, %under	284	2
	3.05	SWC.265, sfseedling, %EW	287	3
	3.06	SWC.265, sfseedling, %LW	289	3
	3.07	SWC.265, sfseedling, %under	286	3
	3.08	SWC.265, %EW, %LW	286	3
	3.09	**SWC.265, %EW, %under**	**282**	**3**
	3.1	SWC.265, %LW, %under	286	3
	3.11	SWC.265, sfseedling, %EW, %LW	288	4
	3.12	SWC.265, sfseedling, %EW, %under	284	4
	3.13	SWC.265, sfseedling, %LW, %under	288	4
	3.14	SWC.265, %EW, %LW, %under	284	4
	3.15	SWC.265,sfseedling,%EW,%LW,%under	286	5
	3.16	SWC.265, %under, SWC.265*%under	283	3
	3.17	SWC.265, %under, %LW, SWC.265*%under, %LW*%under	287	5
	3.18	SWC.265, %under, %LW, SWC.265*%under, %LW*SWC.265	286	5
	3.19	SWC.265, %under, %LW, SWC.265*%LW	287	4
	3.2	SWC.265, %under, %LW, sfseedling, SWC.265*%under, %LW*SWC.265, Sf*SWC.265	290	7
	3.21	SWC.265, %under, sfseedling, SWC.265*%under, Sf*SWC.265	287	5

	3.22	SWC.265, %under, %LW, sfseedling, %LW*SWC.265, Sf*SWC.265	291	6
	3.23	SWC.265, %under, %LW, SWC.265*%under, %LW*SWC.265, %under*%LW	288	6
	3.24	SWC.265, %under, %EW, %under*SWC.265	282	4
2a.Understory	4.01	SWC.265, %under, %EW, sfsapling	284	4
	4.02	SWC.265, %under, %EW, sfsapling, sfsapling*SWC.265	284	5
2b. Overstory	5.01	SWC.265, %under, %EW, %cover	282	4
	5.02	SWC.265, %under, %EW, QMD	280	4
	5.03	SWC.265, %under, %EW, ht.min	281	4
	5.04	SWC.265, %under, %EW, BA.SF	281	4
	5.05	SWC.265, %under, %EW, BA.ES.L	282	4
	5.06	**SWC.265, %under, %EW, BA.D**	**266**	**4**
	5.07	SWC.265, %under, %EW, %cover, QMD	282	5
	5.08	SWC.265, %under, %EW, %cover, Ht	283	5
	5.09	SWC.265, %under, %EW, %cover,BA.SF	283	5
	5.1	SWC.265, %under, %EW, %cover, BA.ES.L	284	5
	5.11	SWC.265, %under, %EW, %cover, BA.D	270	5
	5.12	SWC.265, %under, %EW, QMD, Ht	279	5
	5.13	SWC.265, %under, %EW, QMD, BA.SF	278	5
	5.14	SWC.265, %under, %EW, QMD, BA.ES.L	282	5
	5.15	SWC.265, %under, %EW, QMD, BA.D	270	5
	5.16	SWC.265, %under, %EW, Ht, BA.SF	283	5
	5.17	SWC.265, %under, %EW, Ht, BA.ES.L	283	5
	5.18	SWC.265, %under, %EW, Ht, BA.D	270	5
	5.19	SWC.265, %under, %EW, BA.SF, BA.ES.L	283	5
	5.20	SWC.265, %under, %EW, BA.SF, BA.D	267	5
	5.21	SWC.265, %under, %EW, BA.ES.L, BA.D	270	5
	5.22	SWC.265, %under, %EW, %cover, QMD, Ht	281	6
	5.23	SWC.265, %under, %EW, %cover, QMD, BA.SF	280	6
	5.24	SWC.265, %under, %EW, %cover, QMD, BA.ES.L	284	6
	5.25	SWC.265, %under, %EW, %cover, QMD, BA.D	272	6
	5.26	SWC.265, %under, %EW, %cover, Ht, BA.SF	284	6
	5.27	SWC.265, %under, %EW, %cover, Ht, BA.ES.L	285	6
	5.28	SWC.265, %under, %EW, %cover, Ht, BA.D	272	6

	5.29	SWC.265, %under, %EW, %cover, BA.SF, BA.ES.L	285	6
	5.30	SWC.265, %under, %EW, %cover, BA.SF, BA.D	268	6
	5.31	SWC.265, %under, %EW, %cover, BA.ES.L, BA.D	272	6
	5.32	SWC.265, %under, %EW, QMD, Ht, BA.SF	279	6
	5.33	SWC.265, %under, %EW, QMD, Ht, BA.ES.L	281	6
	5.34	SWC.265, %under, %EW, QMD, Ht, BA.D	272	6
	5.35	SWC.265, %under, %EW, QMD, BA.SF, BA.ES.L	280	6
	5.36	SWC.265, %under, %EW, QMD, BA.SF, BA.D	268	6
	5.37	SWC.265, %under, %EW, QMD, BA.ES.L, BA.D	272	6
	5.38	SWC.265, %under, %EW, Ht.min, BA.SF, BA.ES.L	285	6
	5.39	SWC.265, %under, %EW, Ht.min, BA.SF, BA.D	269	6
	5.40	SWC.265, %under, %EW, BA.SF, BA.ES.L, BA.D	268	6
	5.41	SWC.265, %under, %EW, %cover, QMD, Ht, BA.SF	281	7
	5.42	SWC.265, %under, %EW, %cover, QMD, Ht, BA.ES.L	283	7
	5.43	SWC.265, %under, %EW, %cover, QMD, Ht, BA.D	274	7
	5.44	SWC.265, %under, %EW, %cover, QMD, BA.SF, BA.ES.L	282	7
	5.45	SWC.265, %under, %EW, %cover, QMD, BA.SF, BA.D	270	7
	5.46	SWC.265, %under, %EW, %cover, QMD, BA.ES.L, BA.D	274	7
	5.47	SWC.265, %under, %EW, QMD, Ht, BA.SF, BA.ES.L	280	7
	5.48	SWC.265, %under, %EW, QMD, Ht, BA.SF, BA.D	270	7
	5.49	SWC.265, %under, %EW, QMD, Ht, BA.ES.L,BA.D	274	7
	5.50	SWC.265, %under, %EW, QMD, BA.SF, BA.ES.L, BA.D	270	7
	5.51	SWC.265, %under, %EW, Ht, BA.SF, BA.ES.L, BA.D	270	7

	5.52	SWC.265, %under, %EW, %cover, QMD, Ht, BA.SF, BA.ES.L	282	8
	5.53	SWC.265, %under, %EW, %cover, QMD, Ht, BA.SF, BA.D	272	8
	5.54	SWC.265, %under, %EW, %cover, QMD, Ht, BA.ES.L, BA.D	276	8
	5.55	SWC.265, %under, %EW, QMD, Ht, BA.SF, BA.ES.L, BA.D	272	8
	5.56	SWC.265, %under, %EW, %cover, QMD, Ht, BA.SF, BA.ES.L, BA.D	274	9
	5.57	SWC.265, %under, %EW, %cover, %cover*SWC.265	283	5
	5.58	SWC.265, %under, %EW, QMD, QMD*SWC.265	281	5
	5.59	SWC.265, %under, %EW, BA.D, BA.D*SWC.265	268	5
3. Landscape	6.01	SWC.265, %under, %EW, BA.D, CMD	269	5
	6.02	SWC.265, %under, %EW, BA.D, slope	270	5
	6.03	SWC.265, %under, %EW, BA.D, aspect	270	5
	6.04	SWC.265, %under, %EW, BA.D, elevation	269	5
	6.05	SWC.265, %under, %EW, BA.D, CMD, slope	271	6
	6.06	SWC.265, %under, %EW, BA.D, CMD, aspect	271	6
	6.07	SWC.265, %under, %EW, BA.D, slope, aspect	272	6
	6.08	SWC.265, %under, %EW, BA.D, slope, elevation	271	6
	6.09	SWC.265, %under, %EW, BA.D, aspect, elevation	271	6
	6.10	SWC.265, %under, %EW, BA.D, CMD, slope, aspect	273	7
	6.11	SWC.265, %under, %EW, BA.D, slope, aspect, elevation	273	7
	6.12	SWC.265, %under, %EW, BA.D, CMD,CMD*SWC.265	270	6
	6.13	SWC.265, %under, %EW, BA.D, aspect, aspect*SWC.265	272	6

Table C-3. Full model selection process from model using post/during-outbreak seedlings and saplings as response variable. Selected models from each step are highlighted in bold text.

	Step	Variables	AIC	K
	1	Intercept	421	0
1a. Abiotic	2.01	SWC.187	292	1
	2.02	SWC.265	293	1
	2.03	CMD.calc	292	1
	2.04	SWC.187, SWC.265	292	2
	2.05	**SWC.187, CMD.calc**	**291**	**2**
	2.06	SWC.265, CMD.calc	292	2
	2.07	SWC.187, SWC.265,CMD.calc	294	3
	2.08	SWC.187,SWC.265,CMD, SWC.187*CMD	294	4
	2.09	SWC.187,SWC.265,CMD, SWC.265*CMD	292	4
	2.10	SWC.187,CMD_calc, SWC.187*CMD_calc	293	3
1b. Biotic	3.01	SWC.187,CMD_calc, sf seedling	262	3
	3.02	SWC.187,CMD_calc, %EW	262	3
	3.03	**SWC.187,CMD_calc, %LW**	**254**	**3**
	3.04	SWC.187,CMD_calc, %under	260	3
	3.05	SWC.187,CMD_calc, sfseedling, %EW	264	4
	3.06	SWC.187,CMD_calc, sfseedling, %LW	256	4
	3.07	SWC.187,CMD_calc, sfseedling, %under	261	4
	3.08	SWC.187,CMD_calc, %EW, %LW	256	4
	3.09	SWC.187,CMD_calc, %EW, %under	261	4
	3.10	SWC.187,CMD_calc, %LW, %under	253	4
	3.11	SWC.187,CMD_calc, sfseedling, %EW, %LW	258	5
	3.12	SWC.187,CMD_calc, sfseedling, %EW, %under	261	5
	3.13	SWC.187,CMD_calc, sfseedling, %LW, %under	254	5
	3.14	SWC.187,CMD_calc, %EW, %LW, %under	255	5
	3.15	SWC.187,CMD_calc,sfseedling,%EW, %LW, %under	256	6
	3.16	SWC.187,CMD_calc, %under, SWC.187*%under	258	4
	3.17	SWC.187,CMD_calc, %under, %LW, %LW*%under	251	5
	3.18	SWC.187,CMD_calc, %under, %LW, SWC.187*%LW	255	5

	3.19	SWC.187,CMD_calc, %under, %LW, sfseedling, SWC.187*%under, %LW*SWC.187, Sf*SWC.187	257	8
	3.20	SWC.187,CMD_calc, %under, sfseedling, SWC.187*%under, Sf*SWC.187	260	6
	3.21	SWC.187,CMD_calc, %under, %LW, sfseedling, %LW*SWC.187, Sf*SWC.187	258	7
	3.22	SWC.187,CMD_calc, %under, %LW, SWC.187*%under, %LW*SWC.187, %under*%LW	250	7
	3.23	SWC.187,CMD_calc,%LW, %LW *SWC.187	256	4
	3.24	SWC.187,CMD_calc, %LW, %under, %under *SWC.187	252	5
2a.Understory	4.01	SWC.187,CMD_calc, %LW, %undercov	256	4
	4.02	SWC.187,CMD_calc, %LW, sfsapling	256	4
	4.03	SWC.187,CMD_calc, %LW, %undercov,sfsapling	258	5
	4.04	SWC.187,CMD_calc, %LW, %undercov, %undercov*SWC.187	250	5
	4.05	SWC.187,CMD_calc, %LW, sfsapling, sfsapling*SWC.187	258	5
	4.06	SWC.187,CMD_calc, %LW, sfsapling, %undercov, sfsapling*%undercov	260	6
2b. Overstory	5.01	SWC.187,CMD_calc, %LW, %cover	256	4
	5.02	SWC.187,CMD_calc, %LW, QMD	256	4
	5.03	SWC.187,CMD_calc, %LW, ht.min	253	4
	5.04	SWC.187,CMD_calc, %LW, BA.SF	255	4
	5.05	SWC.187,CMD_calc, %LW, BA.ES.L	254	4
	5.06	SWC.187,CMD_calc, %LW, BA.D	256	4
	5.07	SWC.187,CMD_calc, %LW, %cover, QMD	257	5
	5.08	SWC.187,CMD_calc, %LW, %cover, Ht	254	5
	5.09	SWC.187,CMD_calc, %LW, %cover,BA.SF	257	5
	5.10	SWC.187,CMD_calc, %LW, %cover, BA.ES.L	256	5
	5.11	SWC.187,CMD_calc, %LW, %cover, BA.D	258	5
	5.12	SWC.187,CMD_calc, %LW, QMD, Ht	254	5
	5.13	SWC.187,CMD_calc, %LW, QMD, BA.SF	257	5
	5.14	SWC.187,CMD_calc, %LW, QMD, BA.ES.L	256	5
	5.15	SWC.187,CMD_calc, %LW, QMD, BA.D	258	5
	5.16	SWC.187,CMD_calc, %LW, Ht, BA.SF	255	5

	5.17	SWC.187,CMD_calc, %LW, Ht, BA.ES.L	254	5
	5.18	SWC.187,CMD_calc, %LW, Ht, BA.D	255	5
	5.19	SWC.187,CMD_calc, %LW, BA.SF, BA.ES.L	256	5
	5.20	SWC.187,CMD_calc, %LW, BA.SF, BA.D	257	5
	5.21	SWC.187,CMD_calc, %LW, BA.ES.L, BA.D	256	5
	5.22	SWC.187,CMD_calc, %LW, %cover, QMD, Ht	255	6
	5.23	SWC.187,CMD_calc, %LW, %cover, QMD, BA.SF	258	6
	5.24	SWC.187,CMD_calc, %LW, %cover, QMD, BA.ES.L	257	6
	5.25	SWC.187,CMD_calc, %LW, %cover, QMD, BA.D	259	6
	5.26	SWC.187,CMD_calc, %LW, %cover, Ht, BA.SF	256	6
	5.27	SWC.187,CMD_calc, %LW, %cover, Ht, BA.ES.L	255	6
	5.28	SWC.187,CMD_calc, %LW, %cover, Ht, BA.D	256	6
	5.29	SWC.187,CMD_calc, %LW, %cover, BA.SF, BA.ES.L	257	6
	5.30	SWC.187,CMD_calc, %LW, %cover, BA.SF, BA.D	259	6
	5.31	SWC.187,CMD_calc, %LW, %cover, BA.ES.L, BA.D	258	6
	5.32	SWC.187,CMD_calc, %LW, QMD, Ht, BA.SF	255	6
	5.33	SWC.187,CMD_calc, %LW, QMD, Ht, BA.ES.L	255	6
	5.34	SWC.187,CMD_calc, %LW, QMD, Ht, BA.D	256	6
	5.35	SWC.187,CMD_calc, %LW, QMD, BA.SF, BA.ES.L	257	6
	5.36	SWC.187,CMD_calc, %LW, QMD, BA.SF, BA.D	259	6
	5.37	SWC.187,CMD_calc, %LW, QMD, BA.ES.L, BA.D	258	6
	5.38	SWC.187,CMD_calc, %LW, Ht.min, BA.SF, BA.ES.L	256	6
	5.39	SWC.187,CMD_calc, %LW, Ht.min, BA.SF, BA.D	256	6

	5.40	SWC.187,CMD_calc, %LW, BA.SF, BA.ES.L, BA.D	258	6
	5.41	SWC.187,CMD_calc, %LW, %cover, QMD, Ht, BA.SF	256	7
	5.42	SWC.187,CMD_calc, %LW, %cover, QMD, Ht, BA.ES.L	256	7
	5.43	SWC.187,CMD_calc, %LW, %cover, QMD, Ht, BA.D	257	7
	5.44	SWC.187,CMD_calc, %LW, %cover, QMD, BA.SF, BA.ES.L	258	7
	5.45	SWC.187,CMD_calc, %LW, %cover, QMD, BA.SF, BA.D	260	7
	5.46	SWC.187,CMD_calc, %LW, %cover, QMD, BA.ES.L, BA.D	259	7
	5.47	SWC.187,CMD_calc, %LW, QMD, Ht, BA.SF, BA.ES.L	257	7
	5.48	SWC.187,CMD_calc, %LW, QMD, Ht, BA.SF, BA.D	257	7
	5.49	SWC.187,CMD_calc, %LW, QMD, Ht, BA.ES.L,BA.D	257	7
	5.50	SWC.187,CMD_calc, %LW, QMD, BA.SF, BA.ES.L, BA.D	259	7
	5.51	SWC.187,CMD_calc, %LW, Ht, BA.SF, BA.ES.L, BA.D	258	7
	5.52	SWC.187,CMD_calc, %LW, %cover, QMD, Ht, BA.SF, BA.ES.L	257	8
	5.53	SWC.187,CMD_calc, %LW, %cover, QMD, Ht, BA.SF, BA.D	258	8
	5.54	SWC.187,CMD_calc, %LW, %cover, QMD, Ht, BA.ES.L, BA.D	258	8
	5.55	SWC.187,CMD_calc, %LW, QMD, Ht, BA.SF, BA.ES.L, BA.D	259	8
	5.56	SWC.187,CMD_calc, %LW, %cover, QMD, Ht, BA.SF, BA.ES.L, BA.D	259	9
	5.57	SWC.187,CMD_calc, %LW, %cover, %cover*SWC.187	258	5
	5.58	SWC.187,CMD_calc, %LW, QMD, QMD*SWC.187	255	5
	5.59	SWC.187,CMD_calc, %LW, QMD, QMD*LW	257	5
	5.60	SWC.187,CMD_calc, %LW, BA.D, BA.D*SWC.187	254	5
	5.61	SWC.187,CMD_calc, %LW, BA.D, Per.under.ave, BA.D*Per.under.ave	257	6

3. Landscape	6.01	SWC.187,CMD_calc, %LW, CMD	255	4
	6.02	SWC.187,CMD_calc, %LW, slope	256	4
	6.03	SWC.187,CMD_calc, %LW, aspect	256	4
	6.04	SWC.187,CMD_calc, %LW, elevation	256	4
	6.05	SWC.187,CMD_calc, %LW, CMD, slope	257	5
	6.06	SWC.187,CMD_calc, %LW, CMD, aspect	257	5
	6.07	SWC.187,CMD_calc, %LW, slope, aspect	257	5
	6.08	SWC.187,CMD_calc, %LW, slope, elevation	258	5
	6.09	SWC.187,CMD_calc, %LW, aspect, elevation	257	5
	6.10	SWC.187,CMD_calc, %LW, CMD, slope, aspect	259	6
	6.11	SWC.187,CMD_calc, %LW, slope, aspect, elevation	259	6
	6.12	SWC.187,CMD_calc, %LW, CMD, CMD*SWC.187	253	5
	6.13	SWC.187,CMD_calc, %LW, aspect, aspect*SWC.187	256	4

APPENDIX D: CHAPTER 3 EXAMPLES OF CODE IN R WRITTEN

FOR ANALYSES

Seedling Density Models
Example: final model for pre-outbreak seedlings and saplings

```
library (MASS)
m.pre.glm.final<-glm.nb (Seed.Sap.pre_100m2 ~ SWC.265 + Per.Under.ave + EW.ave +
            BA.D_ha, data=flat, link=log)
```

Spatial Analysis
Example: Univariate Analysis for all seedlings

```
library (spatstat)
Kest <- lapply(seed.map$V1, pcf, ratio=TRUE)
Ke<- do.call(pool, Kest)
plot(Ke, cbind(pooliso, pooltheo, loiso, hiiso) ~ r, shade=c("loiso", "hiiso"),
    main="Univariate analysis: All Seedlings", ylim=c(0,10))
```

Rose Diagram
Example: diagram for post-outbreak seedlings in relation to closest down log on slope $\geq 10\%$
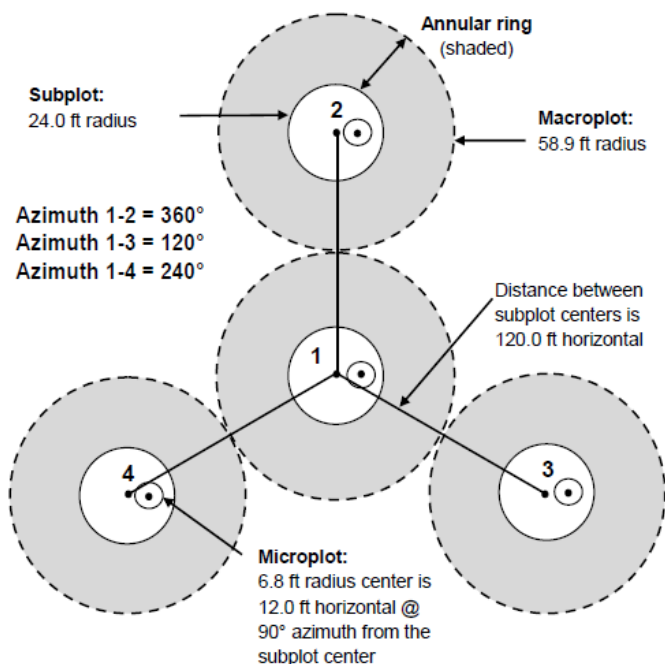
```
library(circular)
x.circL.ste.post <- circular(log.close.1.post$Az2, type="directions", units="degrees",
                template="geographics", rotation="clock")
rose.diag(x.circL.ste.post, bins=18, col="gray", border="dark gray",
      main="Direction of Post-Seedling from closest Log on slopes >9")
```

APPENDIX E: CHAPTER 3 COMPLETE FIELD SAMPLING PROTOCOL

Forest Inventory and Analysis (FIA) Plot Dimensions:

Size Classes:
-Seedling: less than 1 in (2.54 cm) DBH
• Engelmann Spruce (ES) seedlings sampled at subplot level
• Subalpine Fir (SF) and other seedlings sampled at microplot level
-Sapling: diameter between 1 in (2.54 cm) and 5 in (12.7 cm)
• Sampled at microplot level
-Tree: at least 5 in (12.7 cm) diameter
• Sampled at subplot level

Tree Status:
Live (L): contains any living parts
Dead (D): no living parts
Dead and Down (DD): dead trees that have fallen from below DBH

Percent Cover Categories: (less than)
0, 1, 5, 15, 25, 50, 75, 85, 95, 99, 100

1. **PLOT LEVEL DATA**: One plot at each site will be set-up following the above diagram (Macroplots not used). GPS coordinates will be taken at the center of subplot #1 and elevation, slope, and aspect will be measured.

2. **SUBPLOT LEVEL DATA**:
   a. **Canopy Trees:** all standing canopy trees will be counted and their species, DBH, height, and status (L/D) will be recorded. Additionally, their distance and azimuth (using 360 for north) to subplot center will be recorded.
   b. **Saplings:** the number of saplings per species will be counted across the subplot
   c. **ES Seedlings*:** subplots will be systematically surveyed for any Engelmann spruce seedlings. All seedlings will be counted and their basal diameter, height, and substrate type found on will be recorded. Age will also be estimated to decade classes by counting the number of bud scars. Additionally, the distance and azimuth to the surrounding vertical

structures (stump, log, large boulder, and trees outside of subplot) within a 6.8 ft radius (2.07 m) plot will be recorded. The vertical height, species, and decay class (where applicable) will also be recorded (if a tree doesn't fall within the subplot then DBH, and height will also be recorded). Additionally, in the same 6.8 ft (2.07 m) radius plot around each seedling the number of subalpine fir seedlings and percent understory cover will be recorded, as well as the percent cover by vegetation, and late and early stage decay wood.

d. **Soil Moisture*:** soil moisture readings will be taken in 9 places at each subplot. In the cardinal and intercardinal directions 12 ft (about 4 m) from the center of the subplot, as well as in the center of the subplot. Readings will be taken three times during the summer (July, August, September). Additional data will be recorded during each soil moisture reading: time of day and hours since rain.

e. **iButtons***: 1 iButton will be deployed at each subplot (4 per plot). They will be placed in small baggies, folded inside reflective insulation, and taped to a PVC pipe with the top of the envelope 50 cm from the substrate. If a PVC pipe cannot be placed in the soil, then the reflective envelope will be nailed to a tree following the same protocol. They will be deployed at the first visit to each site and left on location until the end of September.

f. **Hemispherical photos*:** Hemispherical photos will be taken above each subplot center. The date and picture number will be recorded. Pictures will be taken from 1m above the soil surface on a leveled tripod, and the top of the photo will face north. Pictures must be taken during uniformly overcast conditions.

g. **Vegetation*:** Percent understory cover (non-tree species) across each subplot estimated (0, 1, 5, 15, 25, 50, 75, 85, 95, 99, 100%). Percent canopy cover above subplot center estimated (same categories as understory cover).

3. **MICROPLOT LEVEL DATA**:
   a. **Sapling Trees**: All sapling trees will be counted and their species, DBH, height, and status (L/D) will be measured. Additionally, their distance and azimuth to microplot center will be recorded.
   b. **Seedlings**: number of seedlings per species in the microplot will be counted.

APPENDIX F: CHAPTER 3 SOIL MOISTURE MODEL

SWC ~ Site + Julian Day + Time Since Rain + Time of Day
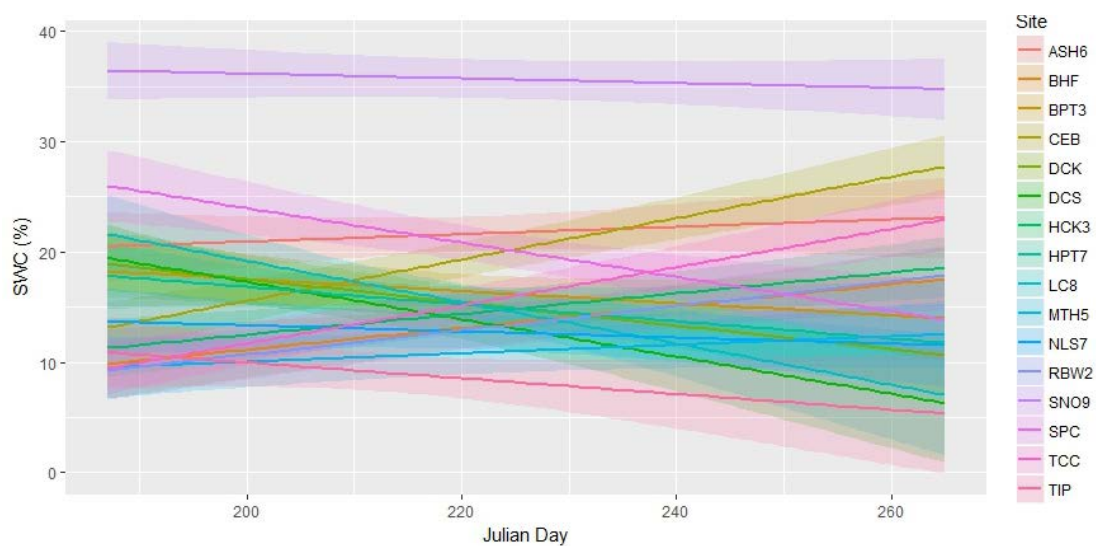($R^2 = 0.48$, $P = 2.2$x 10^{-16})

Fig. F-1. Predicted soil water content (%) for the range of Julian days where soil moisture data was measured across all sites. Line color denotes each site, lighter shading represents confidence intervals.